The CMS-TOTEM Precision Proton Spectrometer

A. Vilela Pereira
On behalf of the CMS and TOTEM Collaborations
Universidade do Estado do Rio de Janeiro, Brazil

High Energy Physics in the LHC Era
6th International Workshop
6-12 January 2016 - Valparaiso - Chile

The CMS-TOTEM Precision Proton Spectrometer

A. Vilela Pereira
On behalf of the CMS and TOTEM Collaborations
Universidade do Estado do Rio de Janeiro, Brazil

Related talk:

C. Mora Herrera

Evidence for Exclusive WW production at 8TeV and other forward physics results from CMS

High Energy Physics in the LHC Era
6th International Workshop
6-12 January 2016 - Valparaiso - Chile

The CT-PPS Project

CERN-LHCC-2014-021

The CT-PPS Project

CT-PPS : CMS-TOTEM Precision Proton Spectrometer

High-energy proton tracks originated from the interaction are measured with detectors located very close to the beam.

A common project of the CMS & TOTEM Collaborations which upgrades the existing Roman Pot (TOTEM) detector system to operate at nominal luminosity at the LHC.

CT-PPS Technical Design Report submitted and project approval (CERN Research Board - December 2014).

Note:

CMS & TOTEM have already taken data jointly using a common trigger configuration during dedicated low luminosity Runs in 2012 and 2015.

This presentation concerns the CT-PPS integrated system aimed at high luminosity operation.

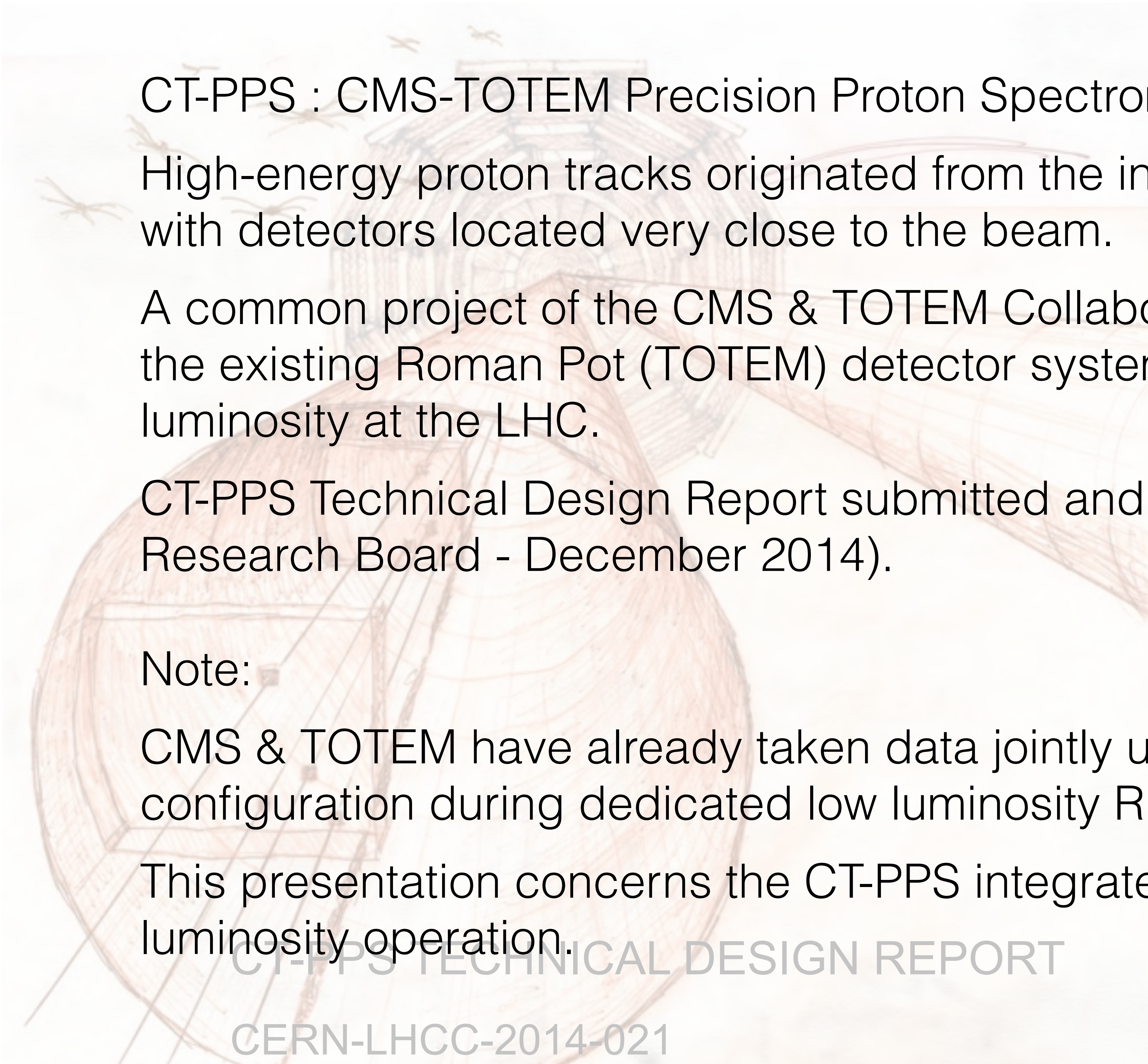

The CT-PPS Project

CT-PPS operation & performance requirements include:

Physics performance at high luminosity: pile-up and beam backgrounds;

Tracking stations with ~10 μm / 1 μrad resolution; Time-of-flight detectors with O(10 ps) resolution;

High rate detector readout fully integrated with CMS Trigger & DAQ;

Detector operation close to beam: RF impedance, LHC collimator setup due to showers originated in the detectors;

Radiation levels in detector and front-end electronics (5×10^{15} protons / cm^2 after 100 fb^{-1} in tracking detectors).

CT-PPS TECHNICAL DESIGN REPORT

CERN-LHCC-2014-021

CT-PPS Detectors

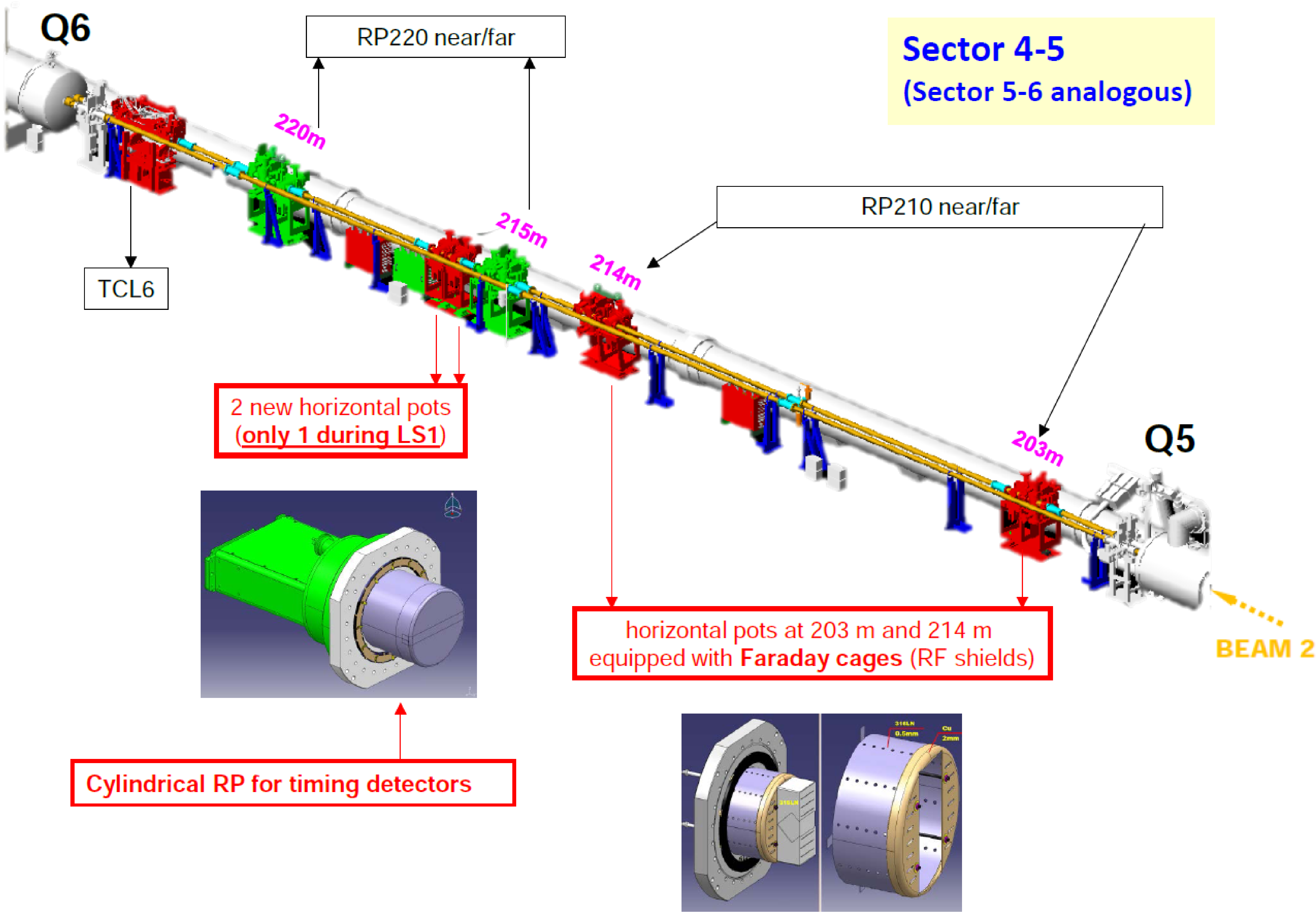

CT-PPS Detectors

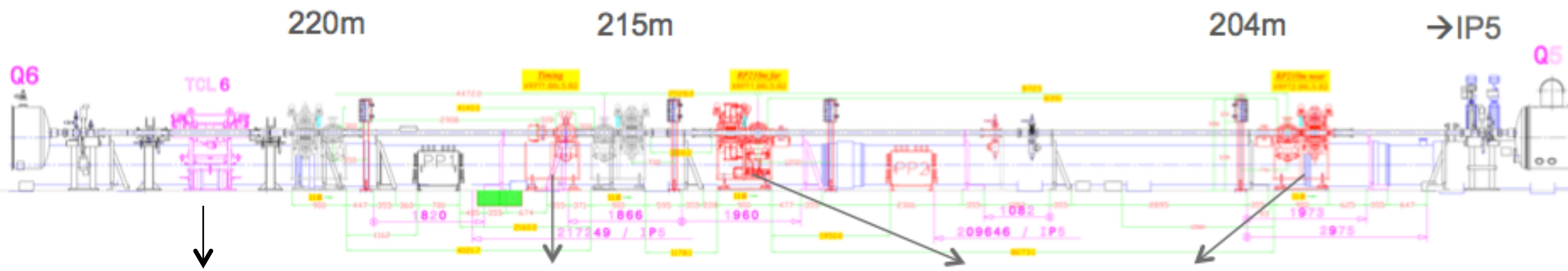

New collimator TCL6 to protect magnet Q6

2 new horizontal cylindrical RPs (1 in LS1)

2 horizontal box-shaped RPs

Timing detectors:
Measures the time-of-flight of scattered protons

Tracking detectors:
Measures the displacement of the scattered protons w.r.t. the beam

Proton reconstruction, i.e. kinematics from interaction, performed using detailed simulation of LHC magnets (optics)

Components installed in tunnel

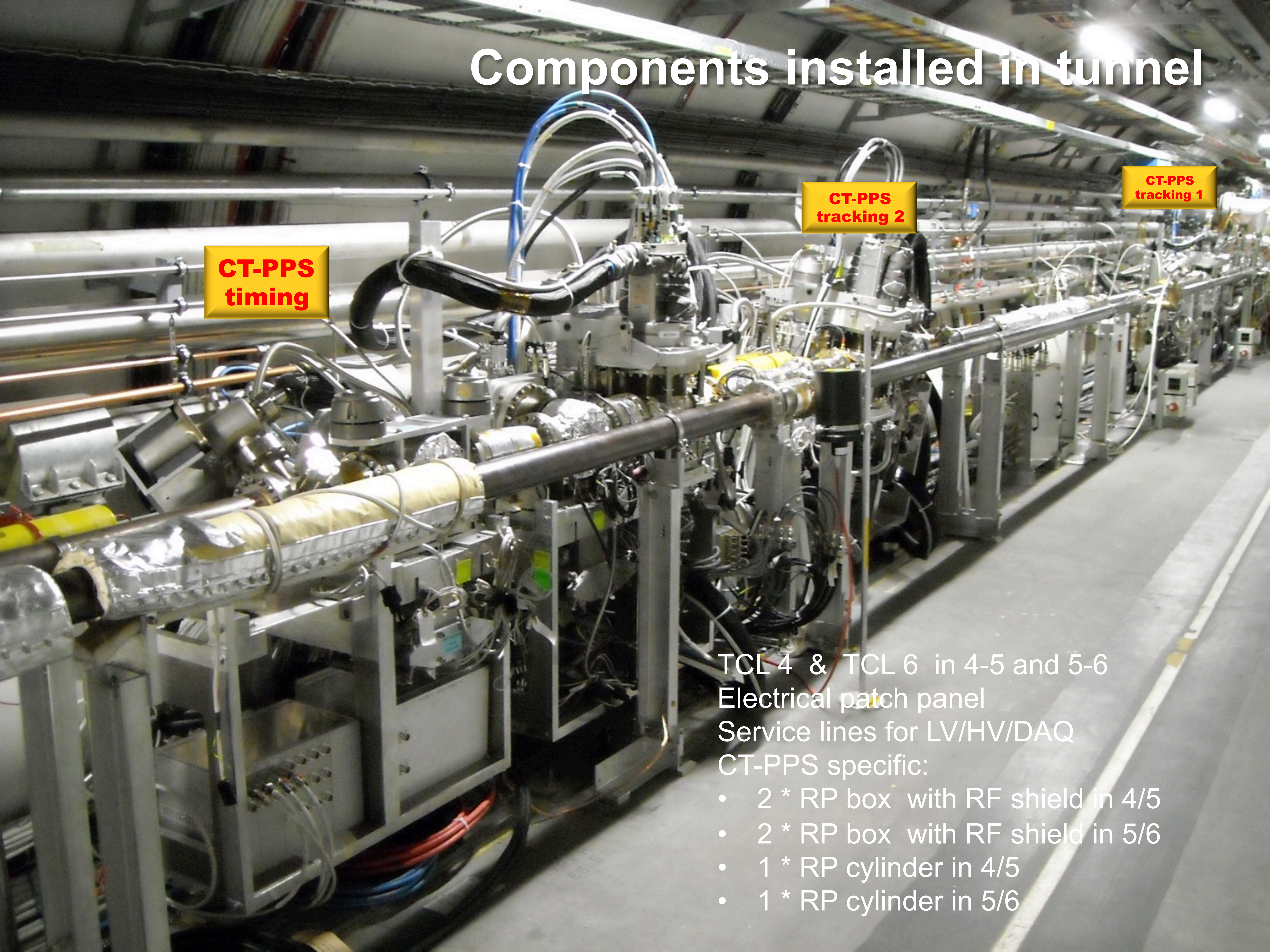

TCL 4 & TCL 6 in 4-5 and 5-6
Electrical patch panel
Service lines for LV/HV/DAQ
CT-PPS specific:

- 2 * RP box with RF shield in 4/5
- 2 * RP box with RF shield in 5/6
- 1 * RP cylinder in 4/5
- 1 * RP cylinder in 5/6

Tracking detectors

Detector Package

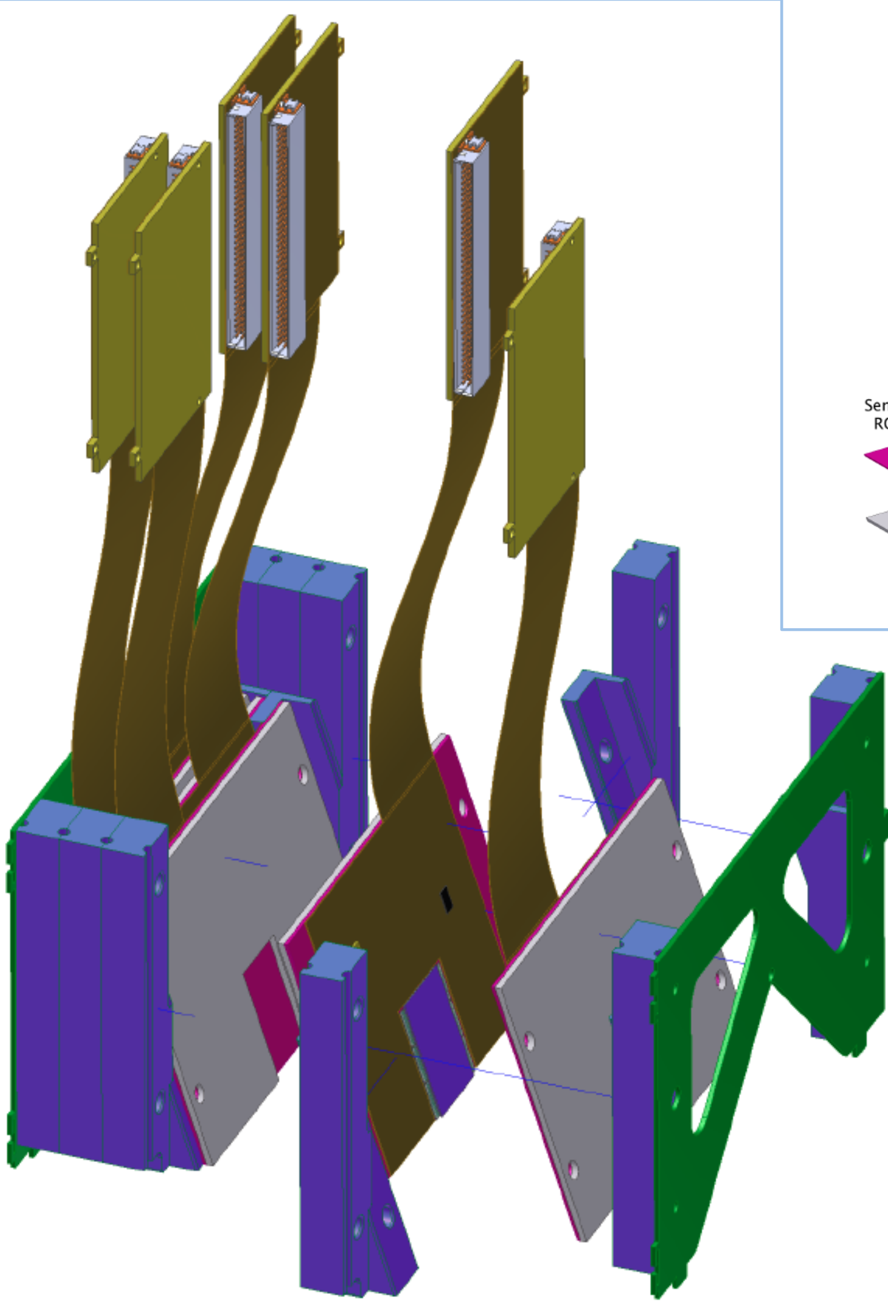

RPix Module

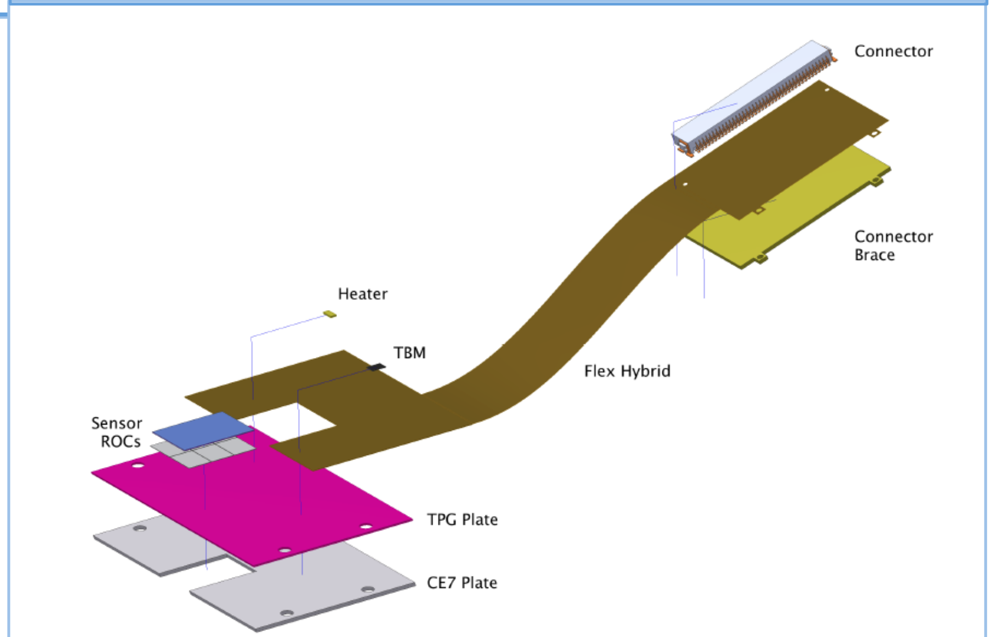

"3D" pixel sensors with columnar electrodes

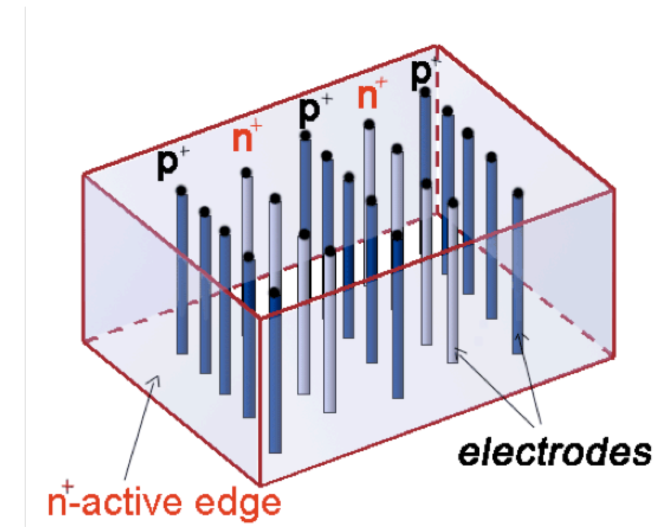

Sensors: 3D pixel (2E). Low depletion voltage, fast charge collection time, radiation hard, slim edge (200 µm);

Readout: PSI46dig readout chip (same as for CMS Pixel Upgrade);

Modules: 6 detector planes per package (1 per station). Detectors are tilted forward do optimize pixel efficiency;

DAQ: Same components (hence very similar firmware, software) as for CMS Pixel Upgrade.

Timing detectors baseline: *Quartic*

Cherenkov light emitted in quartz bar and propagated through light guide (“L-Bar”);

Quartic module has 4 x 5 grid of 3 x 3 mm^2 quartz bars. Each RP carries two modules in sequence;

Early beam test has shown timing resolution of $\sigma \sim 30$ ps, down to ~ 20 ps with measurement on two consecutive bars;

Readout with SiPM, NINO discriminator and HPTDC digitizer. Same back-end DAQ components as for tracking detectors.

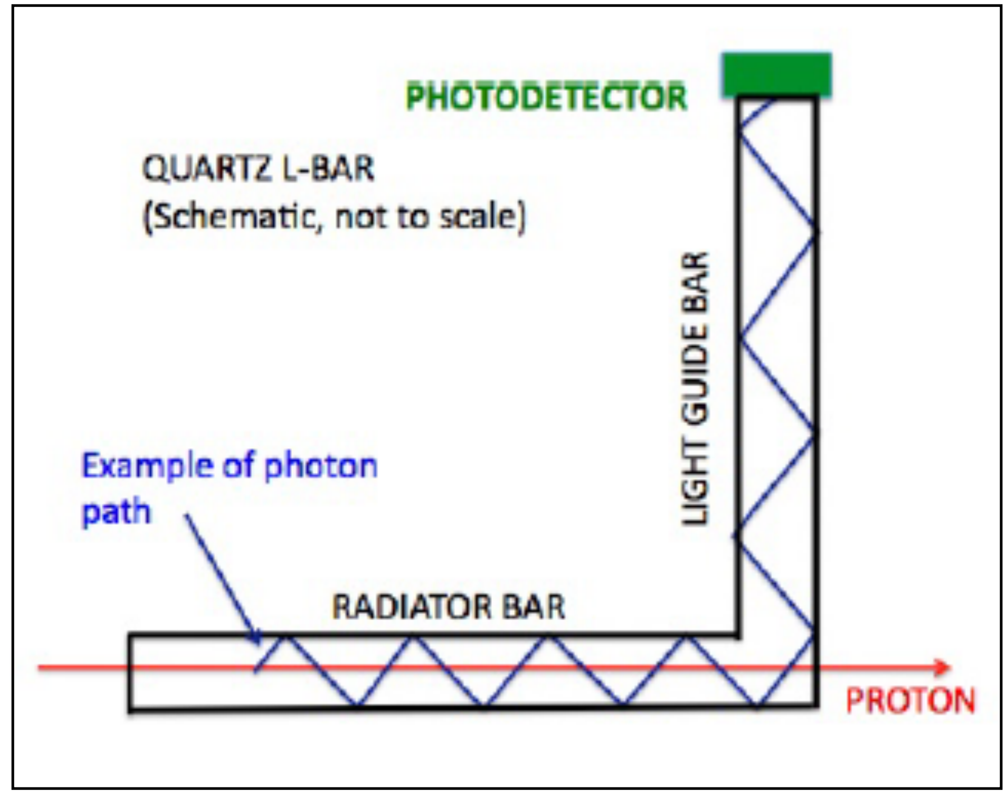

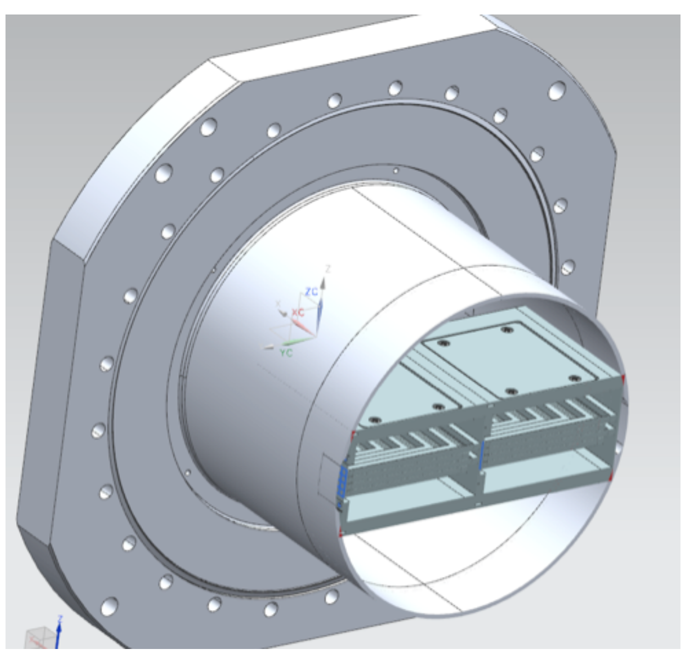

Figure 77: Assembly of two Quartic modules in Roman pot. The beam comes from the left.

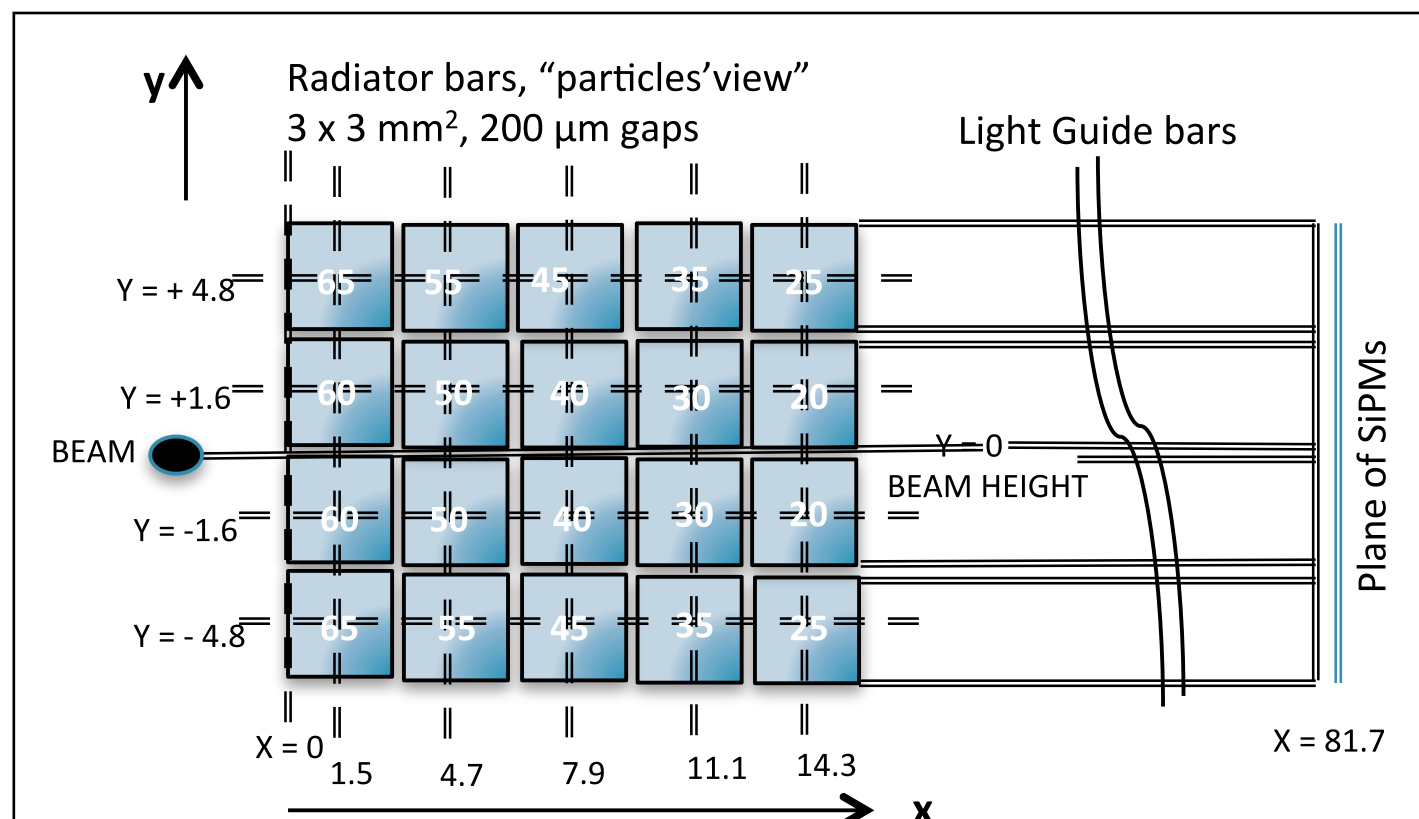

Timing detectors baseline: *Quartic*

Cherenkov light emitted in quartz bar and propagated through light guide ("L-Bar");

Quartic module has 4 x 5 grid of 3 x 3 mm^2 quartz bars. Each RP carries two modules in sequence;

Early beam test has shown timing resolution of σ ~ 30 ps, down to ~ 20 ps with measurement on two consecutive bars;

Readout with SiPM, NINO discriminator and HPTDC digitizer. Same back-end DAQ components as for tracking detectors.

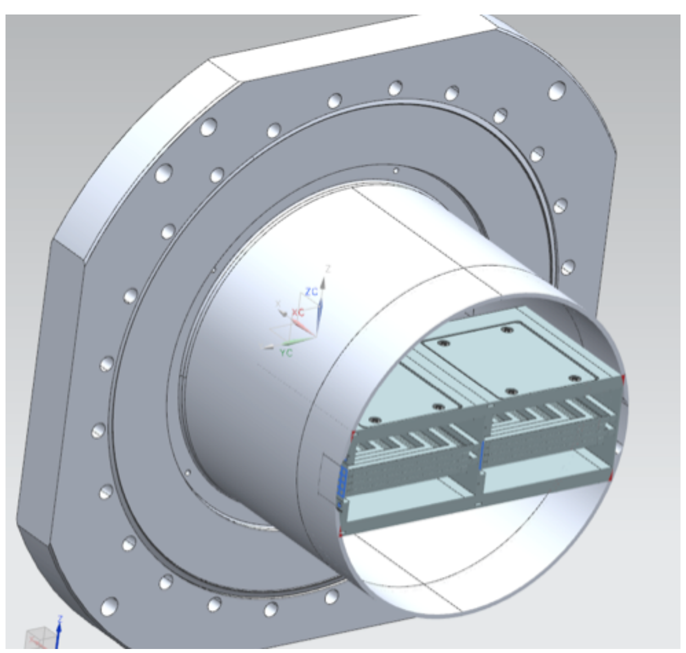

Figure 77: Assembly of two Quartic modules in Roman pot. The beam comes from the left.

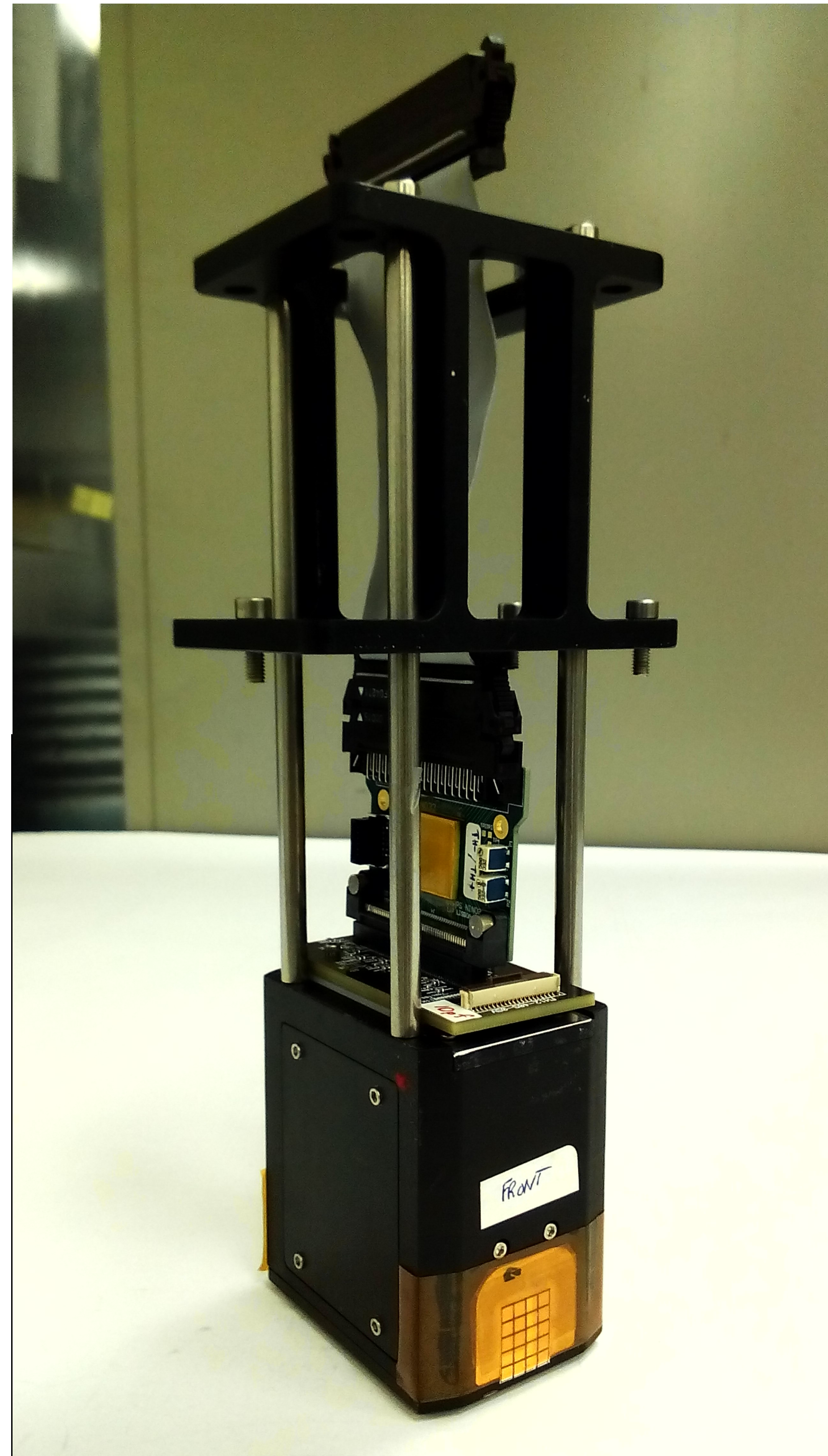

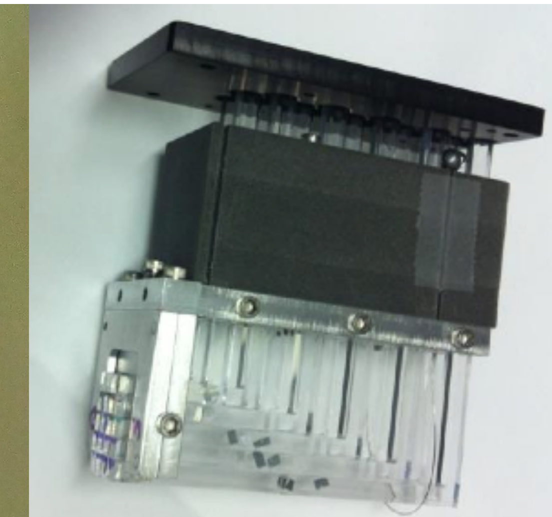

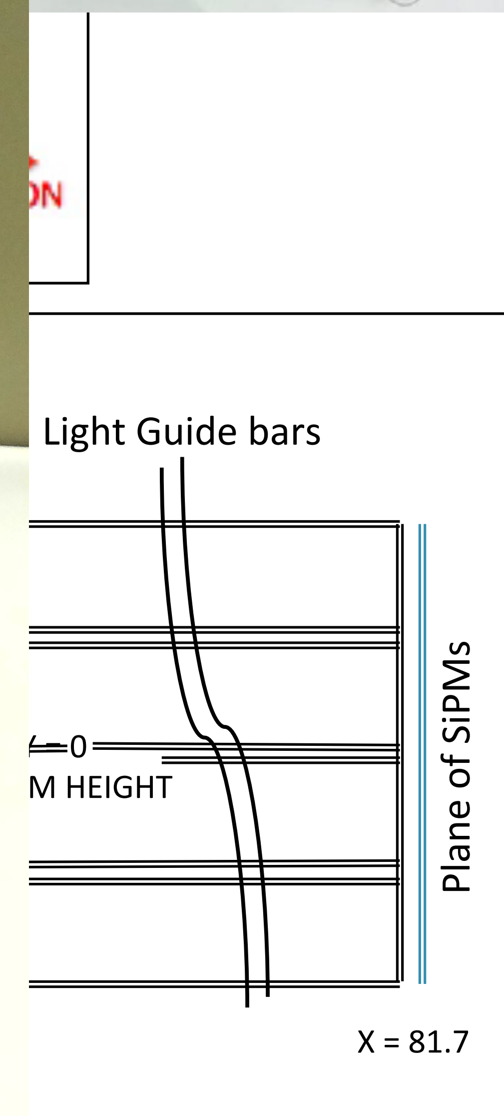

Timing detectors baseline: *Quartic*

Cherenkov light emitted in quartz bar and propagated through light guide ("L-Bar");

Quartic module has 4 x 5 grid of 3 x 3 mm^2 quartz bars. Each RP carries two modules in sequence;

Early beam test has shown timing resolution of $\sigma \sim 30$ ps, down to ~ 20 ps with measurement on two consecutive bars;

Readout with SiPM, NINO discriminator and HPTDC digitizer. Same back-end DAQ components as for tracking detectors.

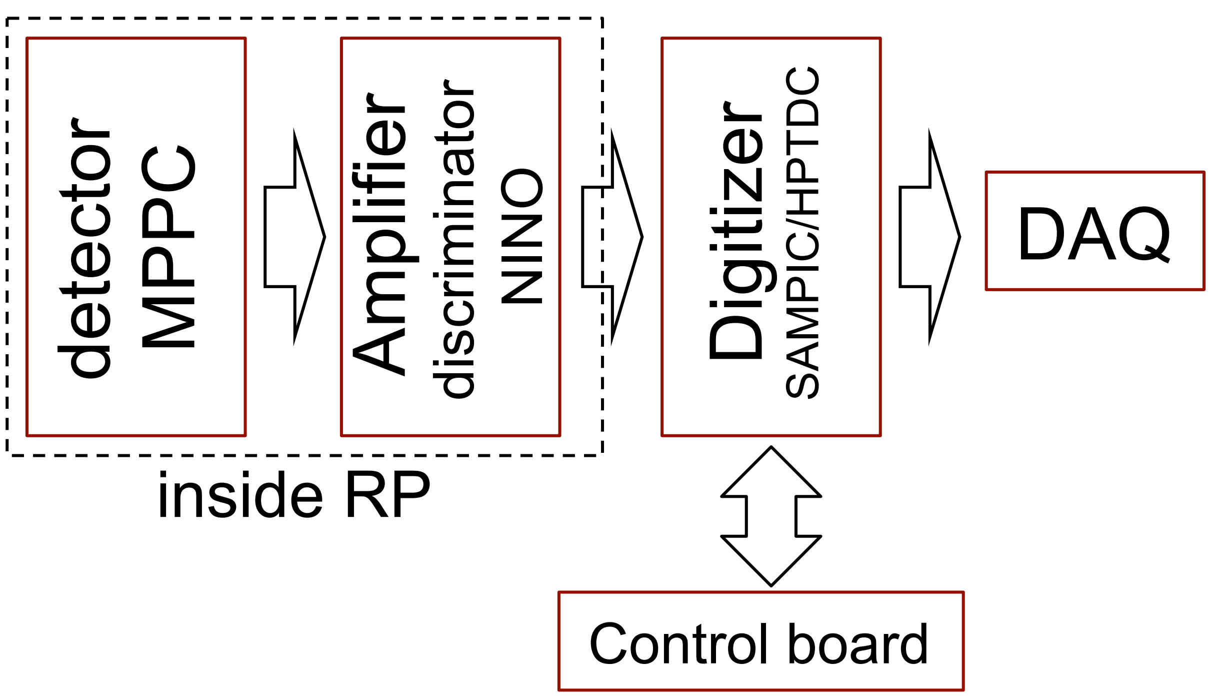

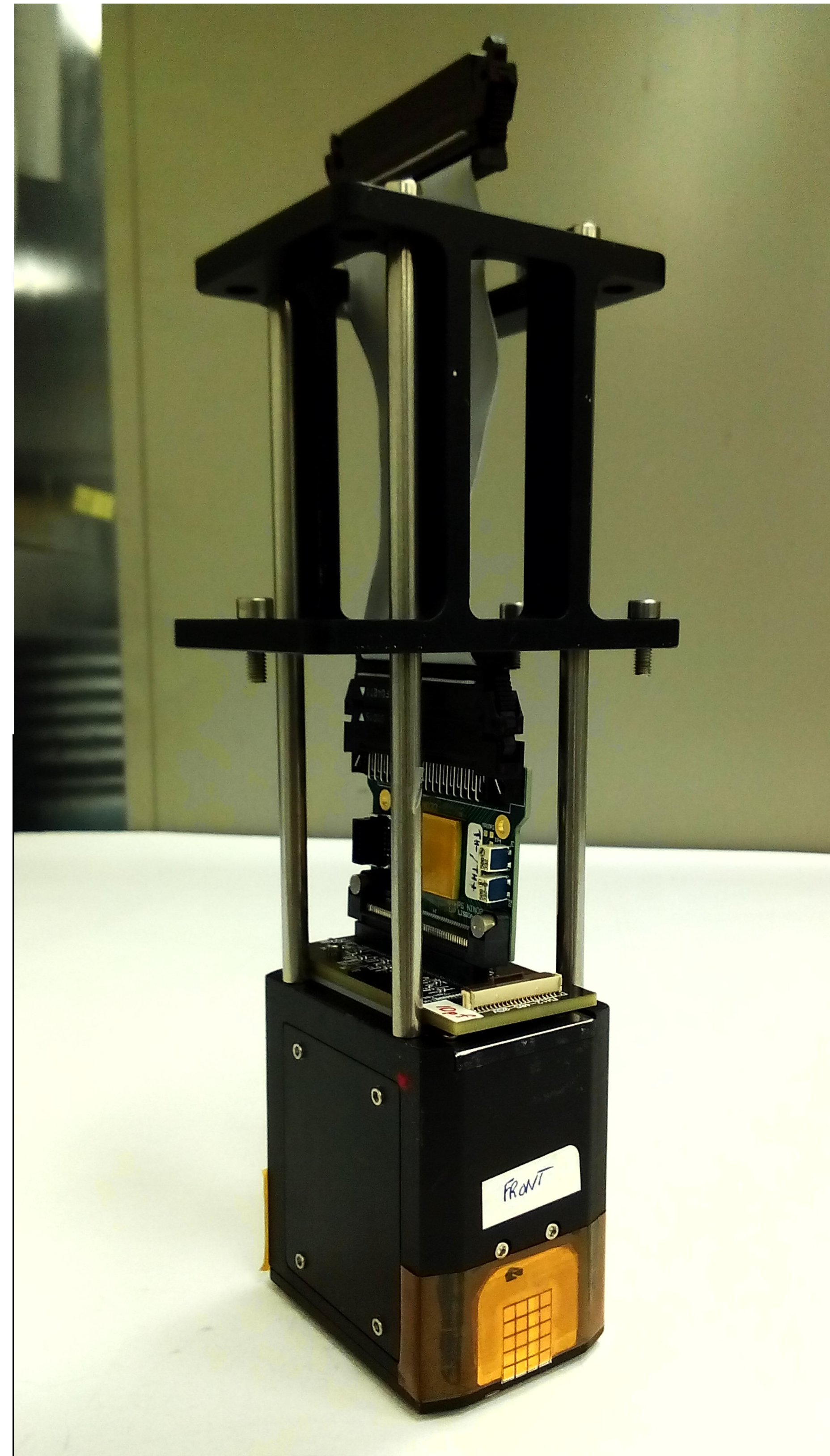

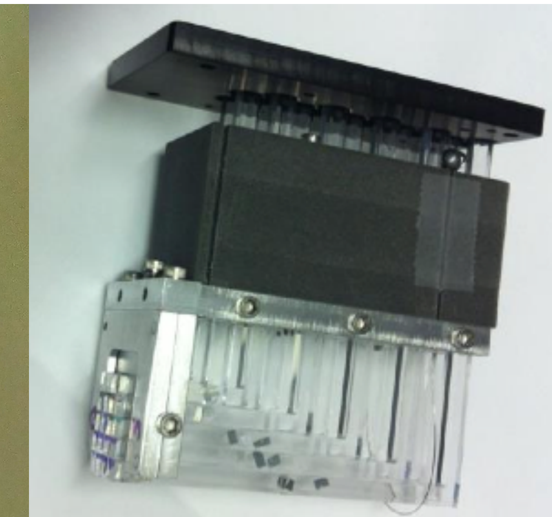

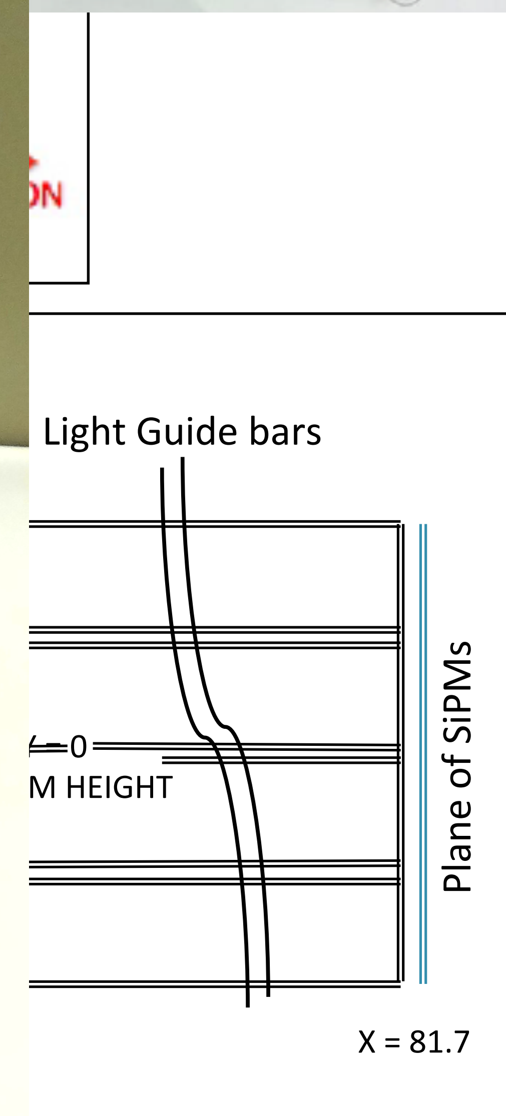

Timing detectors baseline: *Quartic*

Cherenkov light emitted in quartz bar and propagated through light guide (“L-Bar”);

Quartic module has 4 x 5 grid of 3 x 3 mm^2 quartz bars. Each RP carries two modules in sequence;

Early beam test has shown timing resolution of $\sigma \sim 30$ ps, down to ~ 20 ps with measurement on two consecutive bars;

Readout with SiPM, NINO discriminator and HPTDC digitizer. Same back-end DAQ

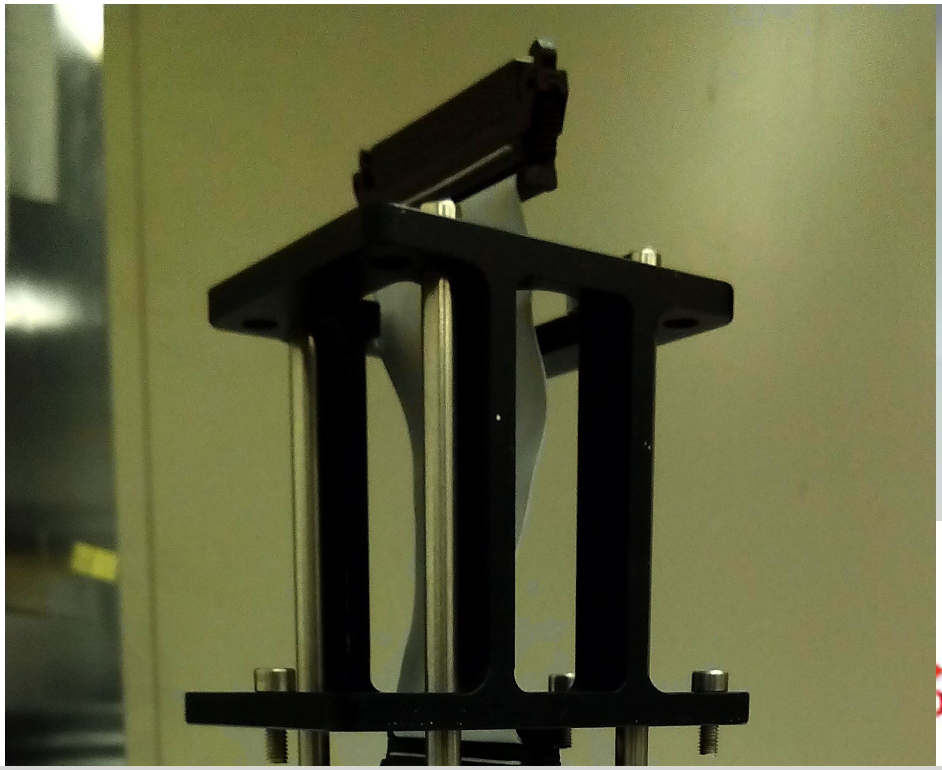

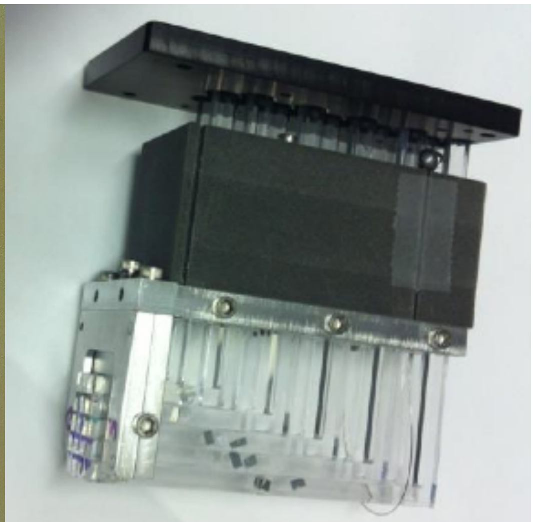

Timing R&D on progress based on solid state technologies: Diamond & silicon detectors.

Possibility for finer segmentation and hence lower occupancy.

Thin and light detectors: reduces nuclear interactions and allow for a larger number of layers (which enhances timing resolution).

Diamond detectors: With 500 µm thick sensors, 5 mm^2 pads, $\sigma_t \sim 80$ ps per plane, better than 50 ps with a package of 4 planes (TOTEM group).

Ultra Fast Silicon Detectors: Expect $\sigma_t \sim 40$ ps per plane with 50 µm thick silicon. Recent beam test results achieve ~115 ps with 300 µm thickness (N. Cartiglia et al, 2015).

Sensor geometry and readout for CT-PPS under development.

Detector acceptance

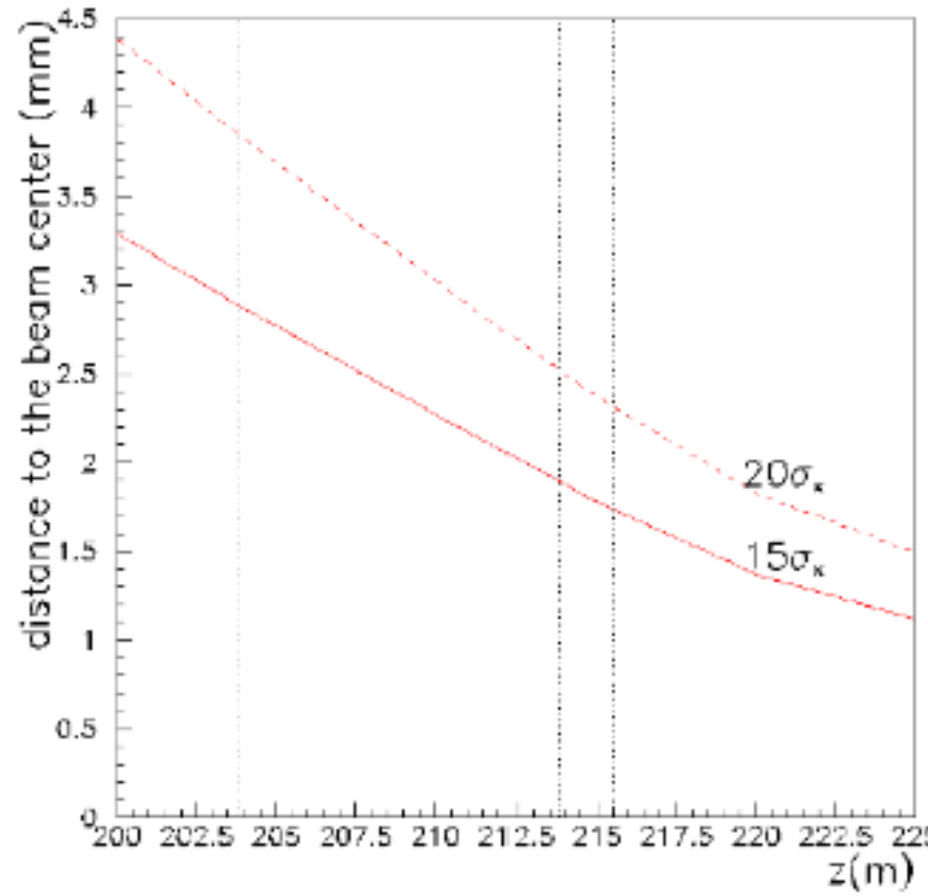

Acceptance region of a scattered proton in a detector plane;

Calculated using a fast simulation of the particle transport in the beamline (HECTOR);

Flat distribution of particles in (ξ,t,ϕ) corresponding to √s = 13 TeV;

Ellipses at constant (ξ,t) and corresponding X-Y detector positions.

z=204m (X as of CMS)

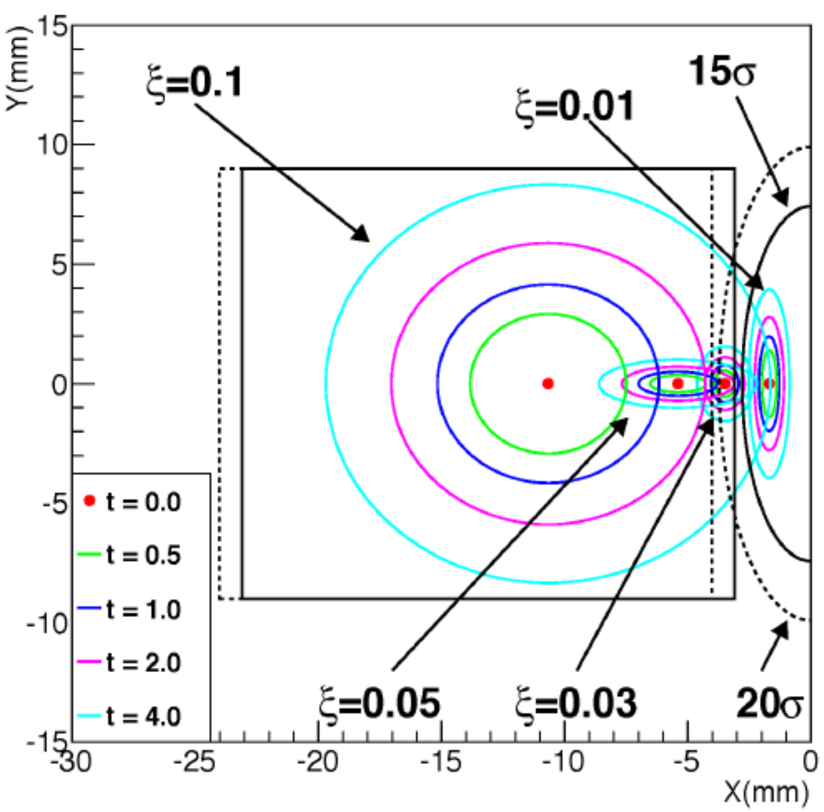

z=215m (X as of CMS)

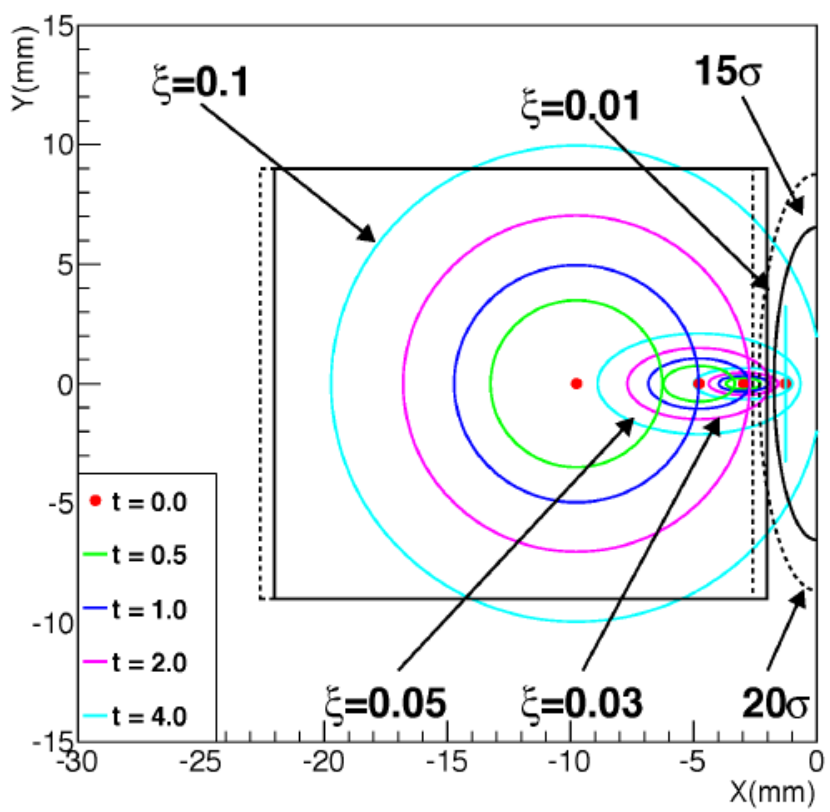

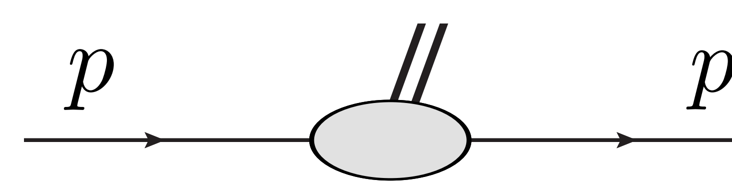

$$\xi = 1 - \frac{p'_z}{p}$$

$$t = (p' - p)^2$$

Physics performance: Central Exclusive Production

Central Exclusive Production as main Physics motivation:

i) photon-photon fusion

ii) gluon-gluon fusion in colour-singlet, $J^{PC} = 0^{++}$, state

High-p_T system X detected by the CMS detectors at central pseudorapidity with high-energy, very low angle scattered protons detected by CT-PPS;

The two outgoing protons must balance perfectly the system X momentum, hence creating strong kinematical constraints;

Its mass M_X is obtained from the momentum loss of the two protons, allowing to study invisible final states with difficult reconstruction in CMS;

The Physics potential includes the study of gauge boson production by photon-photon fusion and anomalous $\gamma\gamma WW$, $\gamma\gamma ZZ$ and $\gamma\gamma\gamma\gamma$ couplings, search for new BSM resonances and the study of QCD in a new domain.

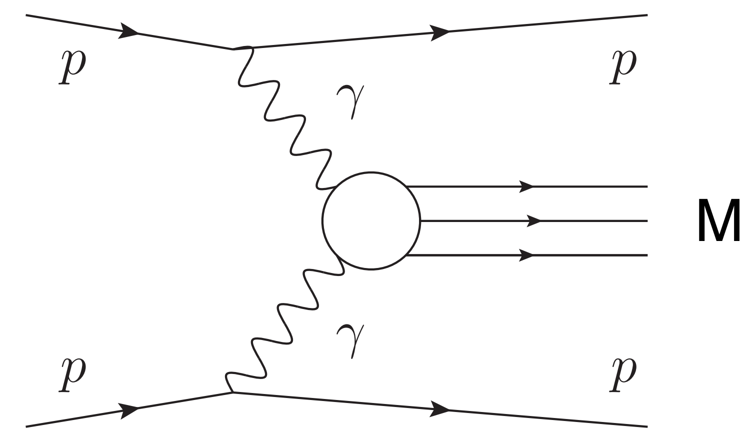

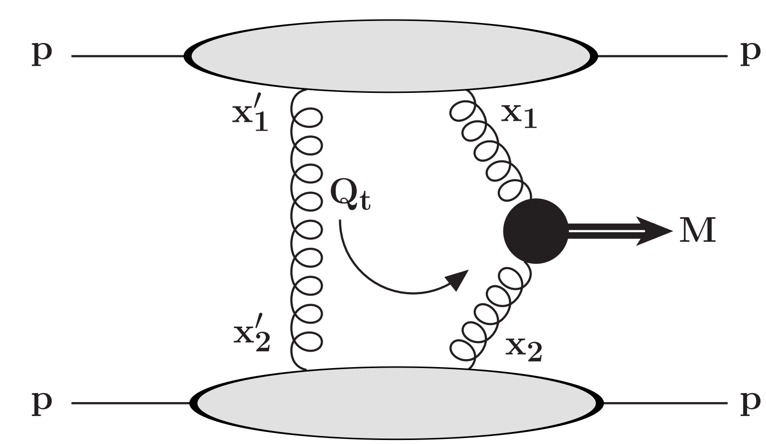

Physics performance: Central Exclusive Production

Central Exclusive Production as main Physics motivation:

i) photon-photon fusion

ii) gluon-gluon fusion in colour-singlet, $J^{PC} = 0^{++}$, state

High-p_T system X detected by the CMS detectors at central pseudorapidity with high-energy, very low angle scattered protons detected by CT-PPS;

The two outgoing protons must balance perfectly the system X momentum, hence creating strong kinematical constraints;

Its mass M_X is obtained from the momentum loss of the two protons, allowing to study invisible final states with difficult reconstruction in CMS;

The Physics potential includes the study of gauge boson production by photon-photon fusion and anomalous $\gamma\gamma WW$, $\gamma\gamma ZZ$ and $\gamma\gamma\gamma\gamma$ couplings, search for new BSM resonances and the study of QCD in a new domain.

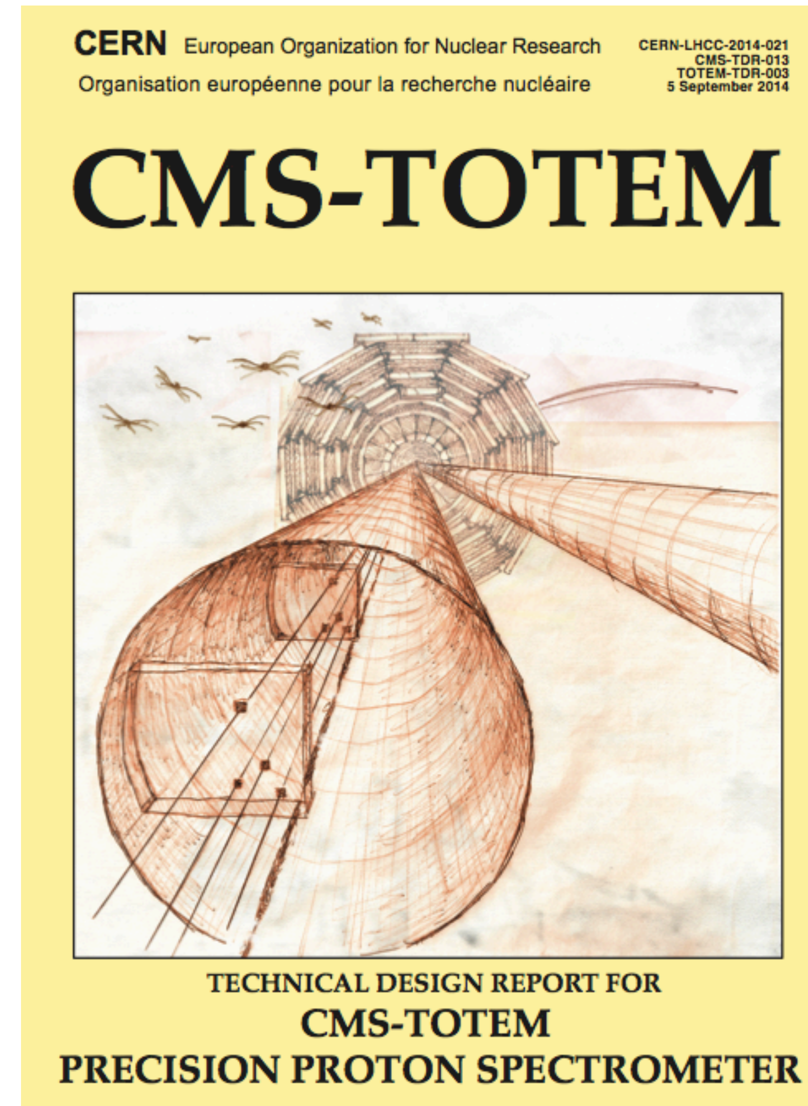

Full simulation studies carried out for two benchmark channels: Exclusive WW production and Exclusive dijet production.

Anomalous quartic couplings

Effective Lagrangian with quartic anomalous operators γγWW and γγZZ:

$$\mathcal{L}_6^0 = \frac{-e^2}{8}\frac{a_0^W}{\Lambda^2}F_{\mu\nu}F^{\mu\nu}W^{+\alpha}W^-_\alpha - \frac{e^2}{16\cos^2\theta_W}\frac{a_0^Z}{\Lambda^2}F_{\mu\nu}F^{\mu\nu}Z^\alpha Z_\alpha$$

$$\mathcal{L}_6^C = \frac{-e^2}{16}\frac{a_C^W}{\Lambda^2}F_{\mu\alpha}F^{\mu\beta}(W^{+\alpha}W^-_\beta + W^{-\alpha}W^+_\beta) - \frac{e^2}{16\cos^2\theta_W}\frac{a_C^Z}{\Lambda^2}F_{\mu\alpha}F^{\mu\beta}Z^\alpha Z_\beta$$

Ansatz coupling form factors introduced to avoid violating unitarity at high energies:

$$a \rightarrow \frac{a}{(1 + W_{\gamma\gamma}^2/\Lambda^2)^n}$$

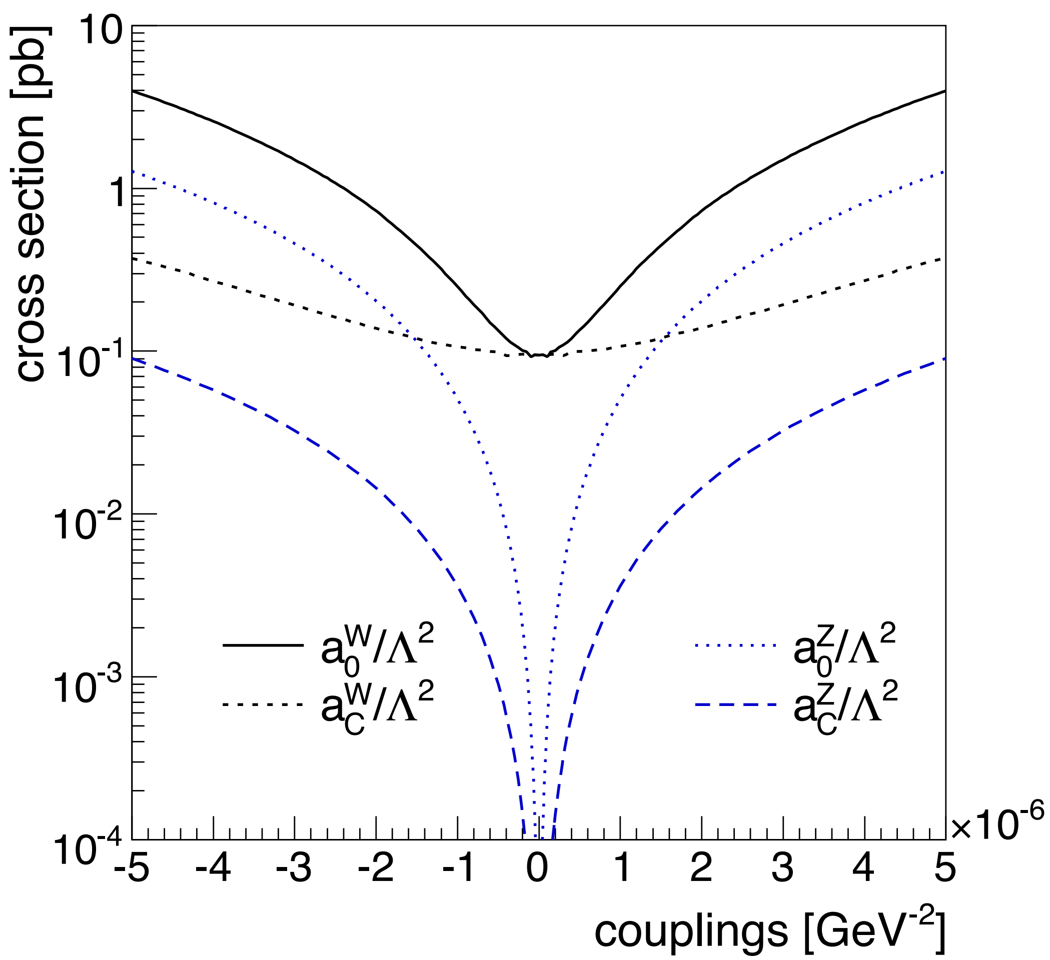

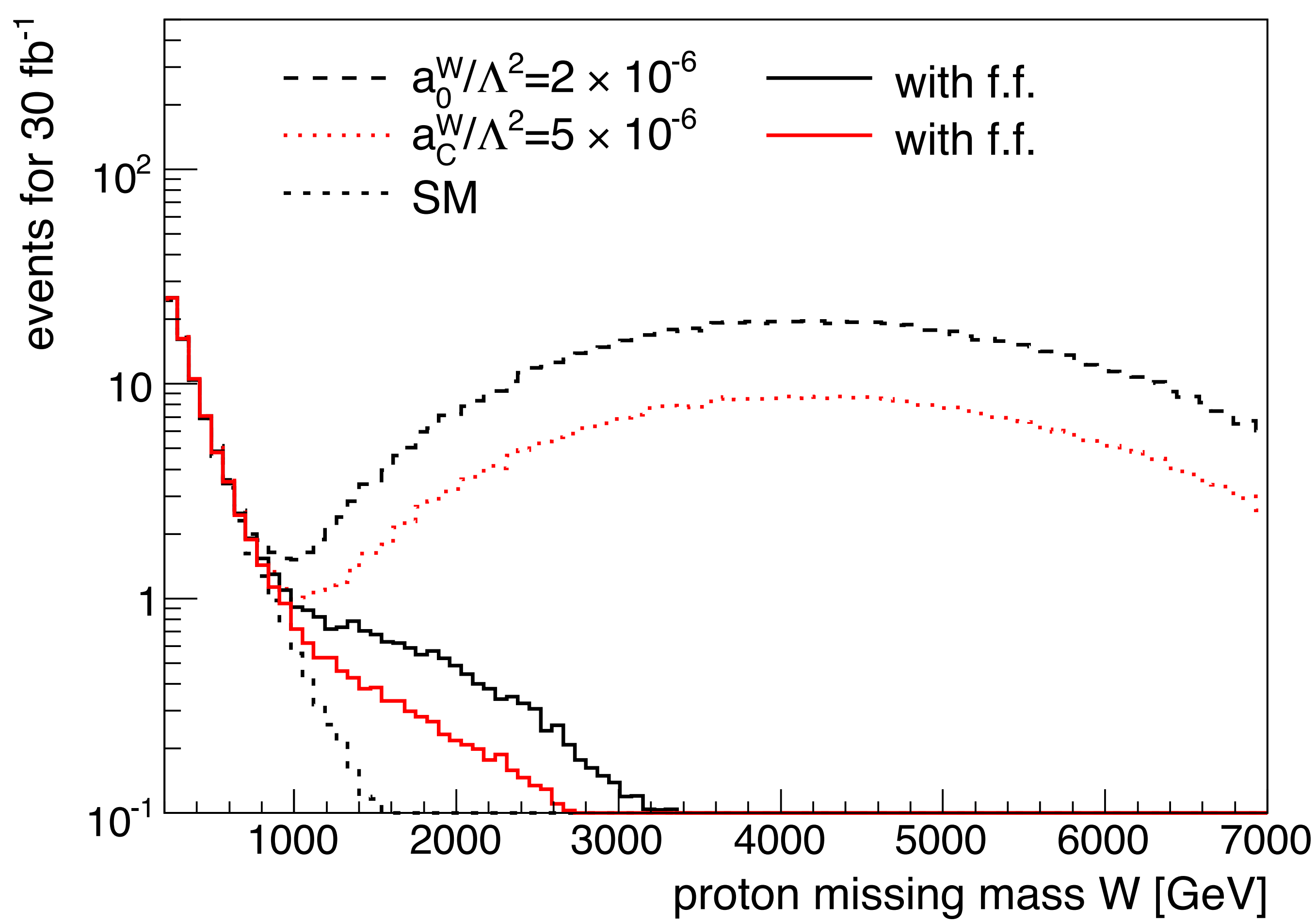

E. Chapon, C. Royon, O. Kepka (2009)

Acceptance & Mass resolution

Acceptance and resolution vs the central system mass (M_X) for two benchmark channels: exclusive dijet production and exclusive WW production;

Lower limit at $M_X \sim 300$ GeV;

Acceptance larger as the detectors are placed closer to the beam: at 15σ a factor two larger than that at 20σ for lower mass values;

Mass resolution around 1.5% at 500 GeV and below 1% for values greater than ~ 900 GeV.

Central system mass M_X calculated from the reconstructed proton kinematics

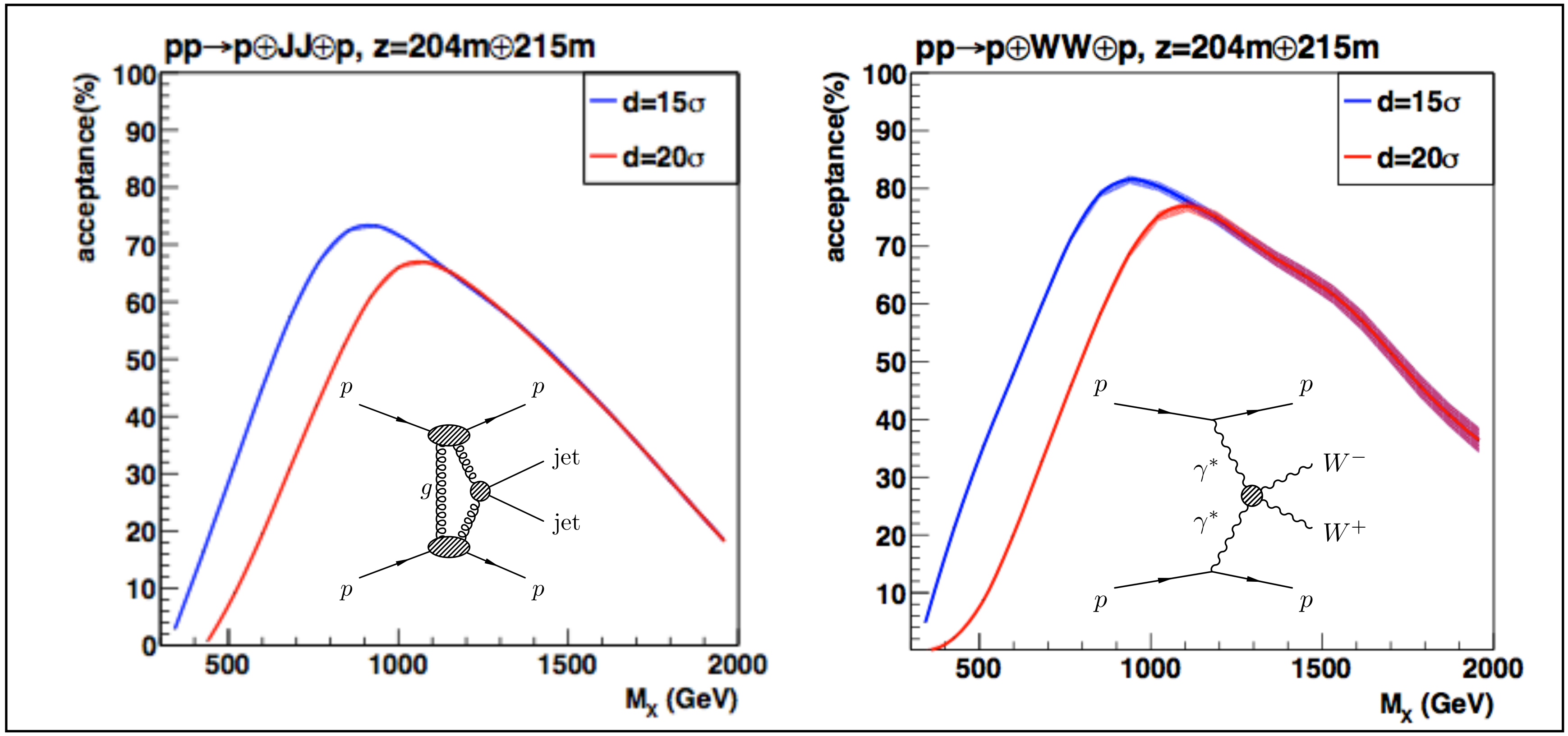

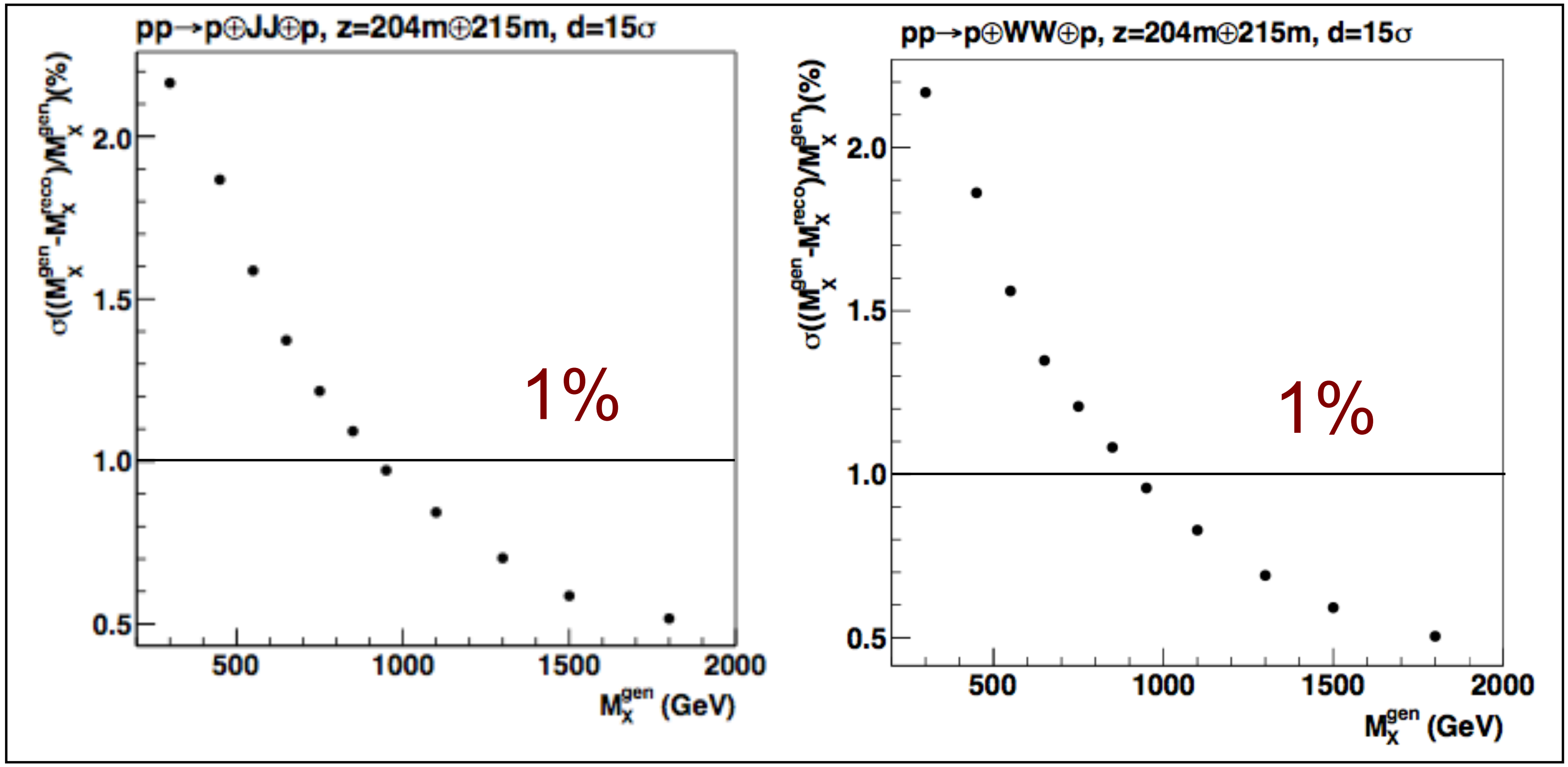

Pile-up background

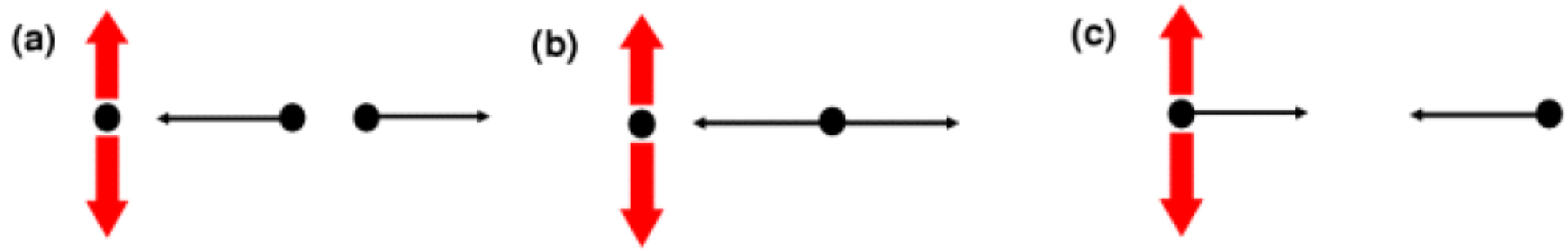

Fig. 114: A schematic diagram of overlap backgrounds to central exclusive production: (a) [p][X][p]: three interactions, one with a central system, and two with opposite direction single diffractive protons (b) [pp][X]: two interactions, one with a central system, and the second with two opposite direction protons (c) [p][pX]: two interactions, one with a central system and a proton, the second with a proton in the opposite direction.

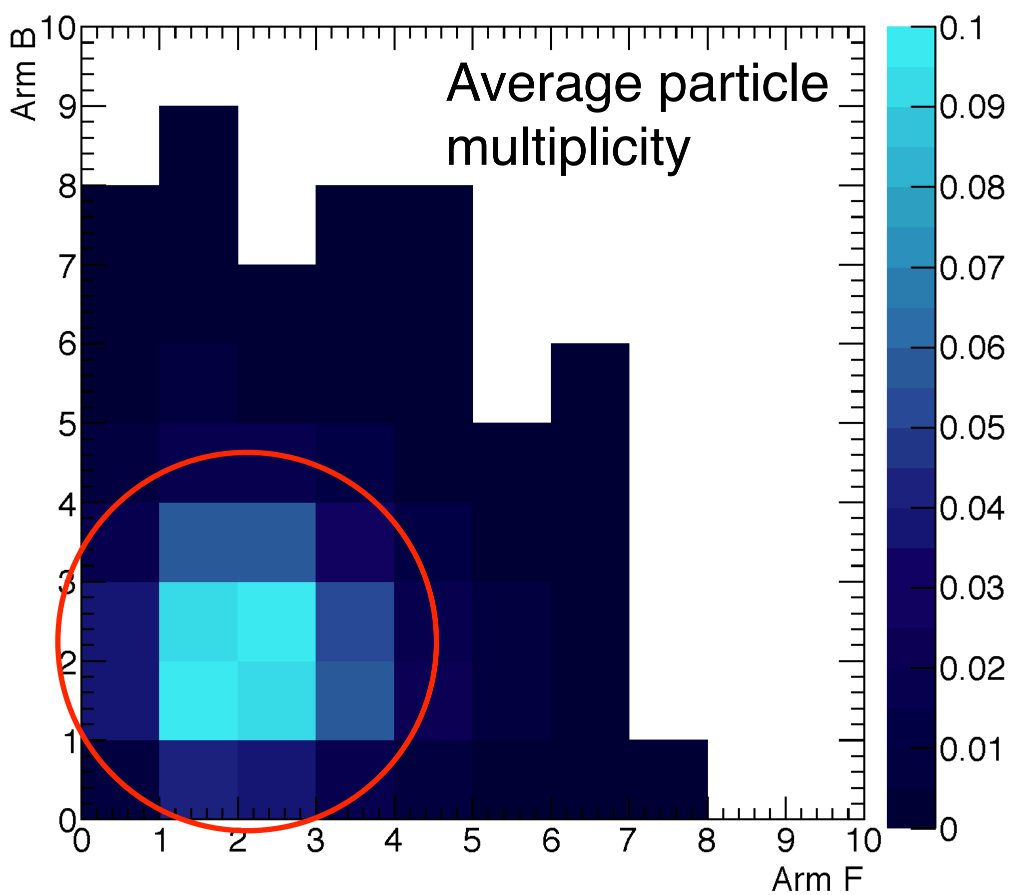

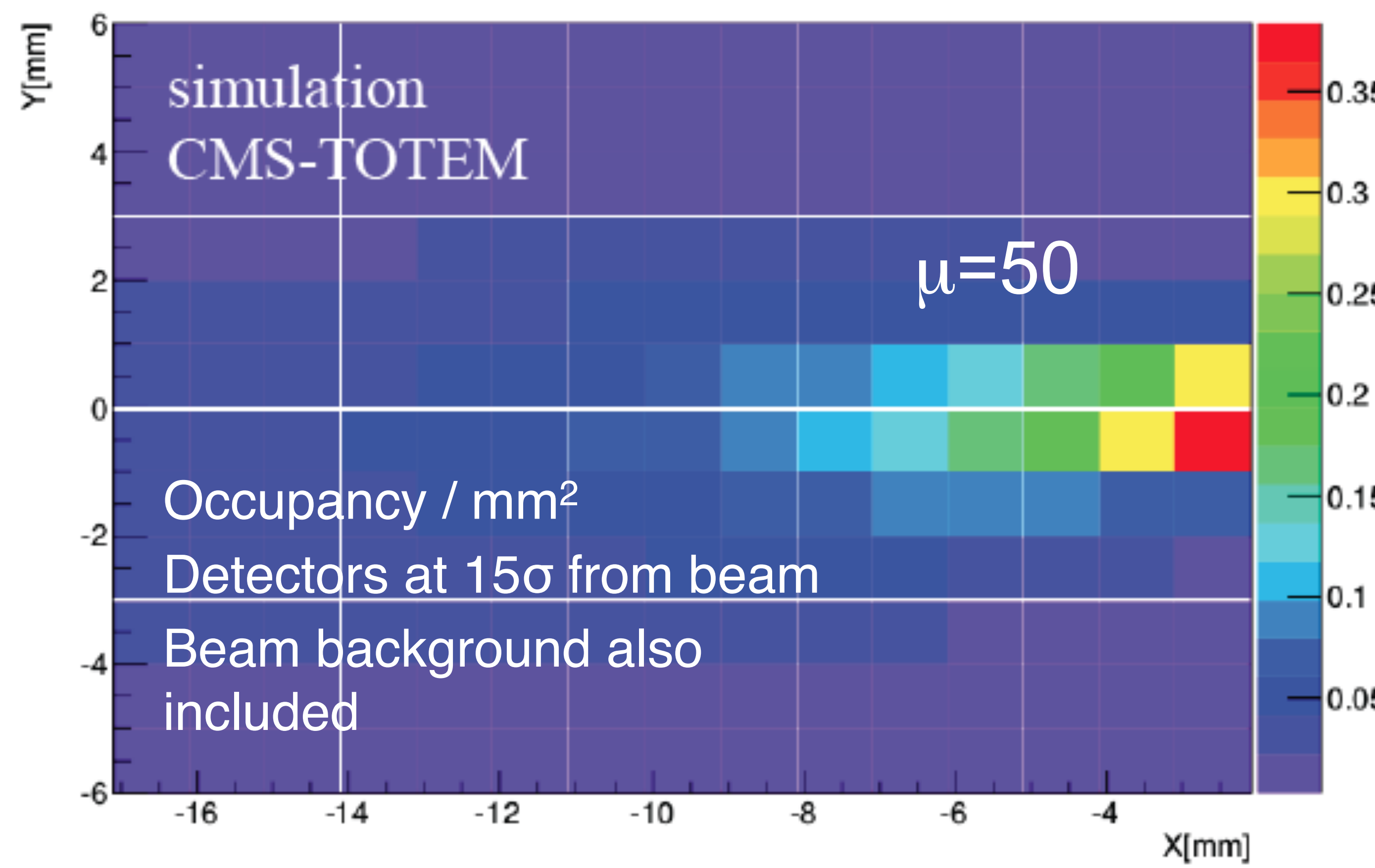

Pile-up background rejection: Timing

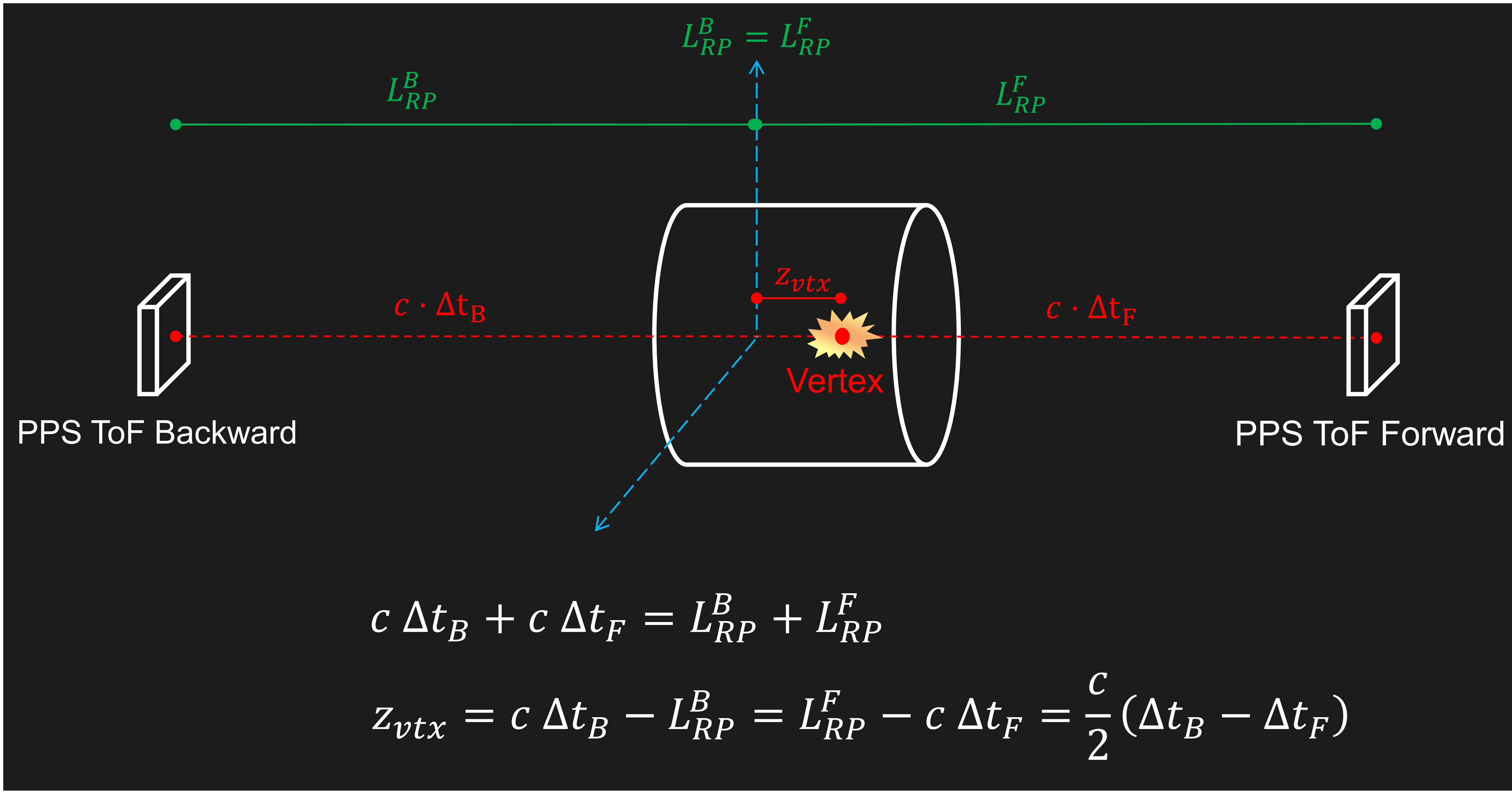

D. Di Croce, 2015

Pile-up background rejection: Timing

$$\sigma_{z_{vtx}} = \frac{c}{2}\sqrt{2\sigma_{\Delta t}^2} \overset{\sigma_{\Delta t}=10\text{ps}}{\approx} 2\text{ mm}$$

$$\overset{\sigma_{\Delta t}=30\text{ps}}{\approx} 6\text{ mm}$$

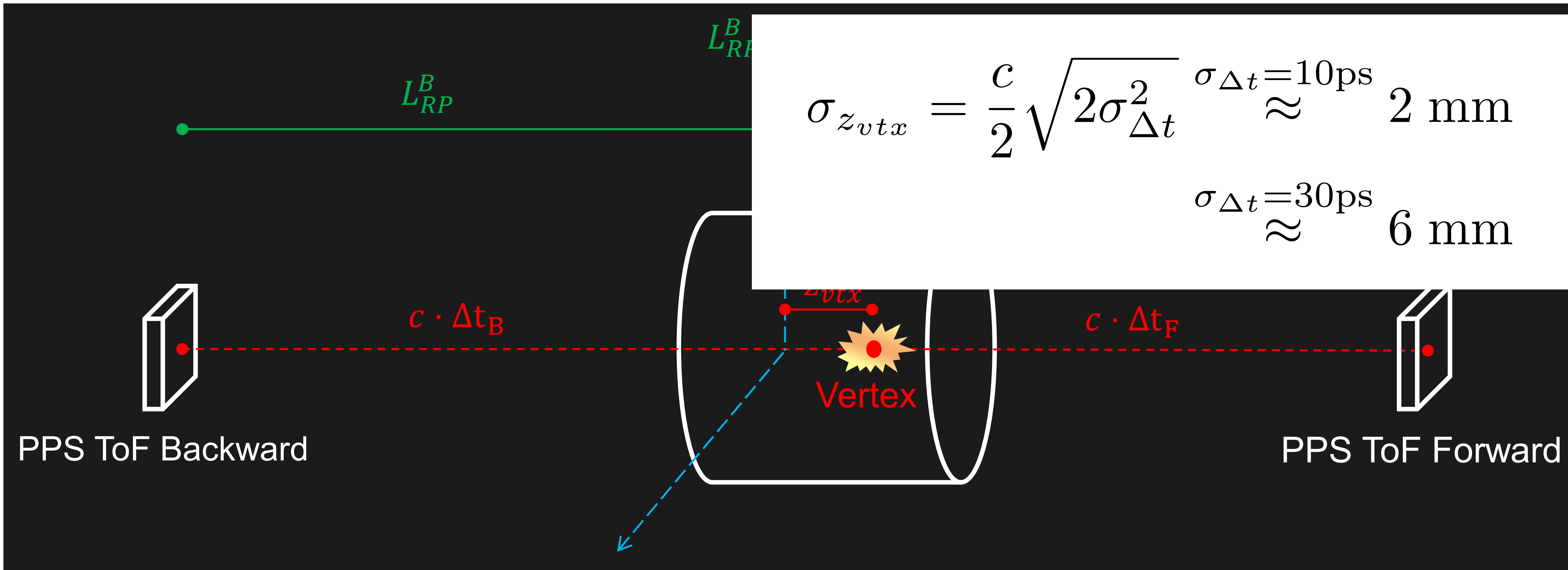

$$c\,\Delta t_B + c\,\Delta t_F = L_{RP}^B + L_{RP}^F$$

$$z_{vtx} = c\,\Delta t_B - L_{RP}^B = L_{RP}^F - c\,\Delta t_F = \frac{c}{2}(\Delta t_B - \Delta t_F)$$

D. Di Croce, 2015

Pile-up background rejection: Timing

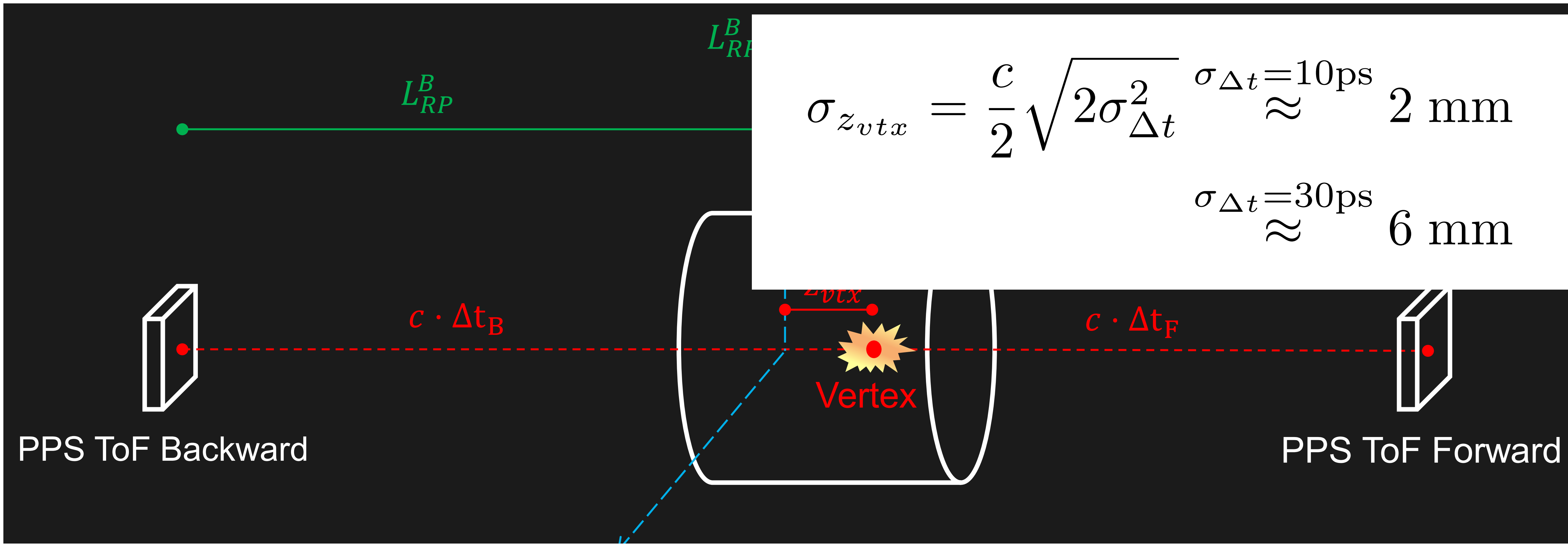

$$\sigma_{z_{vtx}} = \frac{c}{2}\sqrt{2\sigma^2_{\Delta t}} \overset{\sigma_{\Delta t}=10\text{ps}}{\approx} 2\text{ mm}$$

$$\overset{\sigma_{\Delta t}=30\text{ps}}{\approx} 6\text{ mm}$$

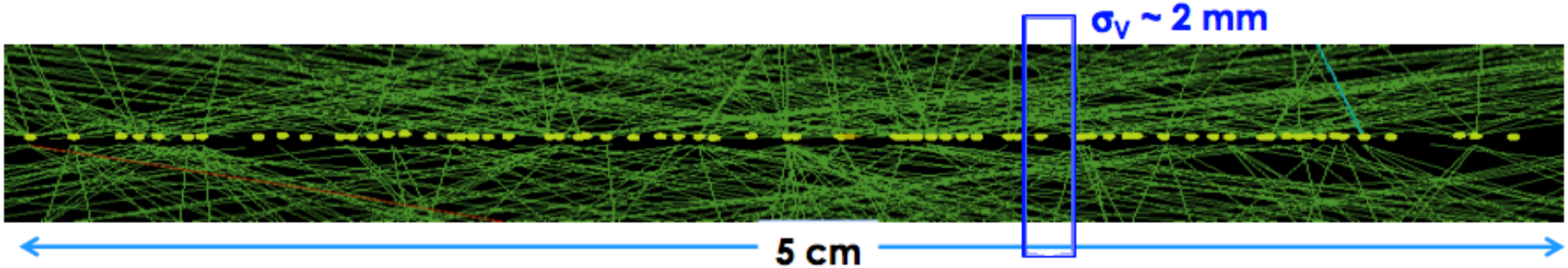

Expected performance: Exclusive WW production

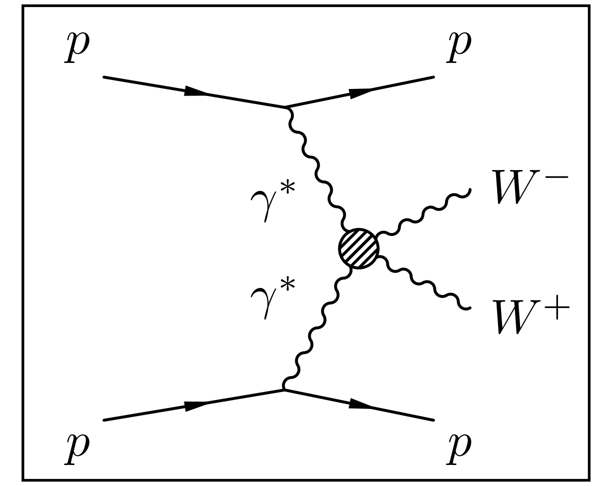

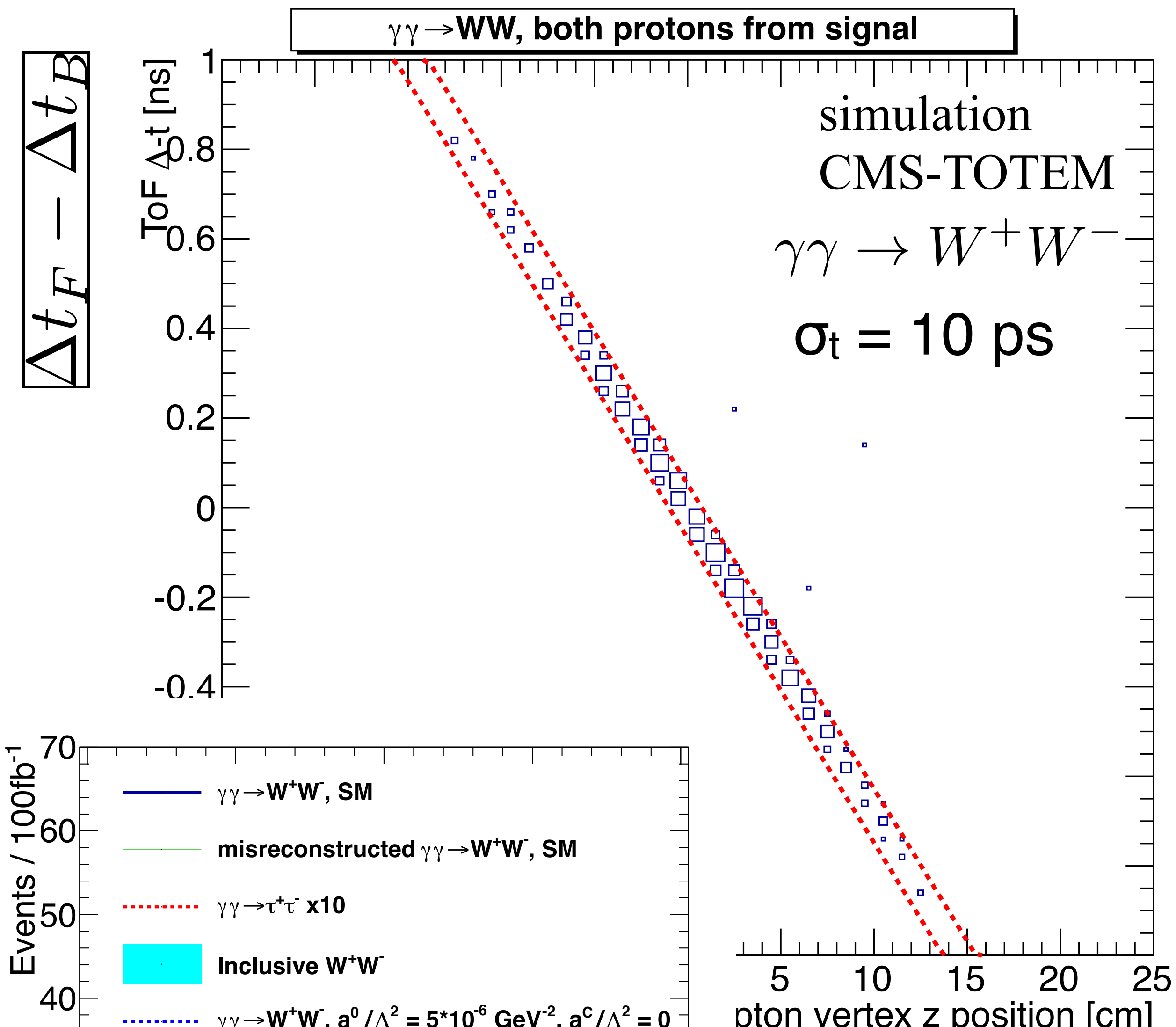

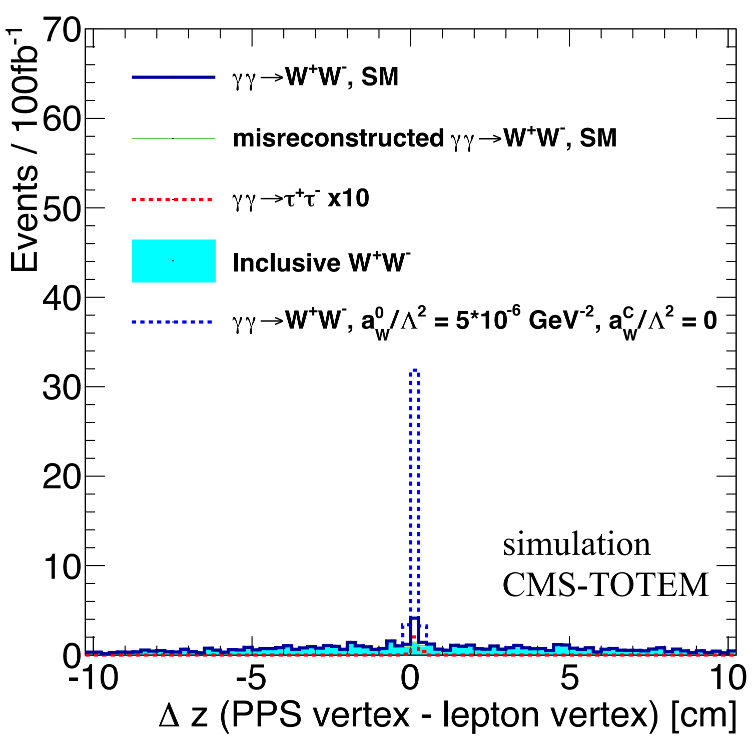

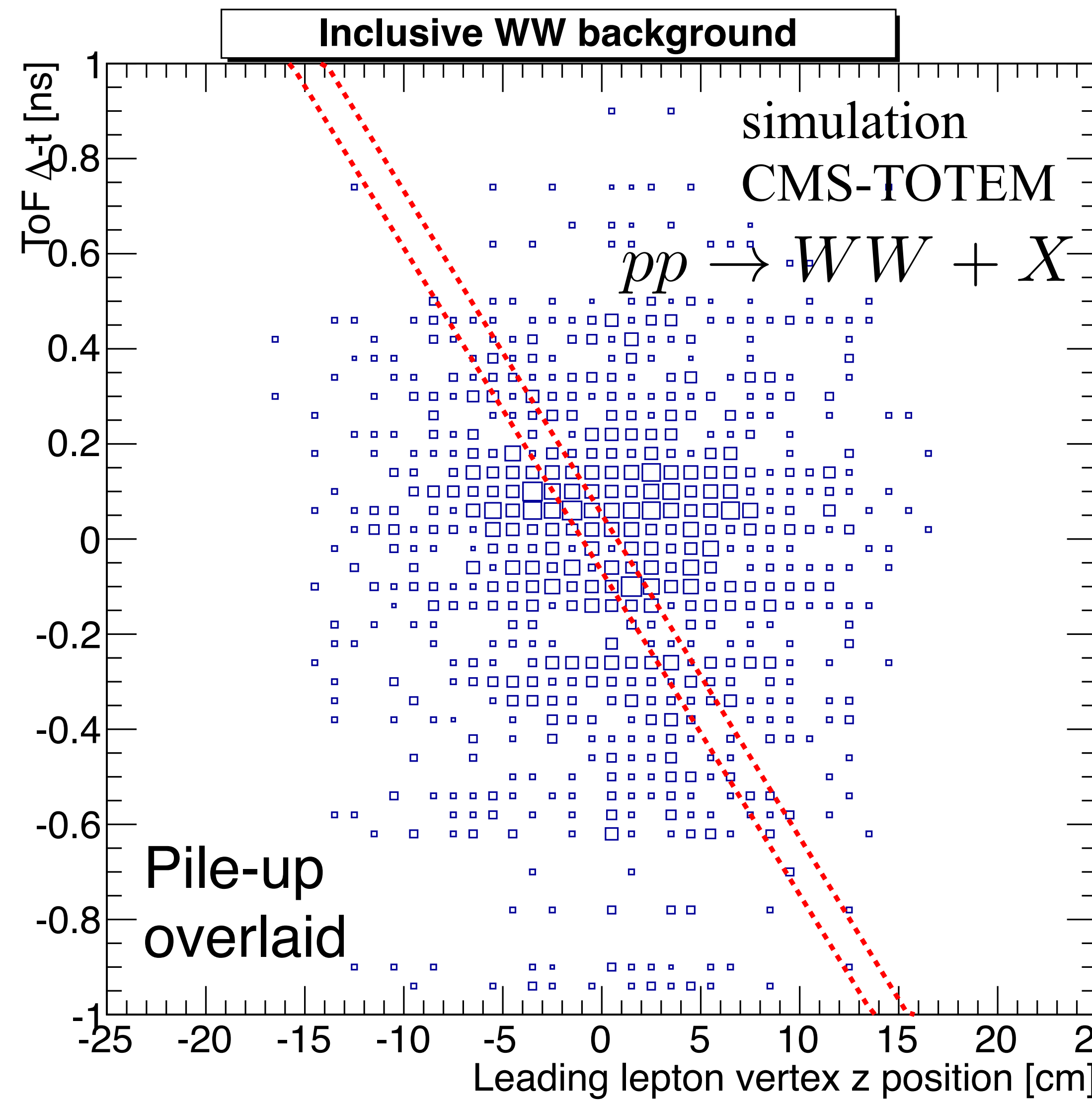

Time-of-flight difference between protons detected in stations z+ (Forward) and z- (Backward) directions;

Important to reject pile-up background mainly from inclusive WW events.

Exclusive WW production

σ_t = 10 ps (30 ps)

Selection	Cross section (fb)			
	exclusive WW	exclusive WW (incorrectly reconstructed)	inclusive WW	exclusive $\tau\tau$
generated $\sigma \times \mathcal{B}(WW \to e\mu\,\nu\bar{\nu})$	0.86±0.01	N/A	2537	1.78±0.01
$\geq$ 2 leptons ($p_T > 20$ GeV, $\eta < 2.4$)	0.47±0.01	N/A	1140±3	0.087±0.003
opposite sign leptons, "tight" ID	0.33±0.01	N/A	776±2	0.060±0.002
dilepton pair $p_T > 30$ GeV	0.25±0.01	N/A	534±2	0.018±0.001
protons in both PPS arms (ToF and TRK)	0.055 (0.054)±0.002	0.044 (0.085)±0.003	11 (22)±0.3	0.004±0.001
no overlapping hits in ToF + vertex matching	0.033 (0.030)±0.002	0.022 (0.043)±0.002	8 (16)±0.2	0.003 (0.002)±0.001
ToF difference, $\Delta t = (t_1 - t_2)$	0.033 (0.029)±0.002	0.011 (0.024)±0.001	0.9 (3.3)±0.1	0.003 (0.002)±0.001
$N_{\text{tracks}} < 10$	0.028 (0.025)±0.002	0.009 (0.020)±0.001	0.03 (0.14)±0.01	0.002±0.001

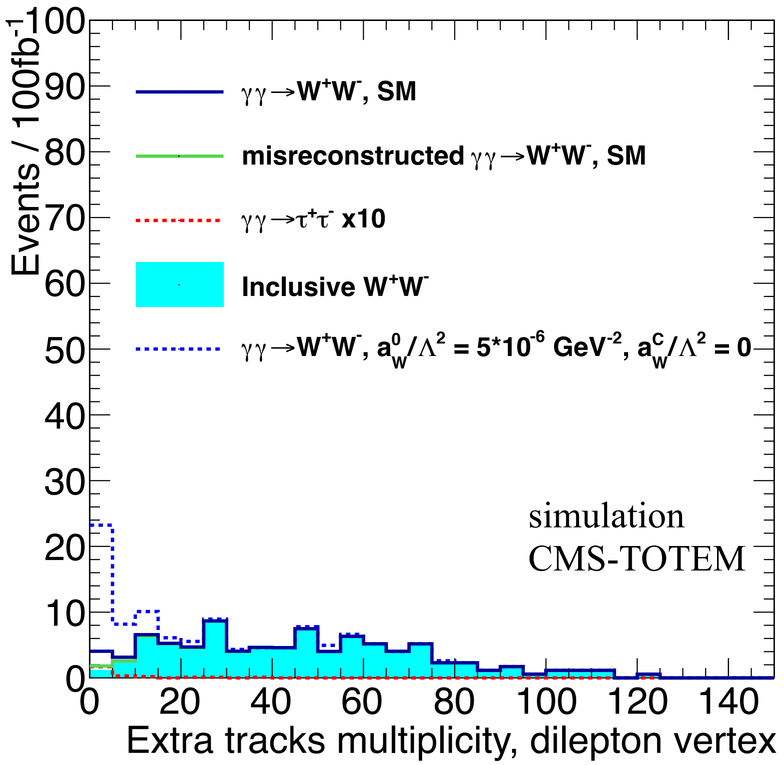

Exclusive WW production

σ_t = 10 ps (30 ps)

Selection	Cross section (fb)			
	exclusive WW	exclusive WW (incorrectly reconstructed)	inclusive WW	exclusive $\tau\tau$
generated $\sigma \times \mathcal{B}(WW \to e\mu\, \nu\bar{\nu})$	0.86±0.01	N/A	2537	1.78±0.01
$\geq$ 2 leptons ($p_T > 20$ GeV, $\eta < 2.4$)	0.47±0.01	N/A	1140±3	0.087±0.003
opposite sign leptons, "tight" ID	0.33±0.01	N/A	776±2	0.060±0.002
dilepton pair $p_T > 30$ GeV	0.25±0.01	N/A	534±2	0.018±0.001
protons in both PPS arms (ToF and TRK)	0.055 (0.054)±0.002	0.044 (0.085)±0.003	11 (22)±0.3	0.004±0.001
no overlapping hits in ToF + vertex matching	0.033 (0.030)±0.002	0.022 (0.043)±0.002	8 (16)±0.2	0.003 (0.002)±0.001
ToF difference, $\Delta t = (t_1 - t_2)$	0.033 (0.029)±0.002	0.011 (0.024)±0.001	0.9 (3.3)±0.1	0.003 (0.002)±0.001
$N_{\text{tracks}} < 10$	0.028 (0.025)±0.002	0.009 (0.020)±0.001	0.03 (0.14)±0.01	0.002±0.001

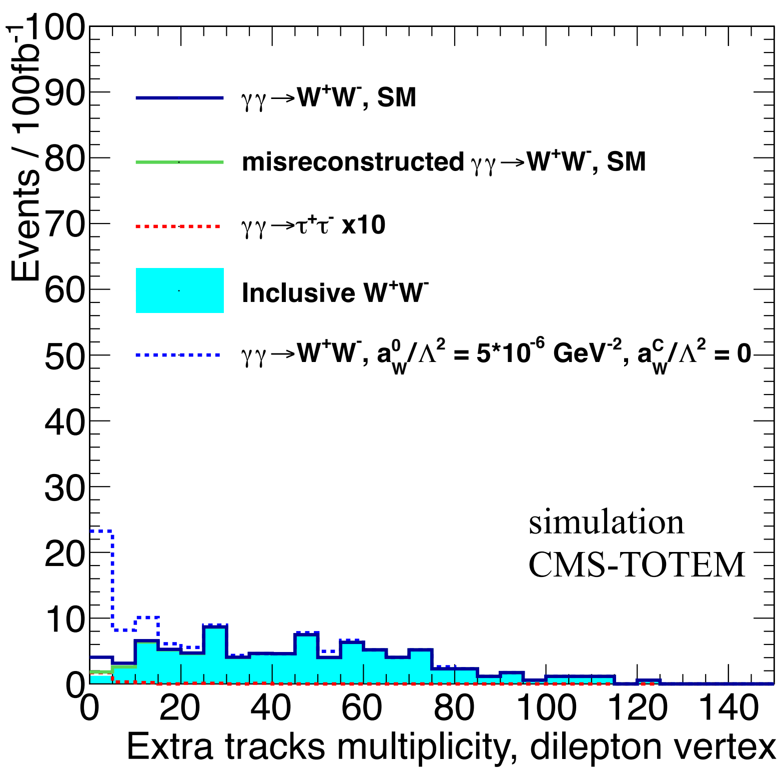

Exclusive WW production

σ_t = 10 ps (30 ps)

Selection	Cross section (fb)			
	exclusive WW	exclusive WW (incorrectly reconstructed)	inclusive WW	exclusive $\tau\tau$
generated $\sigma \times \mathcal{B}(WW \to e\mu\, \nu\bar{\nu})$	0.86±0.01	N/A	2537	1.78±0.01
$\geq$ 2 leptons ($p_T > 20$ GeV, $\eta < 2.4$)	0.47±0.01	N/A	1140±3	0.087±0.003
opposite sign leptons, "tight" ID	0.33±0.01	N/A	776±2	0.060±0.002
dilepton pair $p_T > 30$ GeV	0.25±0.01	N/A	534±2	0.018±0.001
protons in both PPS arms (ToF and TRK)	0.055 (0.054)±0.002	0.044 (0.085)±0.003	11 (22)±0.3	0.004±0.001
no overlapping hits in ToF + vertex matching				
ToF difference, $\Delta t = (t_1 - t_2)$				
$N_{\text{tracks}} < 10$				

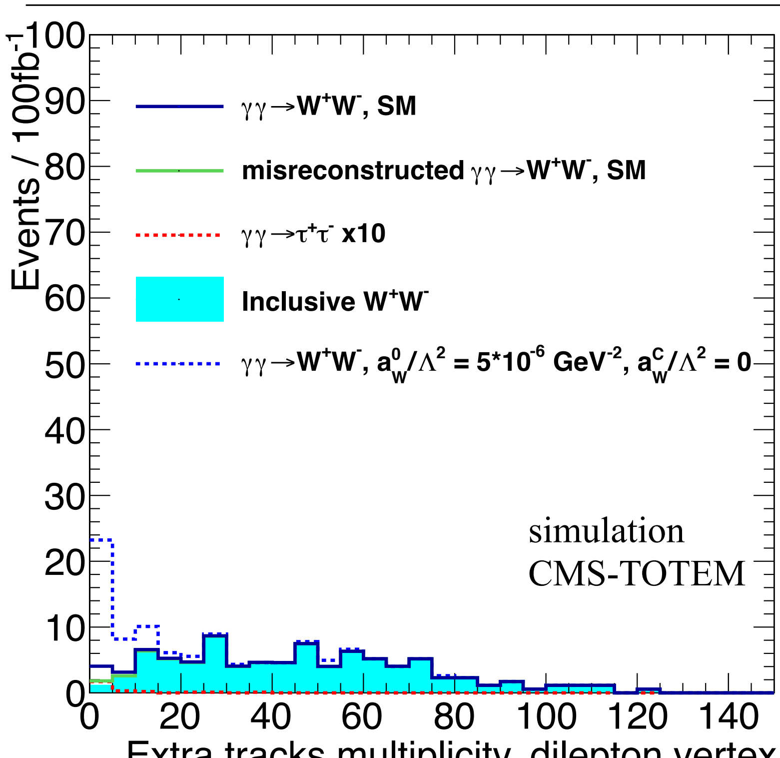

Selection	Cross section (fb)	
	$a_0^W/\Lambda^2 = 5 \cdot 10^{-6}\text{GeV}^{-2}$ ($a_C^W = 0$)	$a_C^W/\Lambda^2 = 5 \times 10^{-6}\text{GeV}^{-2}$ ($a_0^W = 0$)
generated $\sigma \times \mathcal{B}(WW \to e\mu\, \nu\bar{\nu})$	3.10±0.14	1.53±0.07
$\geq$ 2 leptons ($p_T > 20$ GeV, $\eta < 2.4$)	2.33±0.08	1.00±0.04
opposite sign leptons, "tight" ID	1.82±0.08	0.78±0.03
dilepton pair $p_T > 30$ GeV	1.69±0.07	0.68±0.03
protons in both PPS arms (ToF and TRK)	0.52 (0.50)±0.04	0.18 (0.17)±0.02
no overlapping hits in ToF detectors	0.35 (0.32)±0.03	0.12 (0.11)±0.01
ToF difference, $\Delta t = (t_1 - t_2)$	0.35 (0.32)±0.03	0.12 (0.11)±0.01
$N_{\text{tracks}} < 10$	0.27 (0.24)±0.03	0.11 (0.10)±0.01

Exclusive WW production

σ_t = 10 ps (30 ps)

Selection	Cross section (fb)			
	exclusive WW	exclusive WW (incorrectly reconstructed)	inclusive WW	exclusive $\tau\tau$
generated $\sigma \times \mathcal{B}(WW \to e\mu\, \nu\bar{\nu})$	0.86±0.01	N/A	2537	1.78±0.01
$\geq$ 2 leptons ($p_{\mathrm{T}} > 20$ GeV, $\eta < 2.4$)	0.47±0.01	N/A	1140±3	0.087±0.003
opposite sign leptons, "tight" ID	0.33±0.01	N/A	776±2	0.060±0.002
dilepton pair $p_{\mathrm{T}} > 30$ GeV	0.25±0.01	N/A	534±2	0.018±0.001
protons in both PPS arms (ToF and TRK)	0.055 (0.054)±0.002	0.044 (0.085)±0.003	11 (22)±0.3	0.004±0.001
no overlapping hits in ToF + vertex matching				
ToF difference, $\Delta t = (t_1 - t_2)$				
$N_{\mathrm{tracks}} < 10$				

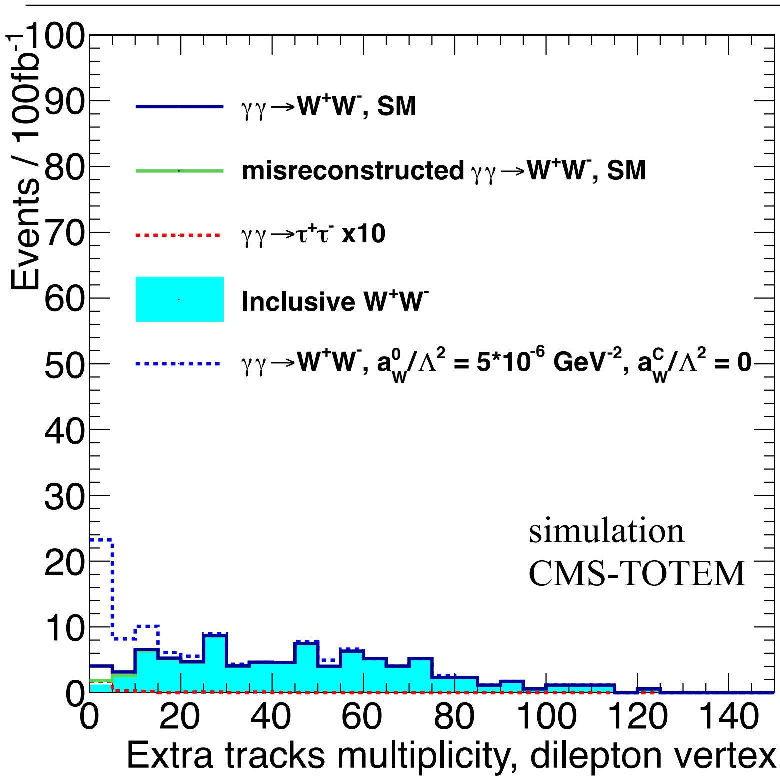

Selection	Cross section (fb)	
	$a_0^W/\Lambda^2 = 5 \cdot 10^{-6}\mathrm{GeV}^{-2}$ ($a_C^W = 0$)	$a_C^W/\Lambda^2 = 5 \times 10^{-6}\mathrm{GeV}^{-2}$ ($a_0^W = 0$)
generated $\sigma \times \mathcal{B}(WW \to e\mu\, \nu\bar{\nu})$	3.10±0.14	1.53±0.07
$\geq$ 2 leptons ($p_{\mathrm{T}} > 20$ GeV, $\eta < 2.4$)	2.33±0.08	1.00±0.04
opposite sign leptons, "tight" ID	1.82±0.08	0.78±0.03
dilepton pair $p_{\mathrm{T}} > 30$ GeV	1.69±0.07	0.68±0.03
protons in both PPS arms (ToF and TRK)	0.52 (0.50)±0.04	0.18 (0.17)±0.02
no overlapping hits in ToF detectors	0.35 (0.32)±0.03	0.12 (0.11)±0.01
ToF difference, $\Delta t = (t_1 - t_2)$	0.35 (0.32)±0.03	0.12 (0.11)±0.01
$N_{\mathrm{tracks}} < 10$	0.27 (0.24)±0.03	0.11 (0.10)±0.01

Expected limits on aQGC

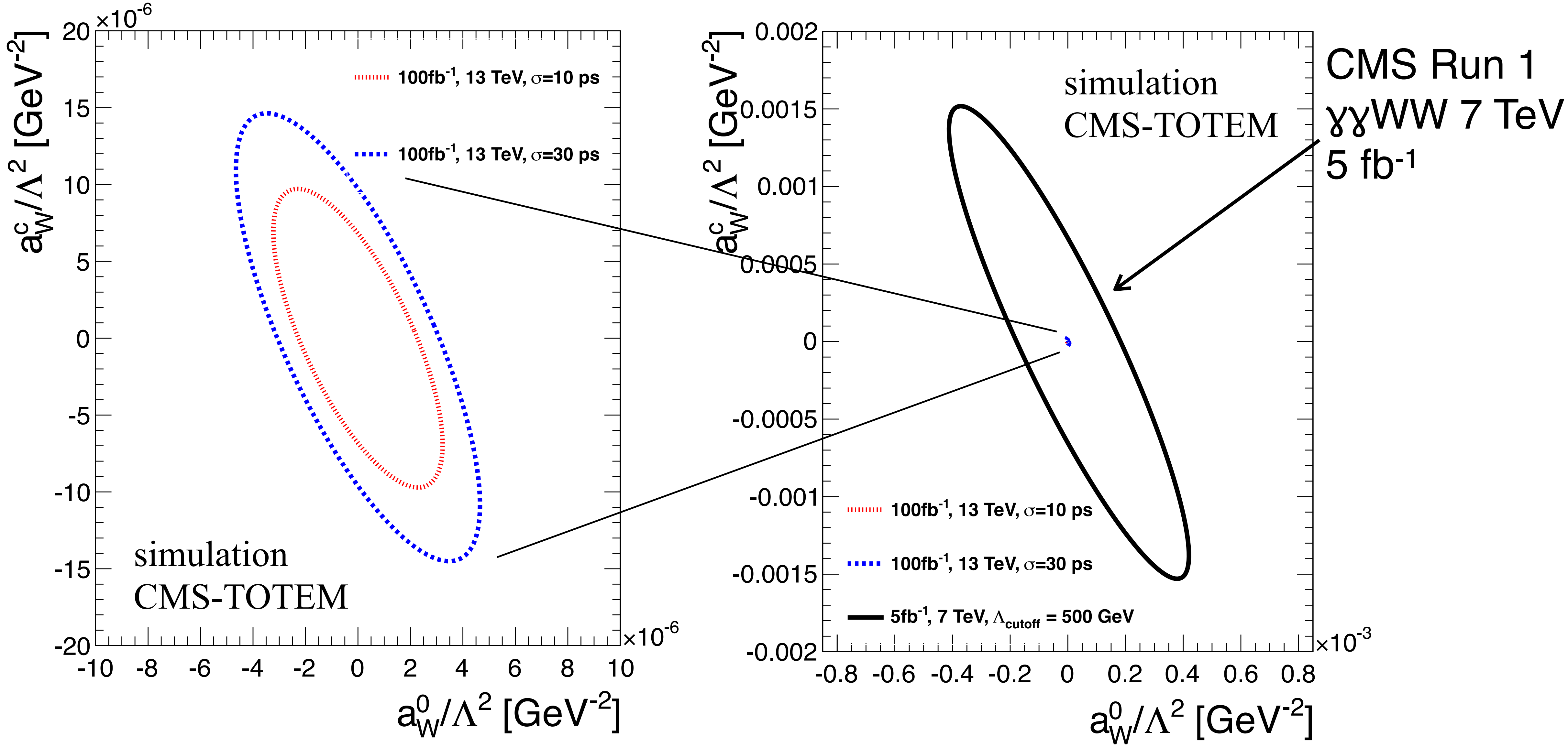

Expected limits assuming 10 ps (30 ps) timing resolution:

$a_0^W/\Lambda^2 = 2 \times 10^{-6}$ (3×10^{-6}), (95% CL)

$a_C^W/\Lambda^2 = 7 \times 10^{-6}$ (10×10^{-6}),

CMS Run 1 γγWW 8 TeV 20 fb^{-1} (95% CL)

$a_0^W/\Lambda^2 < 1.0 \times 10^{-4}\,\mathrm{GeV}^{-2}$

$a_C^W/\Lambda^2 < 3.4 \times 10^{-4}\,\mathrm{GeV}^{-2}$

Summary & Outlook

- CT-PPS will enhance the CMS & TOTEM physics potential by allowing precision proton measurement on both sides of CMS, collecting data at high luminosity
- Sensitivity to anomalous gauge couplings and search for new resonances
- Experimental challenges being addressed:
  - Operation of Roman Pots at high luminosity
  - Timing detectors with high precision
  - Tracking detectors with 3D pixel sensors
- *Exploratory* phase (2015-2016):
  - RP insertion commissioning and operation at low β* and high intensity
  - Install detectors, commissioning & start of data taking

CT-PPS TECHNICAL DESIGN REPORT

CERN-LHCC-2014-021

Additional material

CT-PPS: Beam background extrapolation

- Used TOTEM data at μ=9
- Account for pileup protons (from simulation) to estimate beam background only
- Extrapolate to μ=30 and 50

track multiplicity in the two arms

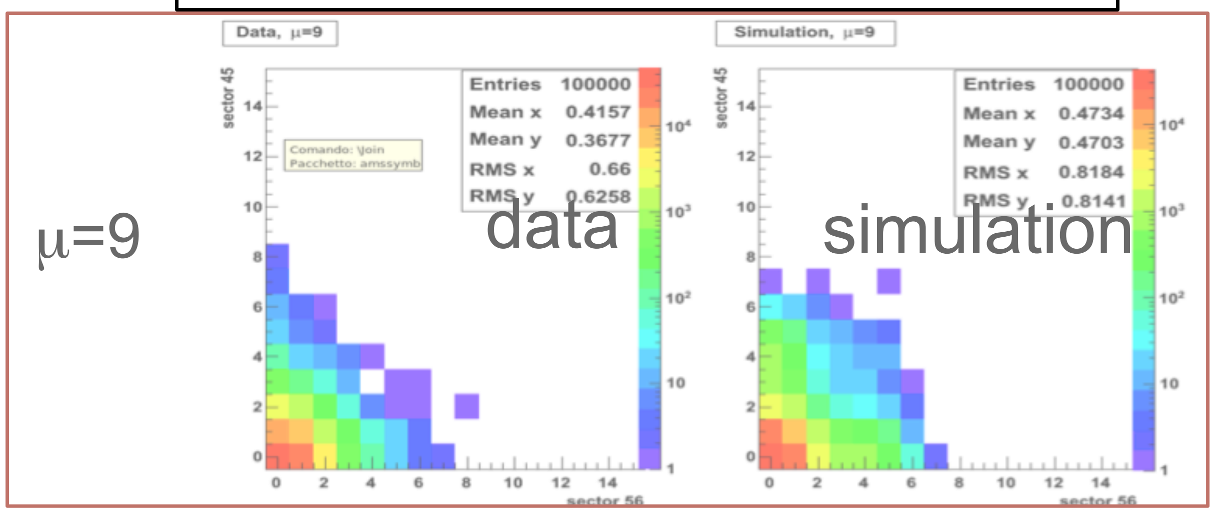

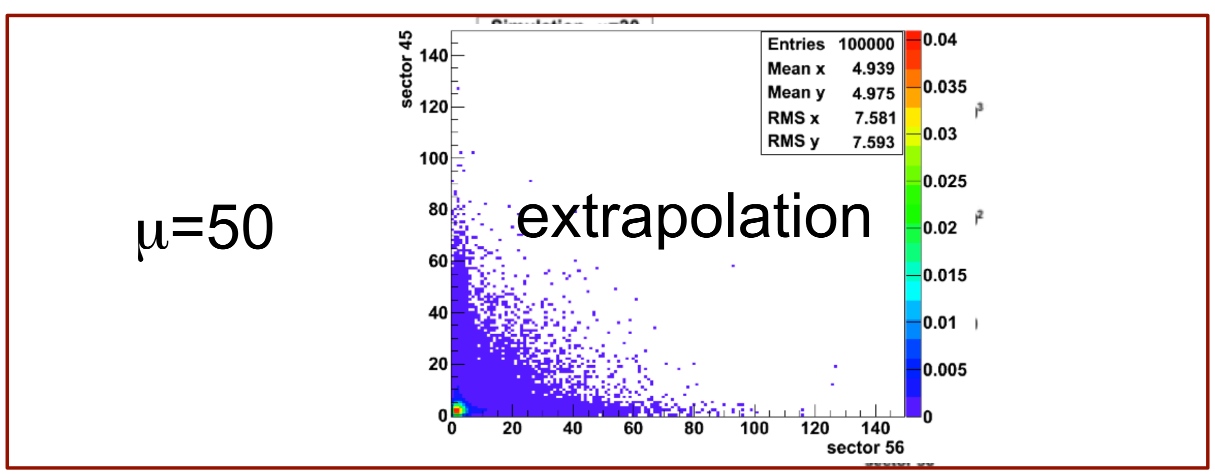

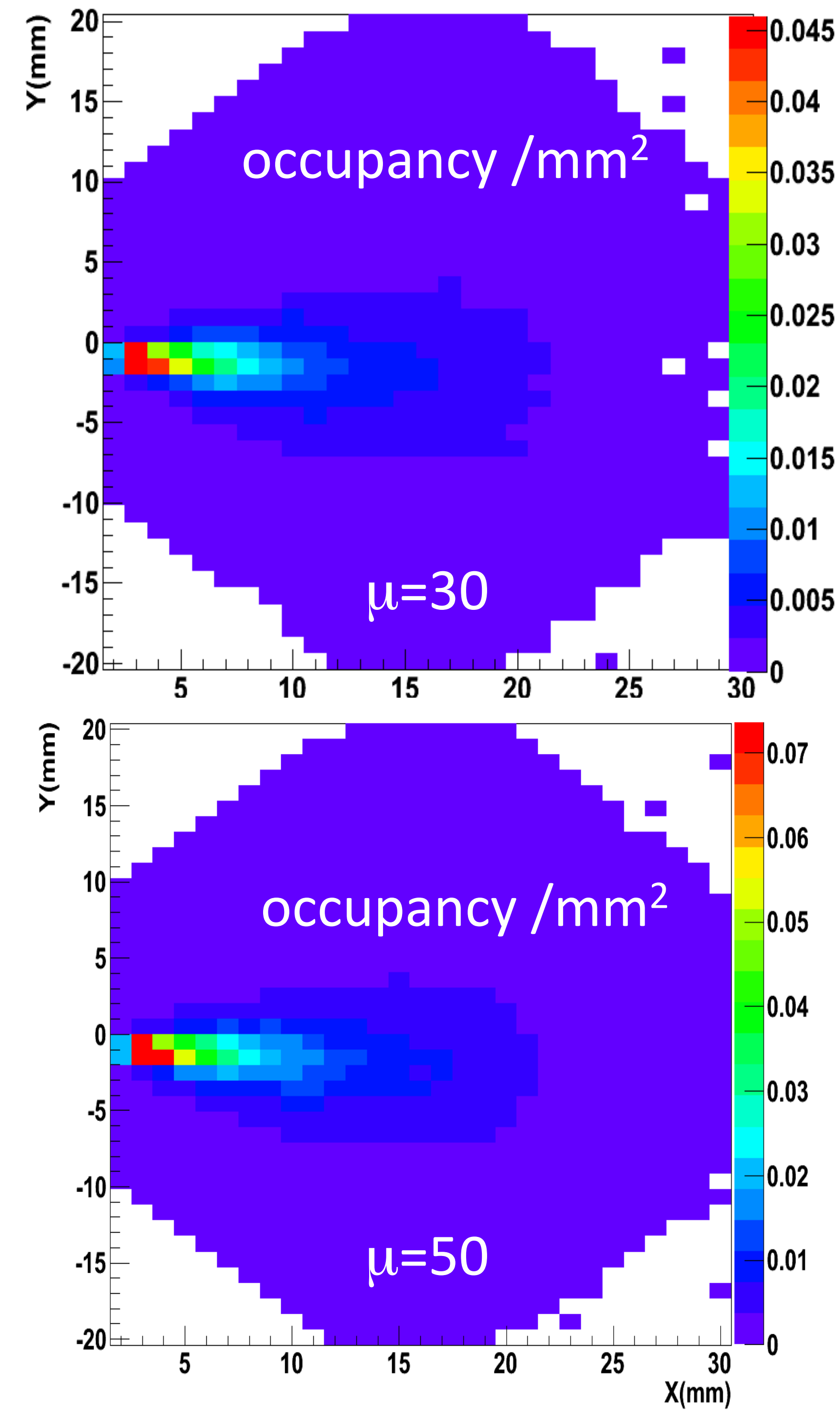

CT-PPS: Expected radiation doses

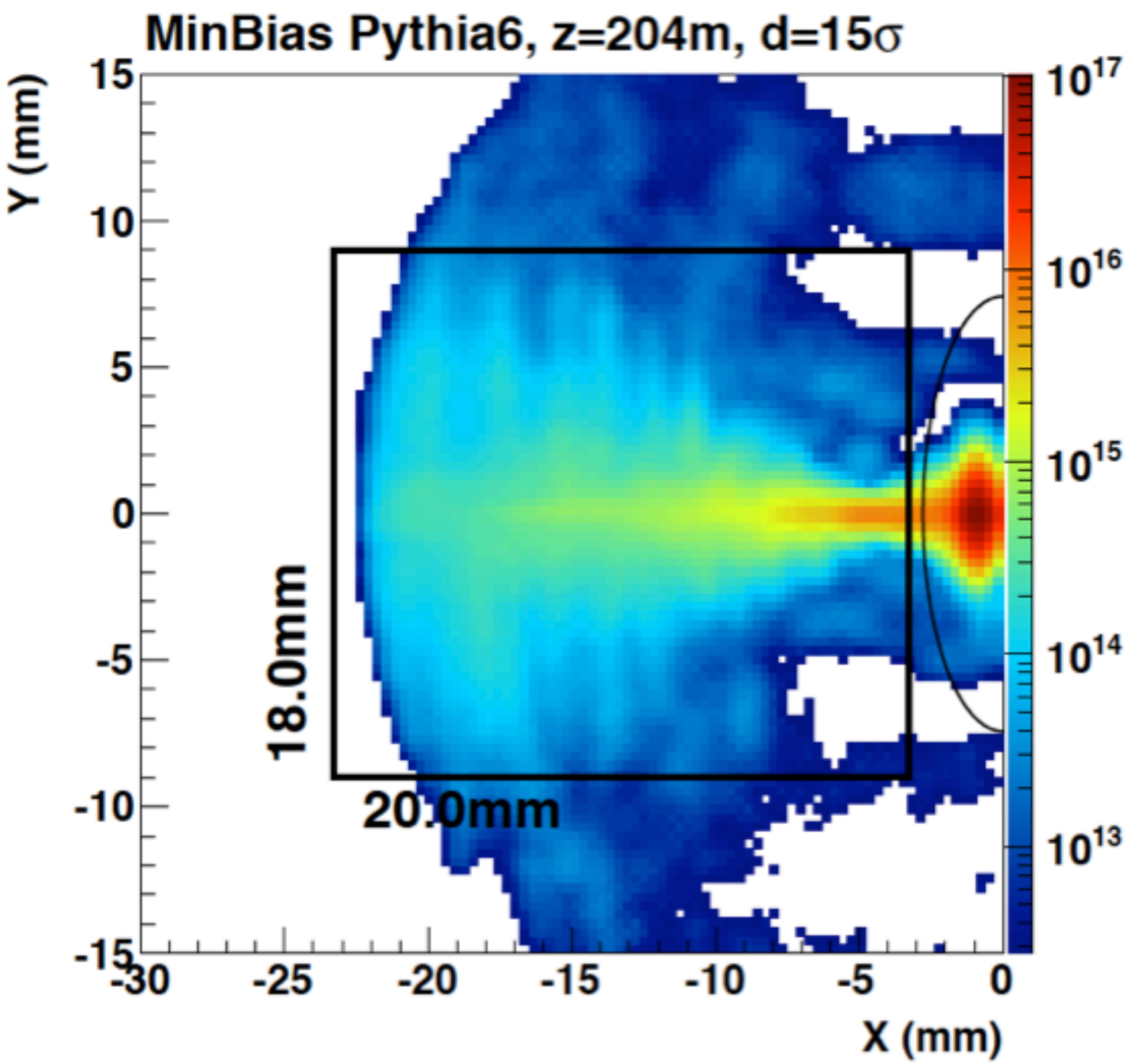

Per 100 fb^{-1}:

- Proton flux up to 5×10^{15} cm^{-2} in the **pixel detectors**
- 10^{12} neq/cm^2 and 100 Gy in **photosensors** and **readout electronics**

CT-PPS Detectors

Only one arm

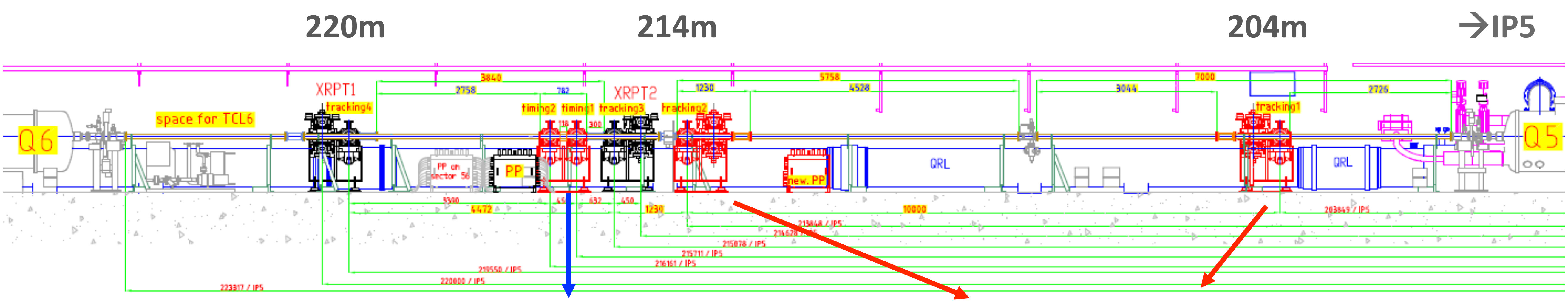

2 new horizontal cylindrical RPs (1 now)

Equipped with timing detectors, for PU rejection

2 horizontal box-shaped RPs

Equipped with tracking detectors to measure the displacement of the scattered protons w.r.t. the beam

Detector acceptance vs β*

β* = 0.55 m (low β* = standard at LHC)

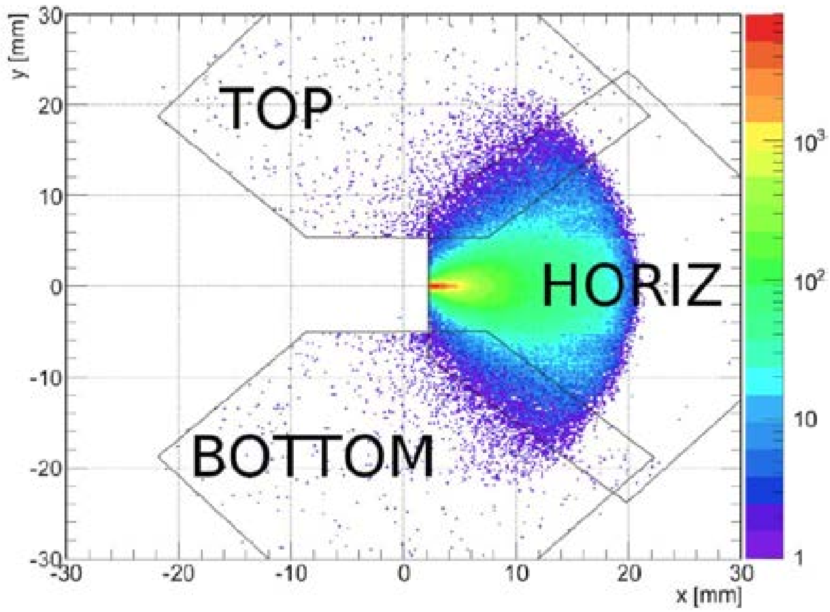

β* = 90 m (special development for RP runs)

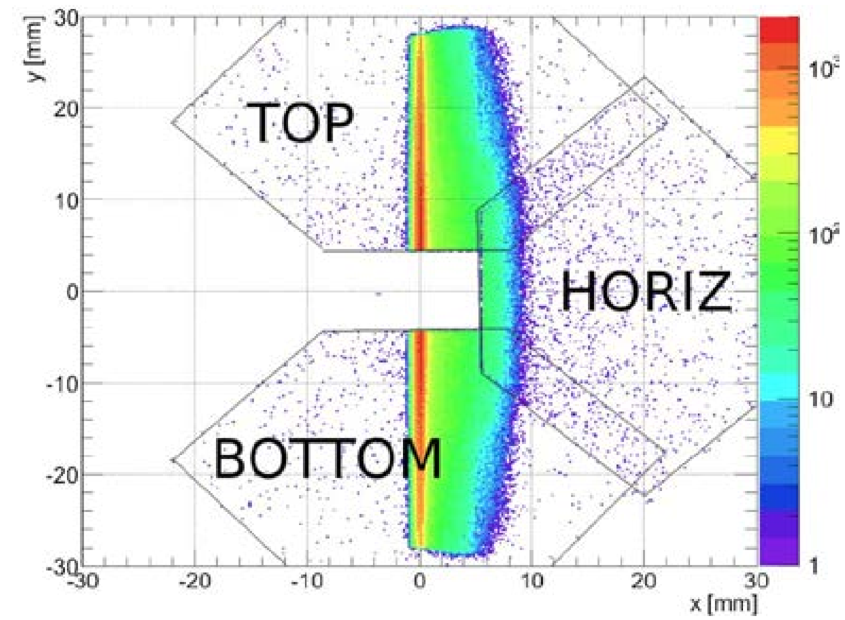

β* = 0.55 m

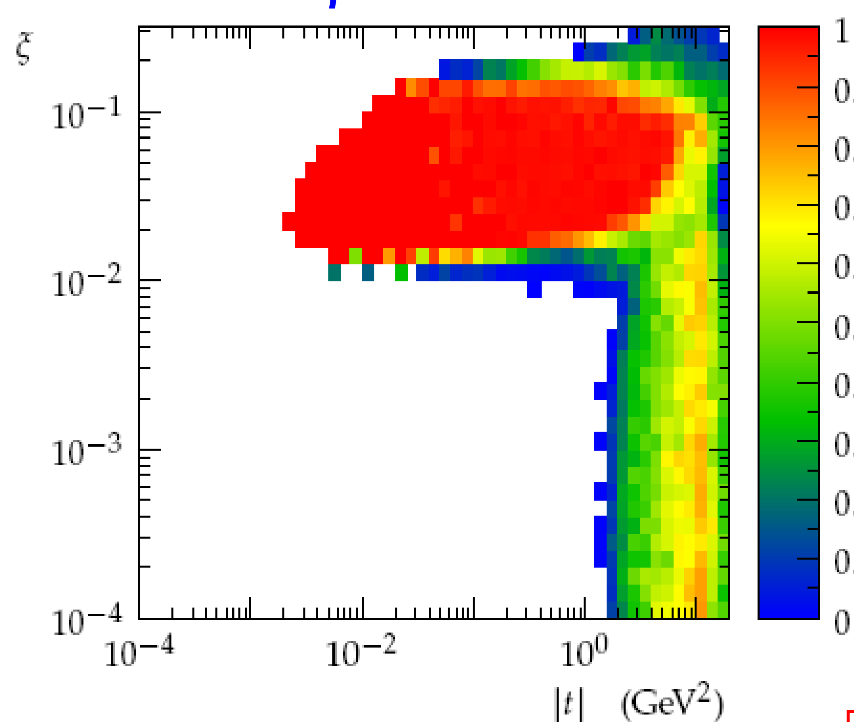

β* = 90 m

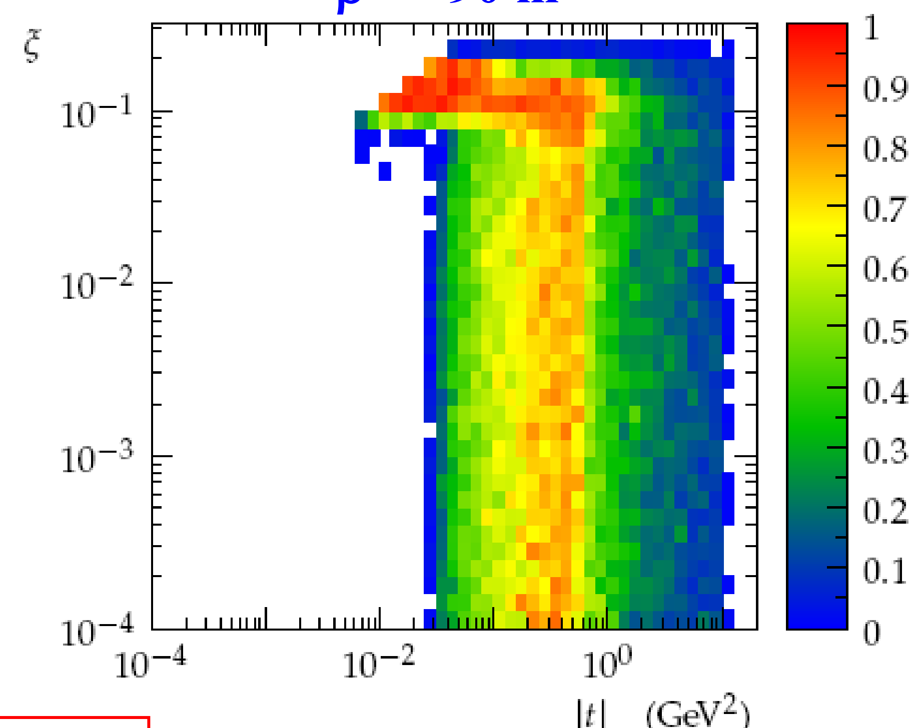

M. Deile, 2015

$$\mathcal{L} \propto \frac{1}{\beta^*}$$

RP Insertions in Regular Fills at Low β*

3 – 4 July: Beam-based alignment of all 14 low-beta RPs in 1½ hours,

5 – 14 July: RP insertions in all intensity steps of 50 ns intensity ramp-up
still nominal TCL configuration: TCL5 in, TCL6 out,
very conservative RP positions due to orbit uncertainties: **~ 30 σ horizontally, ~ 20.5 σ vertically**
3, 50, 152, 296, 476 bunches per beam → **lumi up to 1.3 x 10^{33} cm^{-2} s^{-1}**

13 – 21 August: RP insertions in first part of 25 ns intensity ramp-up
final TCL configuration: TCL5 out, TCL6 @ 25 σ
closer RP positions: **~ 25 σ horizontally, ~ 19.5 σ vertically**
2, 86, 157, 219, 315 bunches per beam → **lumi up to 0.7 x 10^{33} cm^{-2} s^{-1}**

M. Deile, 2015

Technical Stop 2: Installation of Aluminium bar in cylindrical pot in 5-6
mimicking the material of a Cherenkov Quartz bar

Since 5 Sept (ongoing): RP insertions in second part of 25ns intensity ramp-up
So far: 2, 49, 219, 459, 745, 1033, 1177, 1321, 1464, 1608, 1825 bunches per beam
→ **lumi up to 3.9 x 10^{33} cm^{-2} s^{-1}**

So far: no beam instabilities due to RP insertions observed.

Aim for RP positions next year if all insertions successful:
20.7 σ horizontally, 18.2 σ vertically or closer if collimation system allows

BLM Response with and without Dummy Quartic Bar in RP
(Insertion of horizontal pots to ~25 σ from beam centre)

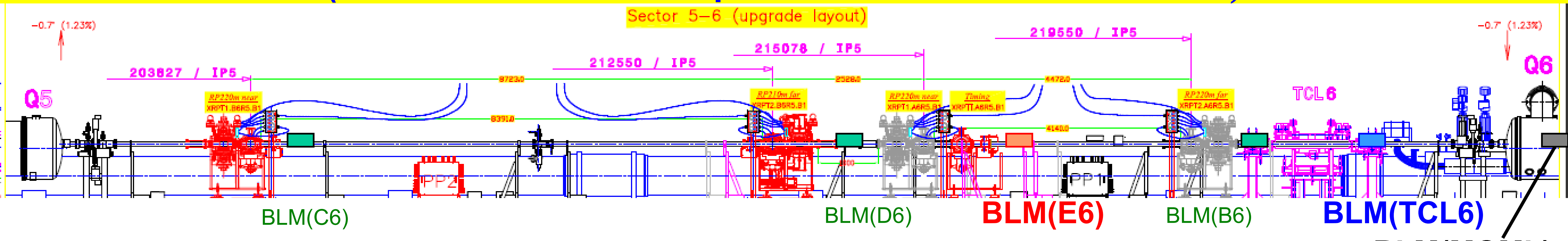

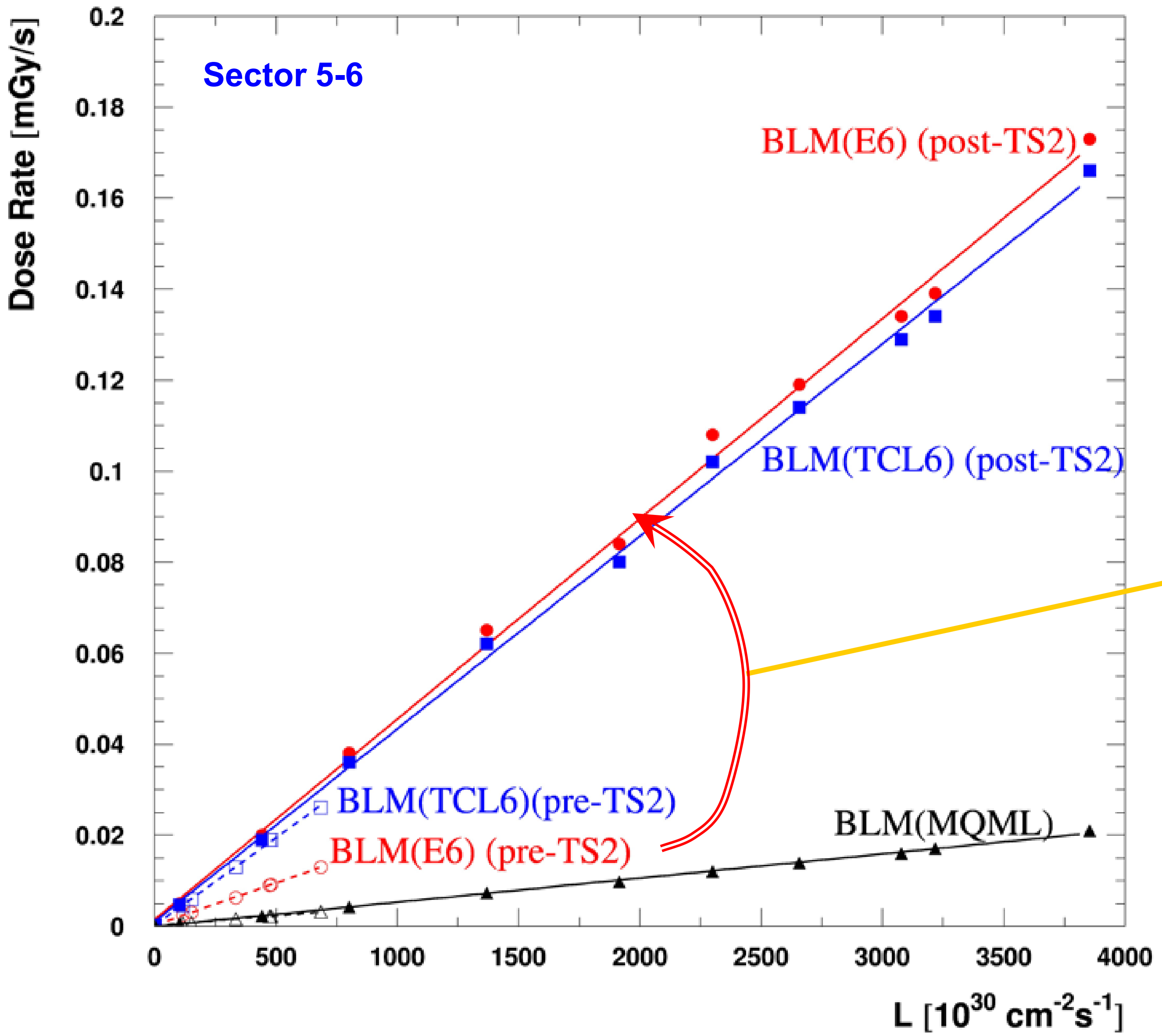

Technical Stop TS2:
Installation of Al bar (Quartic dummy) in the pot

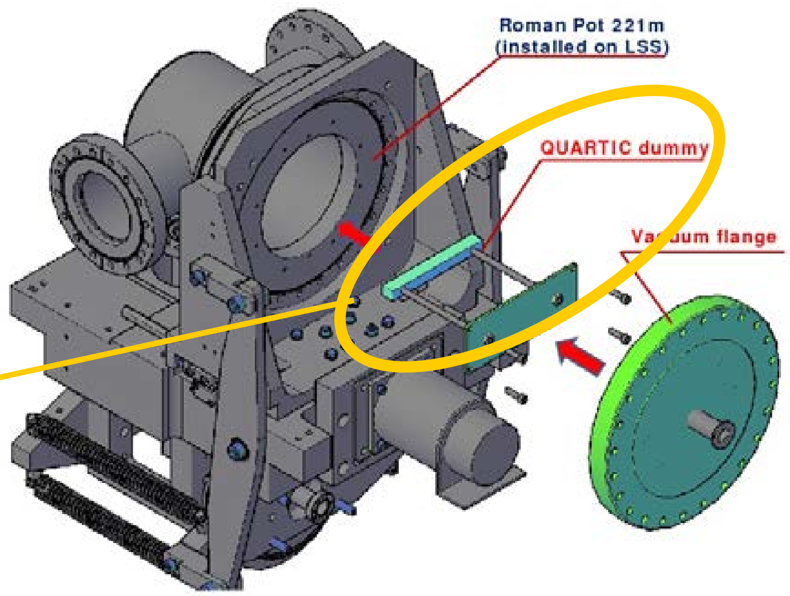

M. Deile, 2015

Installation of dummy QUARTIC bar → dose rate in BLM(E6) increases by ~ factor 2

Roman Pots' updates

- Tests of TOTEM RPs at high luminosity revealed important issues (vacuum, beam dumps, heating).
- Several improvements have been carried by TOTEM (and CMS) in collaboration with BE-ABP.
  - New RF shielding in standard box-shaped RPs
  - New cylindrical RP for timing detectors
  - 10 um thick copper coating
  - New ferrites

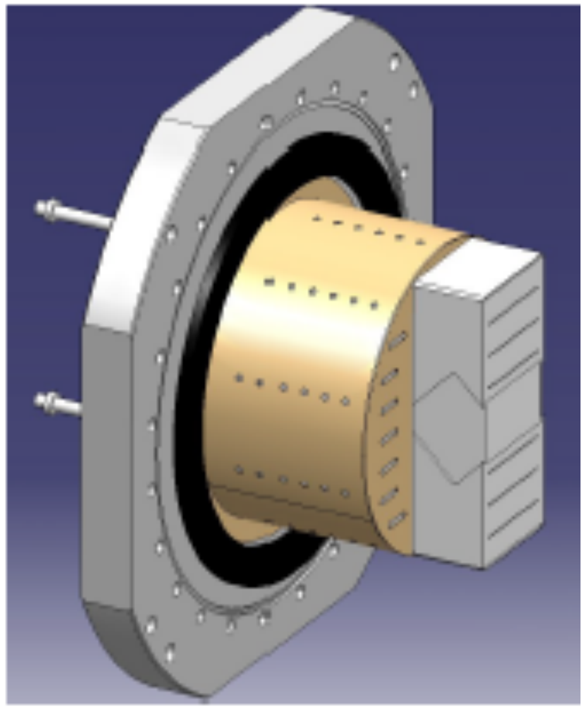

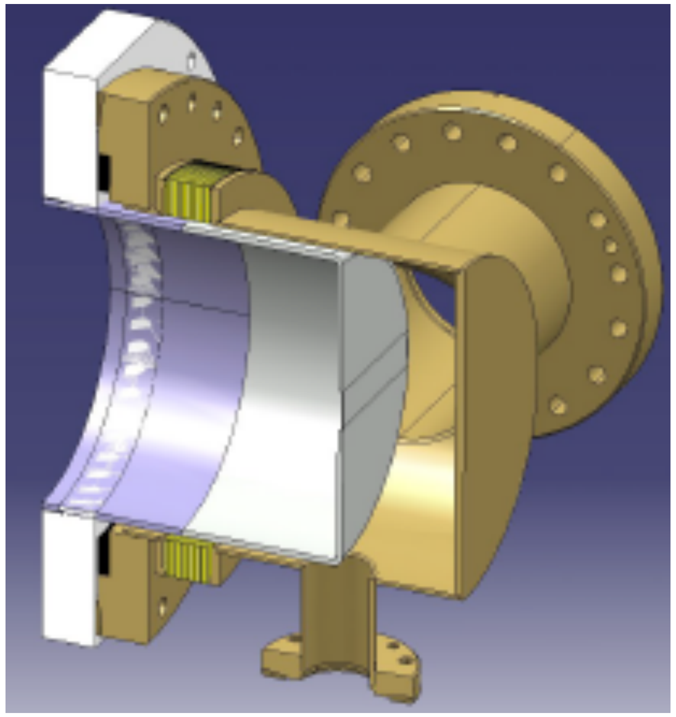

Tracking detectors: sensors

6 detector planes per station

For each plane:

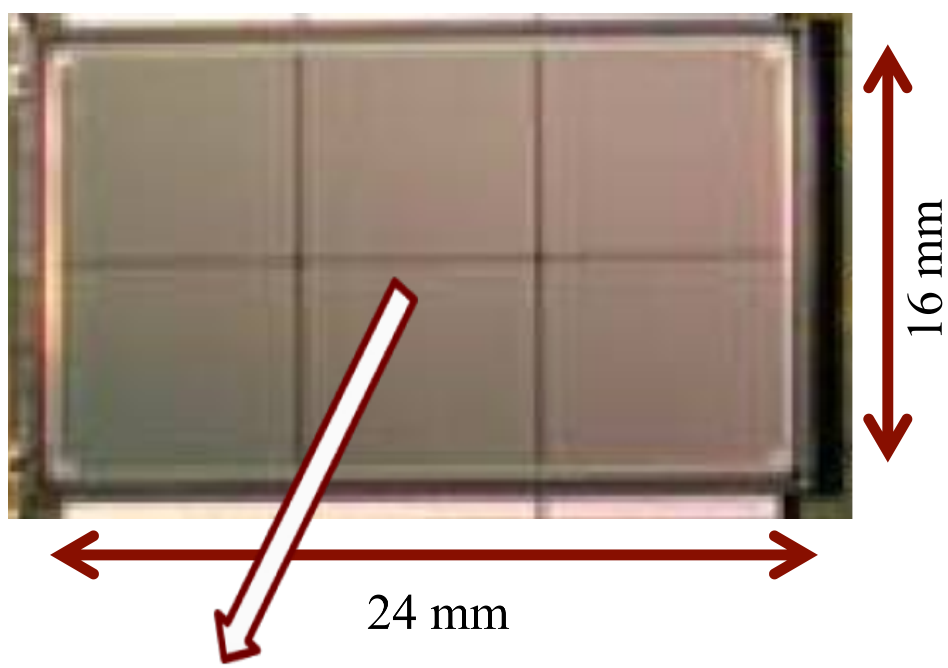

- 16 x 24 mm^2 **3D silicon pixel sensors**
- 150(x) x 100(y) μm^2 pixel pattern same as CMS pixel detectors
- **6 PSI46dig readout chips** (52x80 pixels each)

3D sensors consist of an array of columnar electrodes

- Mature technology after ATLAS IBL

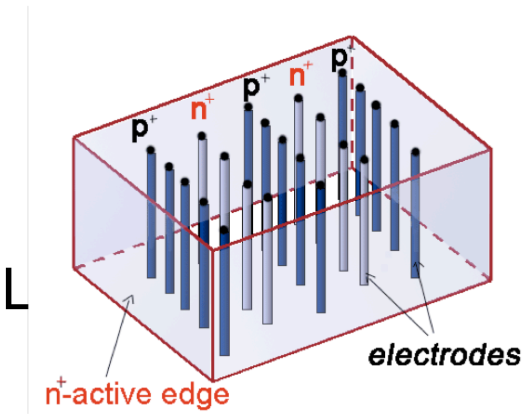

Interesting features w.r.t. planar sensors:

- **Low depletion voltage** (~10 V)
- Fast charge collection time
- Reduced charged trapping probability and therefore **high radiation hardness**
- **Slim edges**, with dead area of ~100-200 μm or **Active edges**, with dead area reduced to a few μm
- Spatial resolution comparable with planar detectors

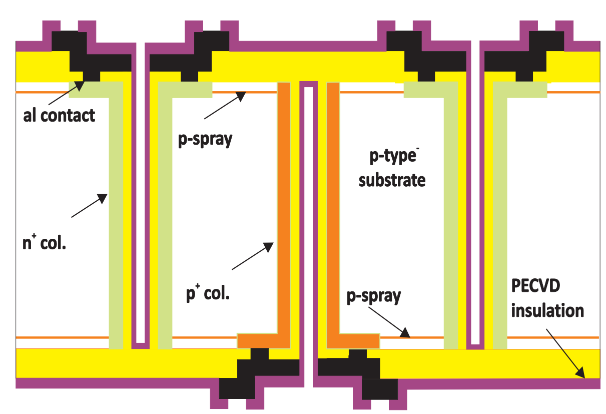

Preferred solution: FBK 3D with inter-electrode distance 62.5 μm

M.Arneodo et al, 2014

Tracking detector modules

- Four detector packages (one per station); six modules per package (one per plane)
- One sensor + 6 PSI46dig, one TBM (token bit manager) on each module
- The supporting structure is used also as heat exchanger
- Design driven by available space and requirement of reusing present TOTEM cooling system without compromising mechanical tolerances, heat removal, ease of access for maintenance, plus minimize material along p path

RPix Module

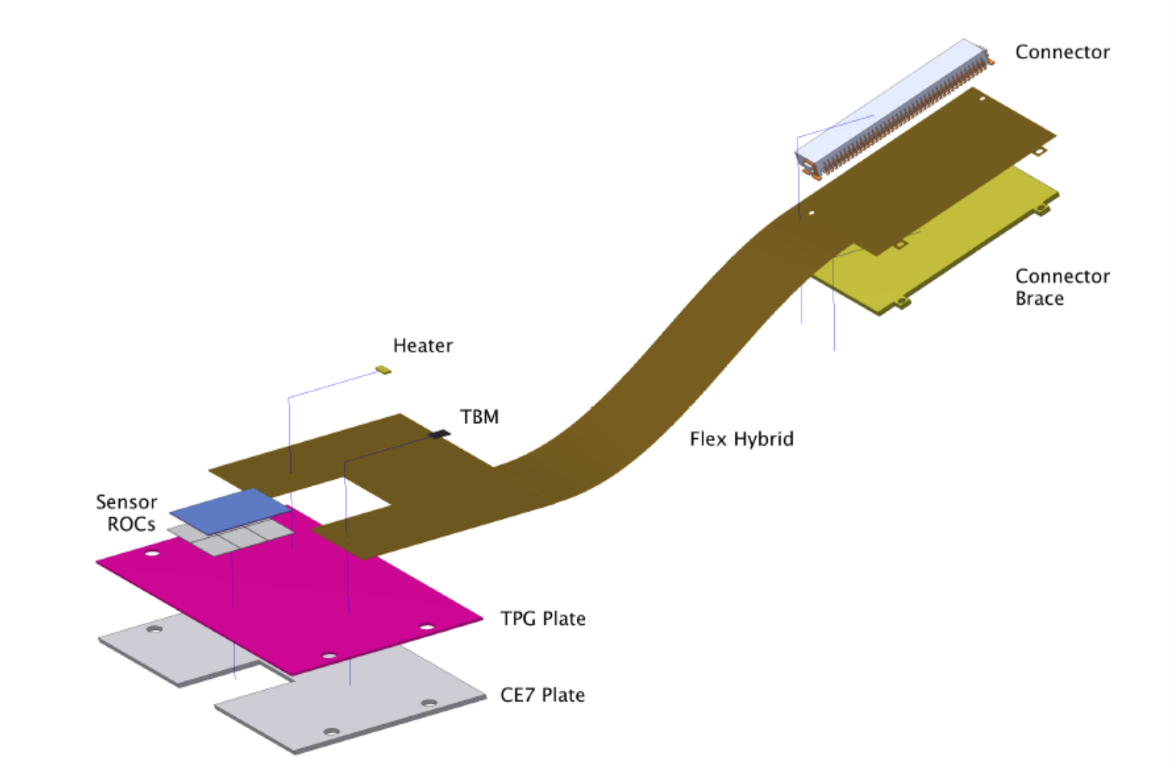

Detector Package

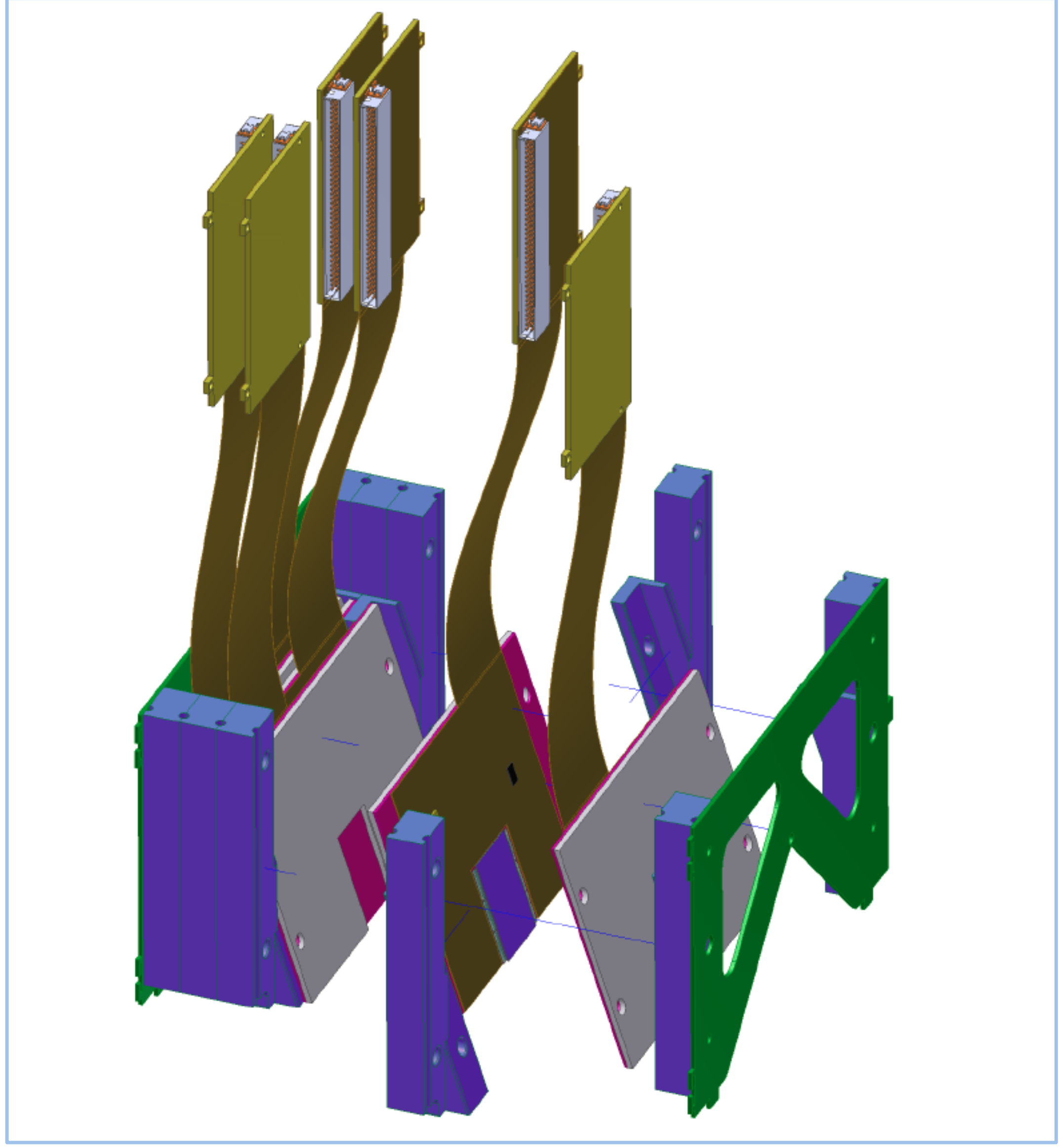

M.Arneodo et al, 2014

Tracking detectors: Front-end & DAQ

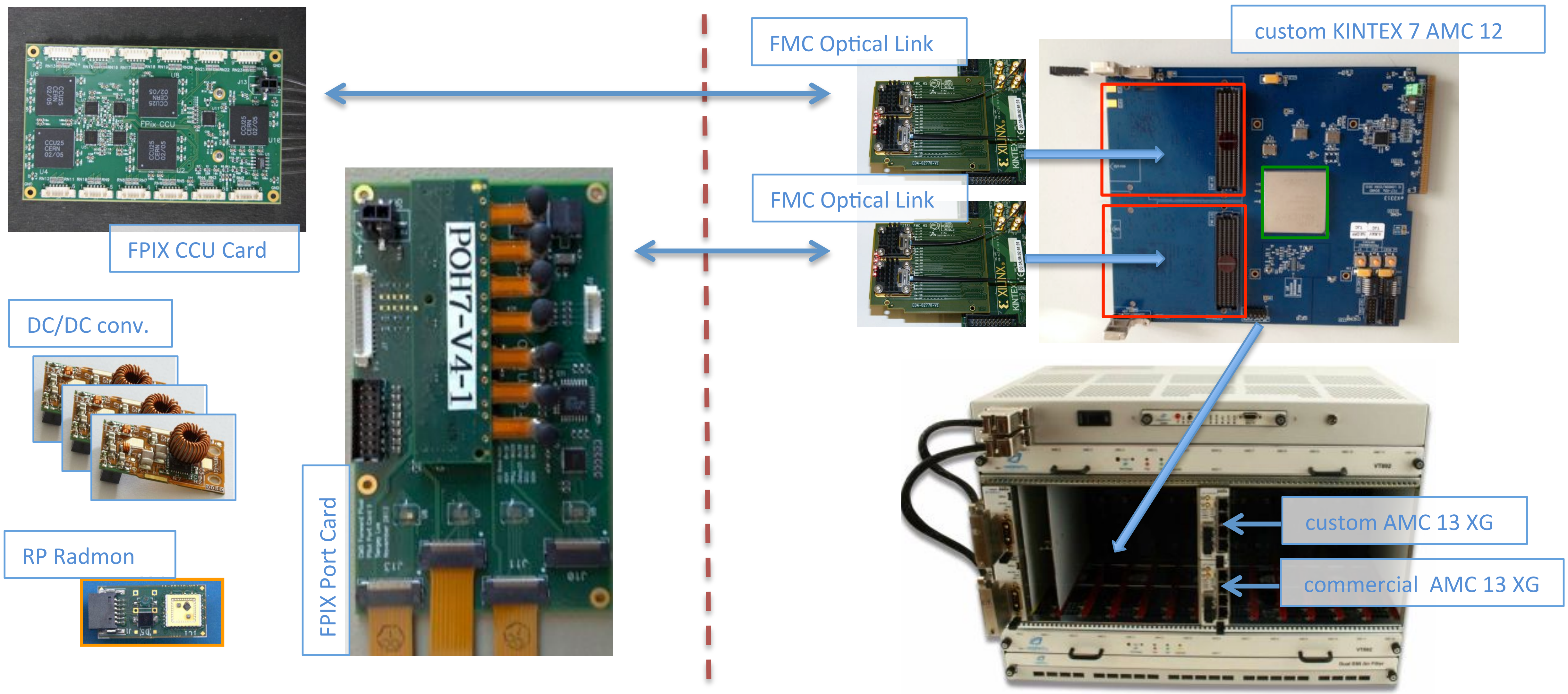

M.Arneodo et al, 2014

Timing detectors baseline: *Quartic*

- Cherenkov light in quartz bars
  - n=1.475, θ=47.3^{o}, at 350 nm.
  - ρ=2.20 g·cm^{-3}, λ_I = 44.5 cm.
- Quartic module:
  - 4x5=20 3x3 mm^2 bar elements
  - 200 µm wire grid separating the bars
  - active area is 12.6 mm x 15.8 mm

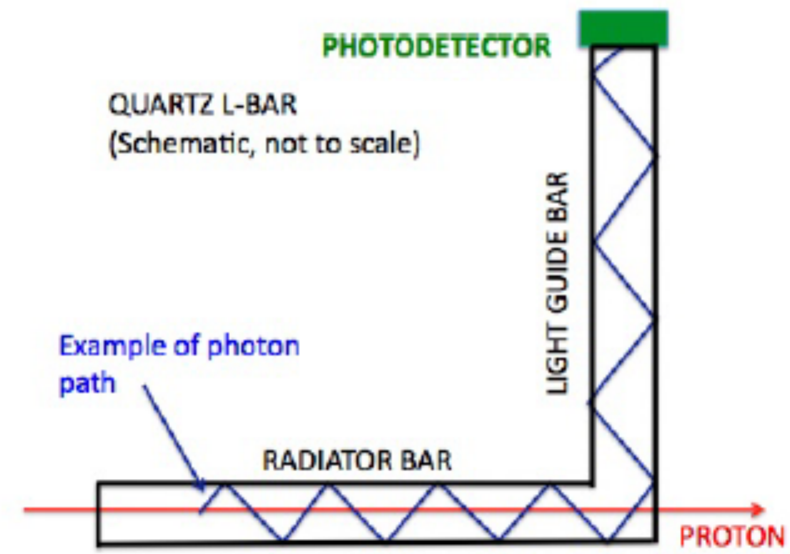

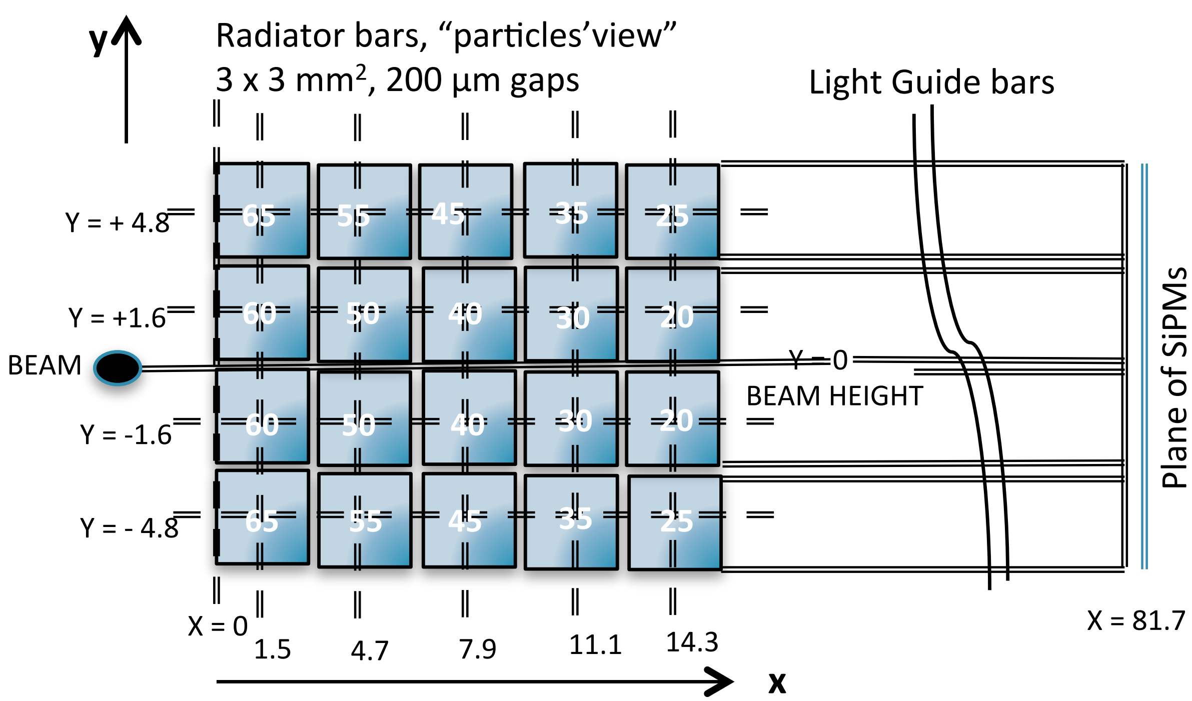

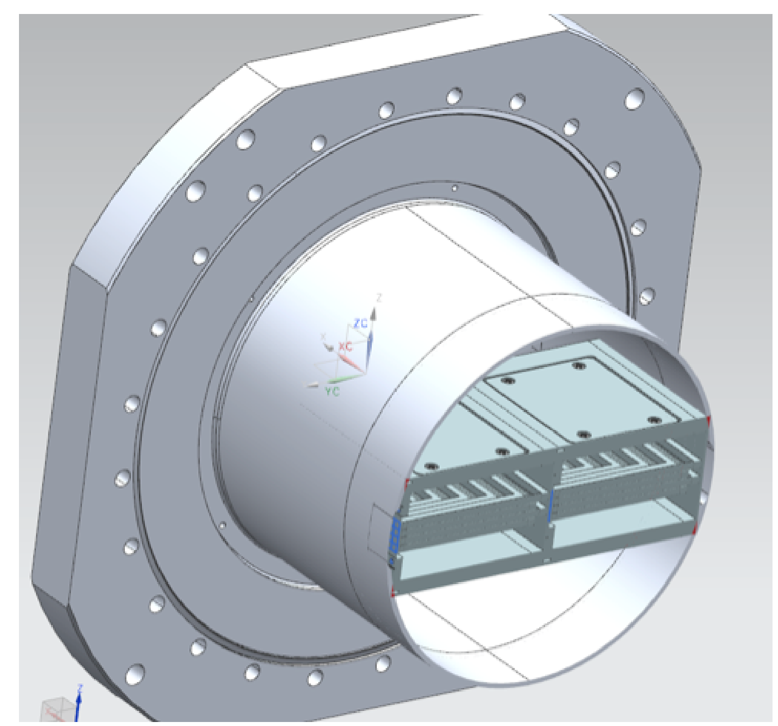

Figure 77: Assembly of two Quartic modules in Roman pot. The beam comes from the left.

M. Arneodo, 2014

Timing detectors: Quartic readout

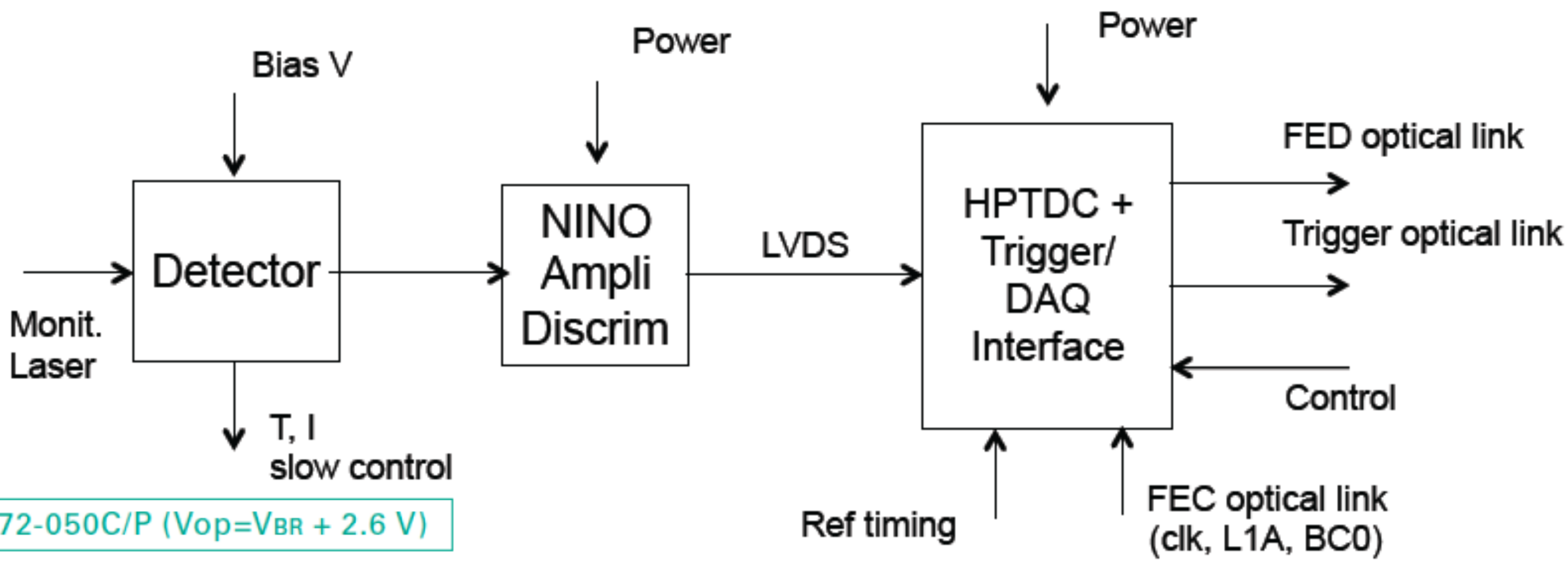

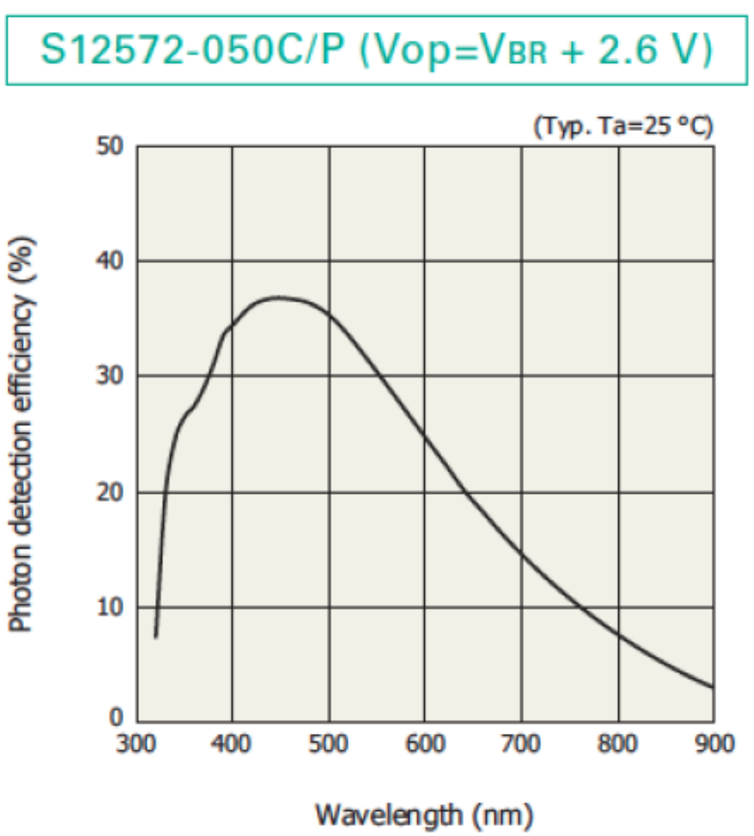

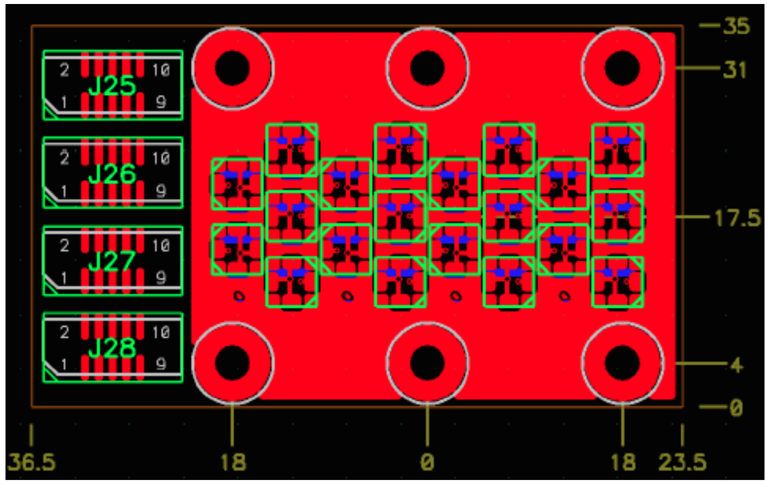

SiPM readout board

Timing detectors R&D: (Very) Fast Silicon Detectors

Diamond detectors

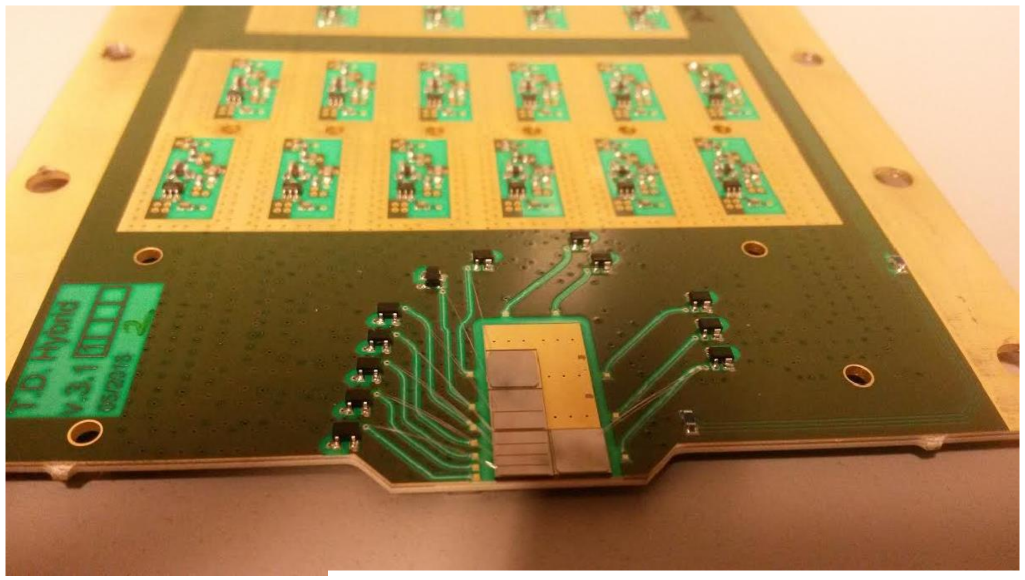

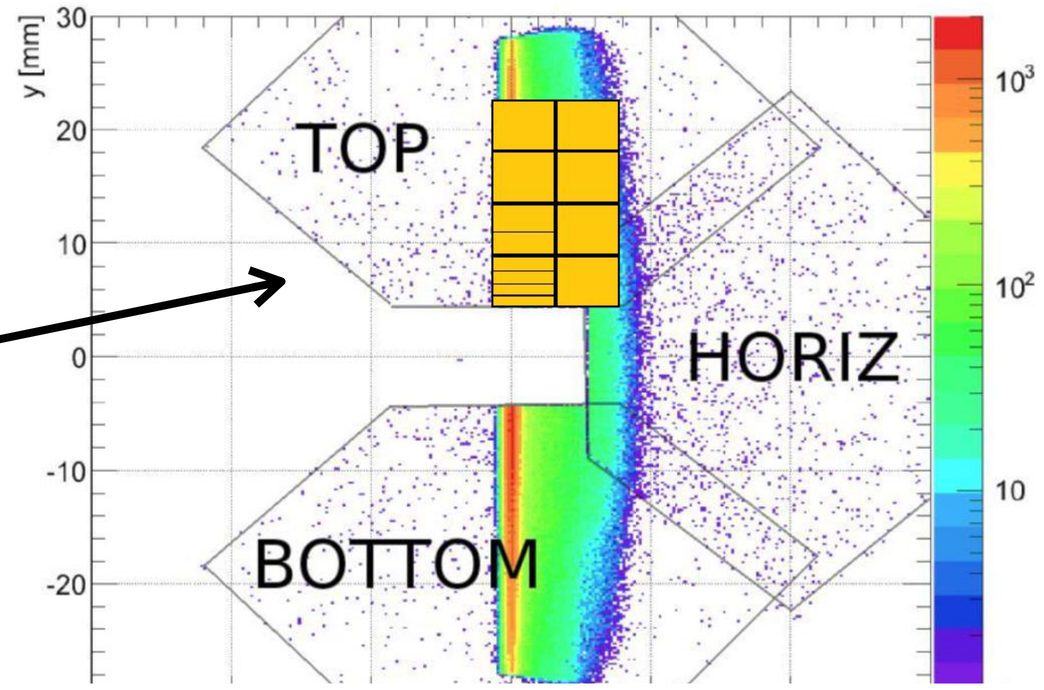

M. Berretti, 2015

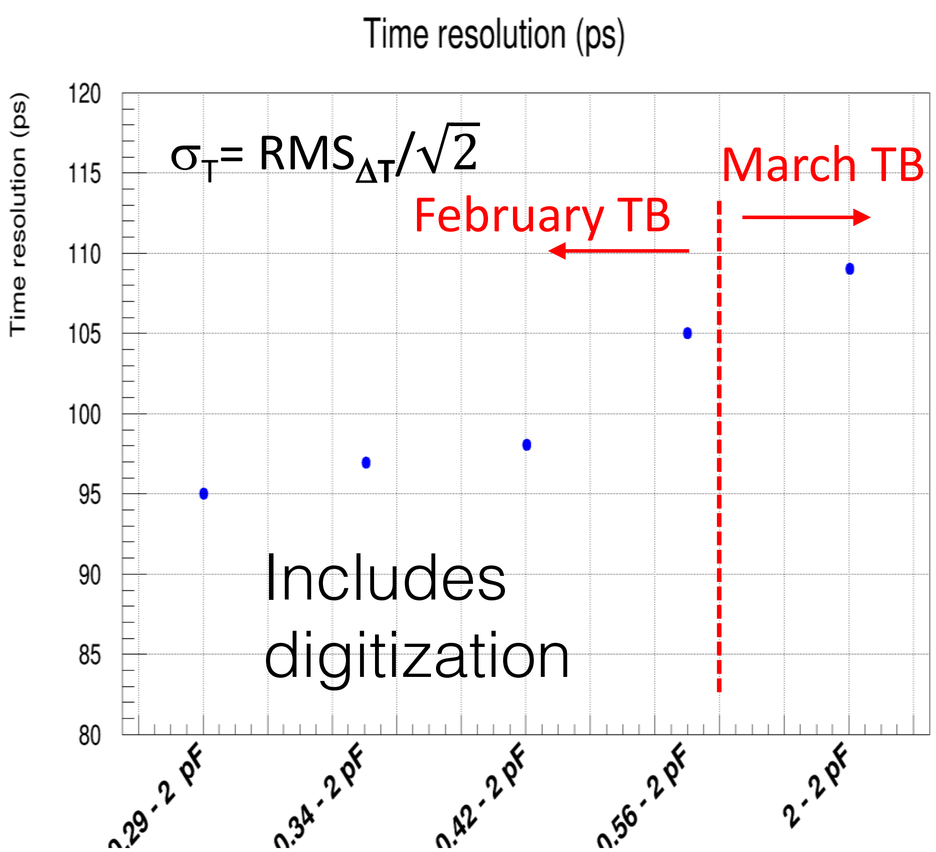

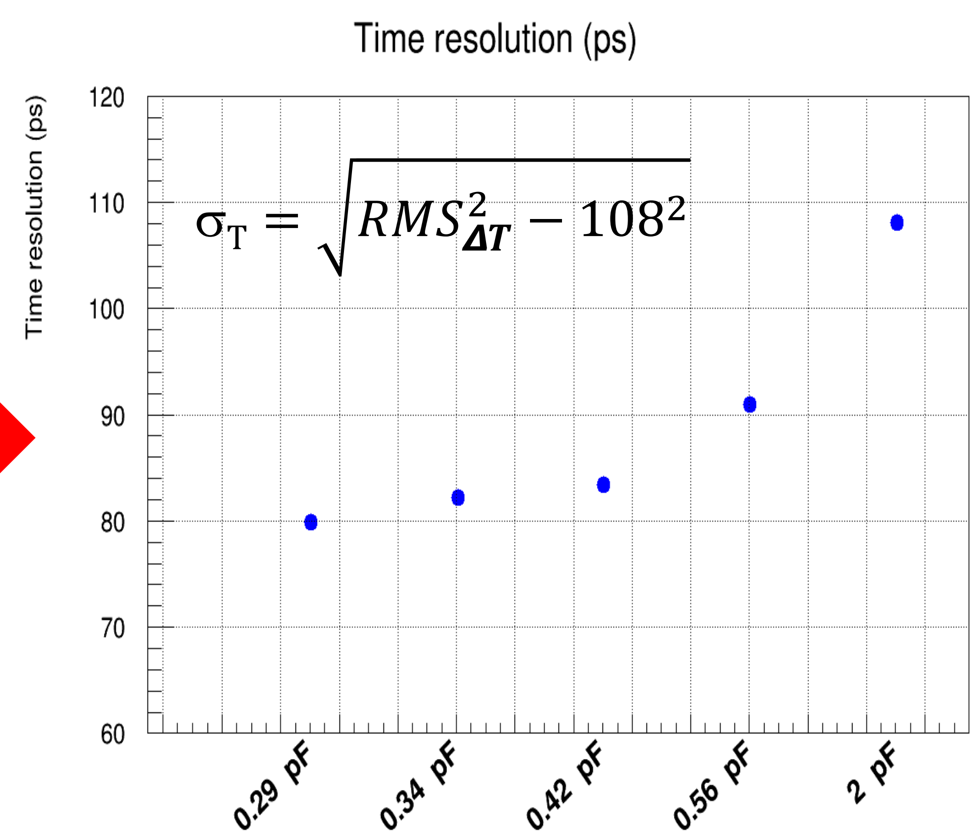

Timing detectors R&D: (Very) Fast Silicon Detectors

Ultra Fast Silicon Detectors

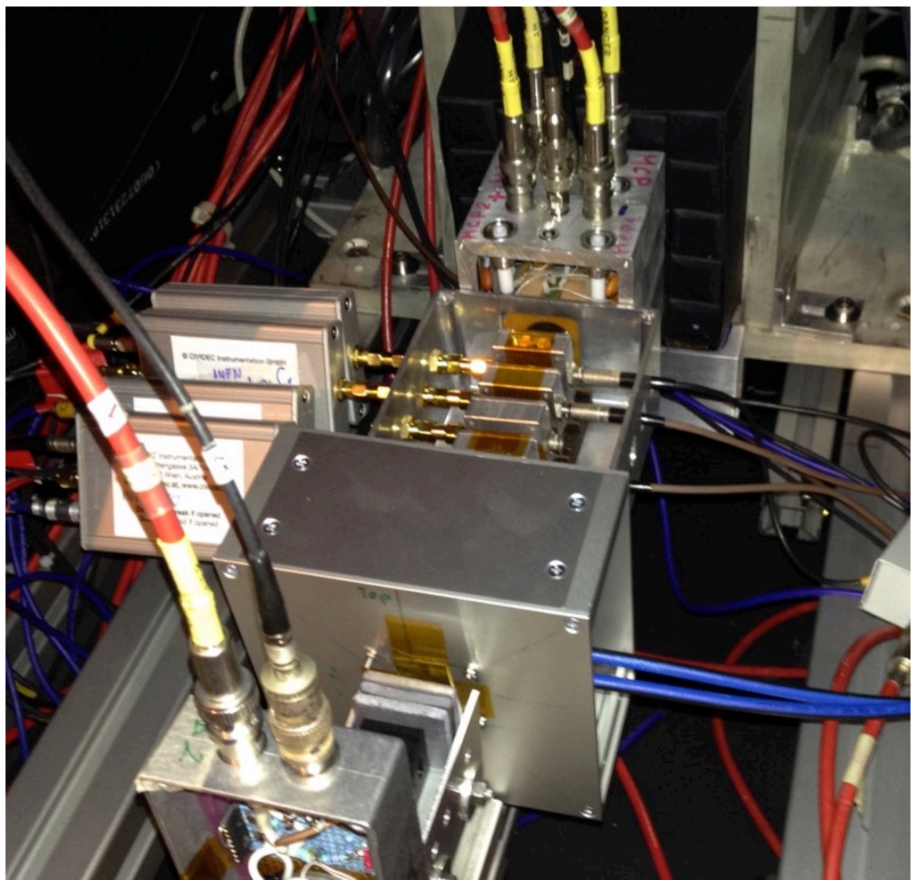

N. Cartiglia, 2015

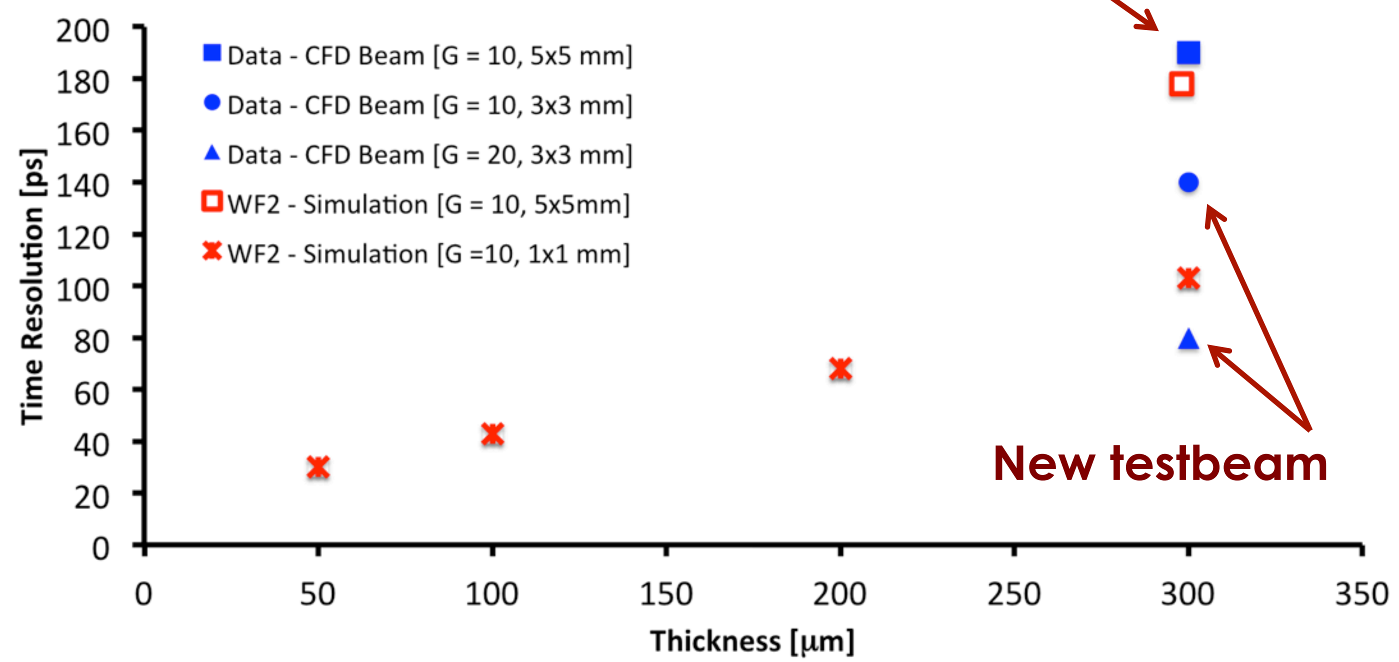

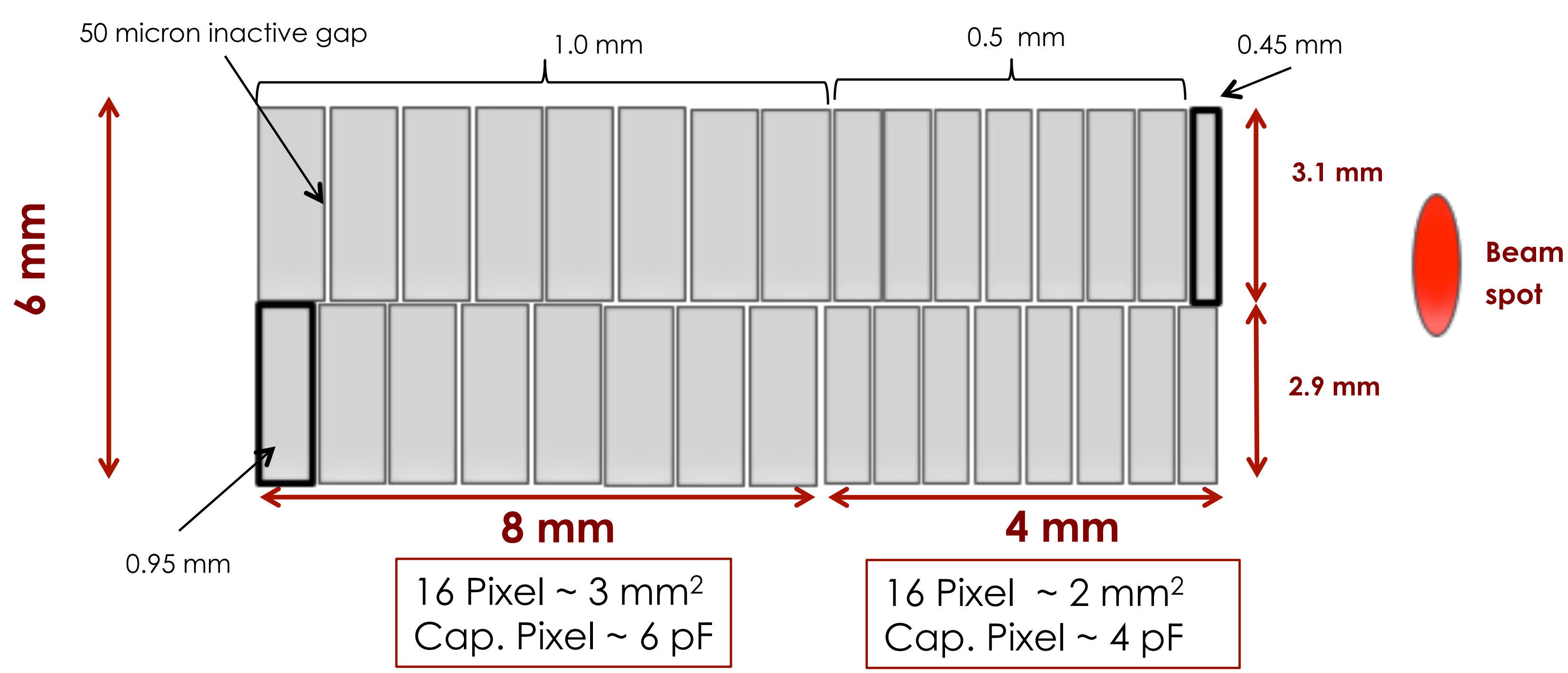

Timing detectors R&D: (Very) Fast Silicon Detectors

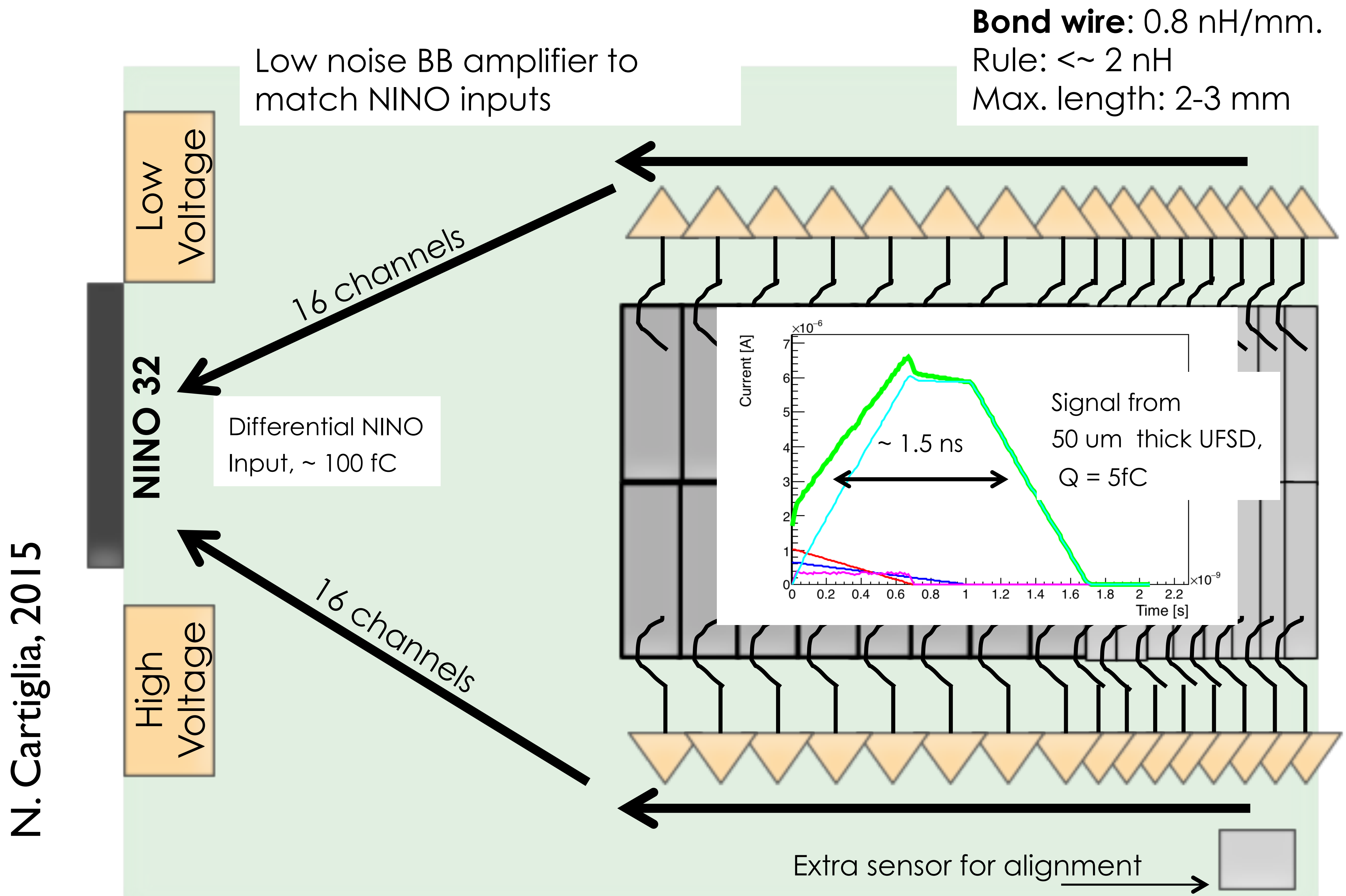

Ultra Fast Silicon Detectors

Basic idea: use specially designed silicon detectors as a backup solution for the timing detectors of the PPS

Ultra-Fast Silicon Detectors

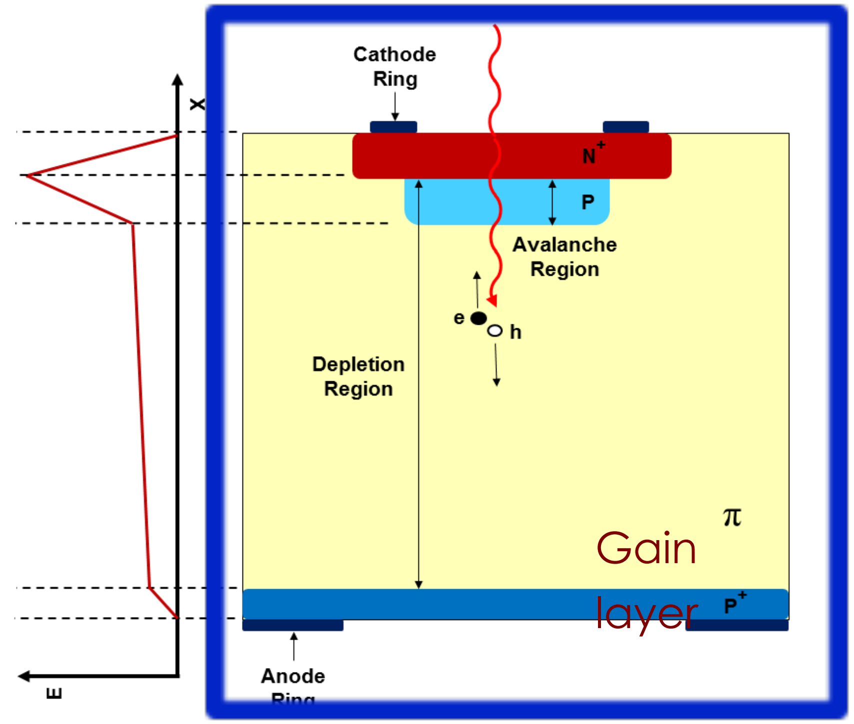

UFSDs: Silicon detectors with enhanced signal
Add an extra deep p+ implant
➔ High local field generates multiplication

Large signals bring good timing resolution.

Prototype UFSDs show good gain (~ 10)
Currently manufactured by CNM, FBK interested in joining the effort.

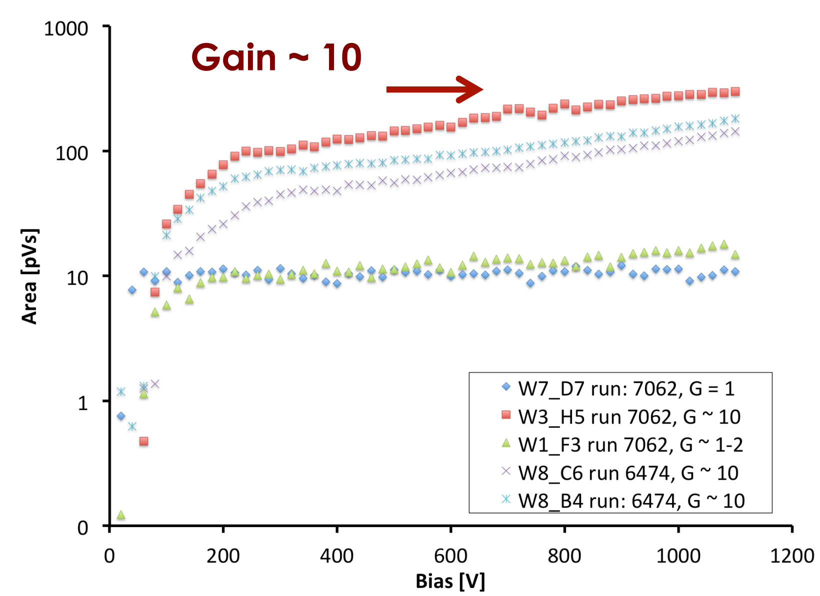

N. Cartiglia, 2014

Detector acceptance

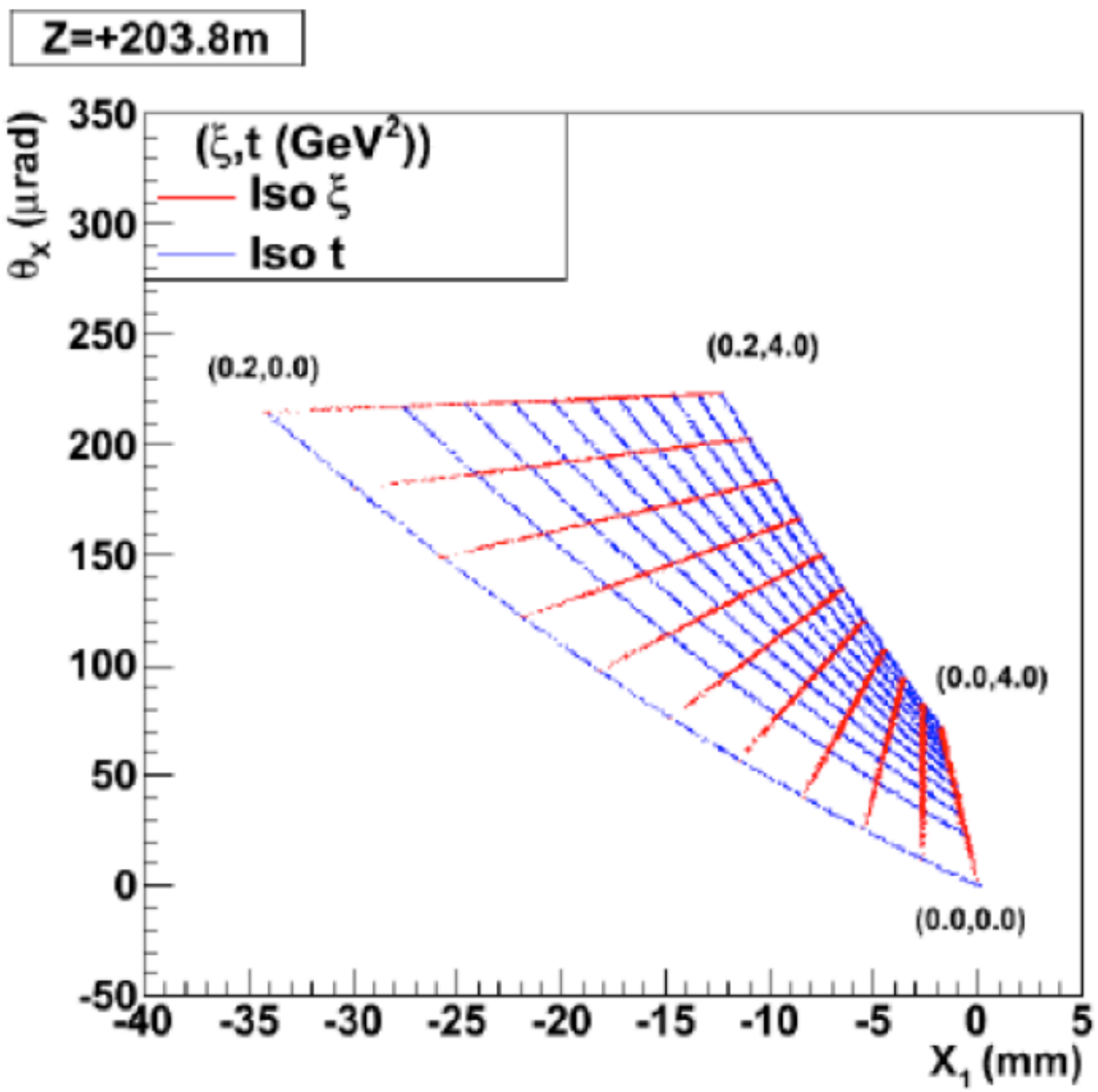

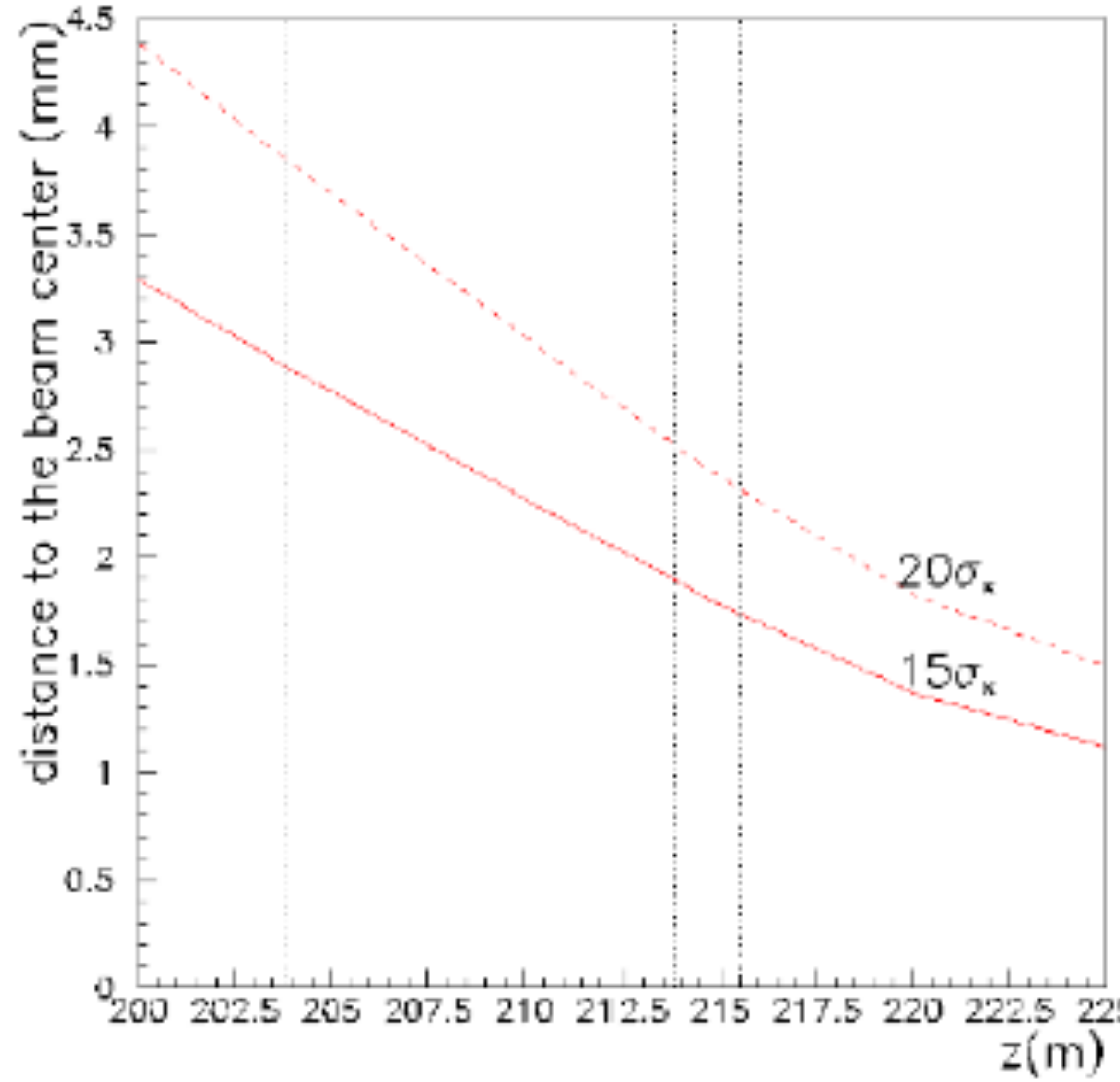

Physics performance: Central Exclusive Production

1) LHC as tagged photon-photon collider

EWK

- Measure $\gamma\gamma \rightarrow W^+W^-$, e^+e^-, $\mu^+\mu^-$, $\tau^+\tau^-$
- Search for AQGC with high sensitivity
- Search for SM forbidden $ZZ\gamma\gamma$, $\gamma\gamma\gamma\gamma$ couplings

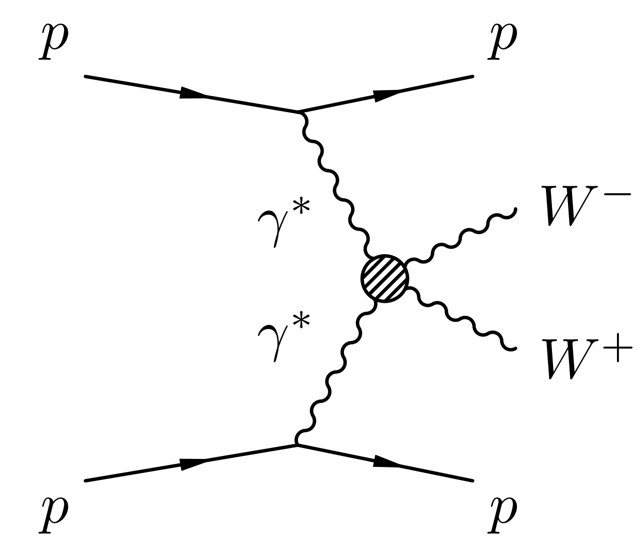

2) LHC as tagged gluon-gluon collider

QCD

- Exclusive two and three jet events, M up to ~ 700-800 GeV.
- Test of pQCD mechanisms of exclusive production.
- Gluon jet samples with small quark jet component
- Proton structure (GPDs)

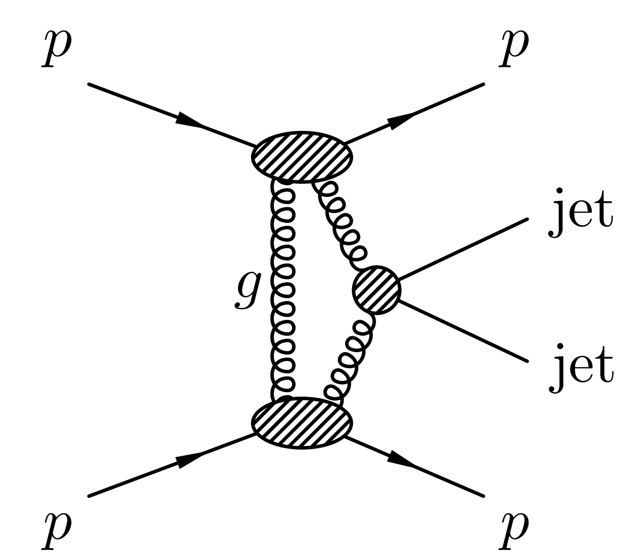

BSM

Search for new resonances in CEP

- Clean events (no underlying pp event)
- Independent mass measurement from pp system
- J^PC quantum numbers 0++, 2++

M. Arneodo, 2014

Exclusive production

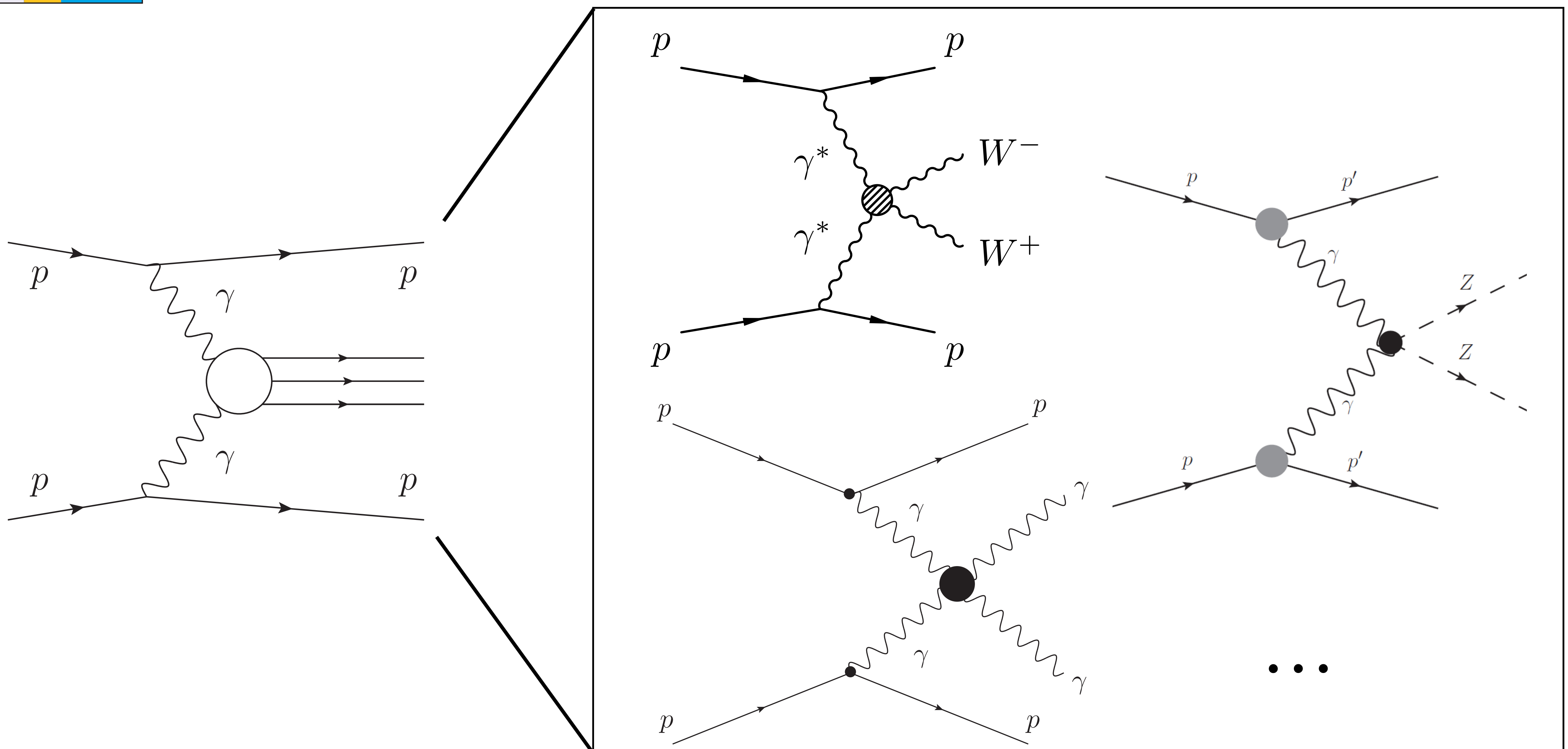

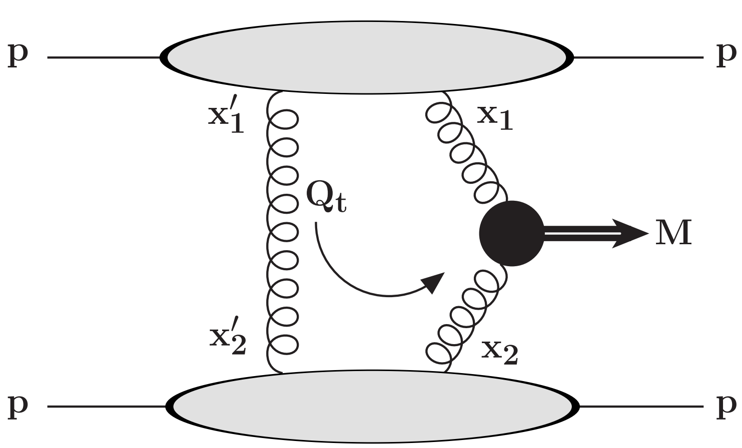

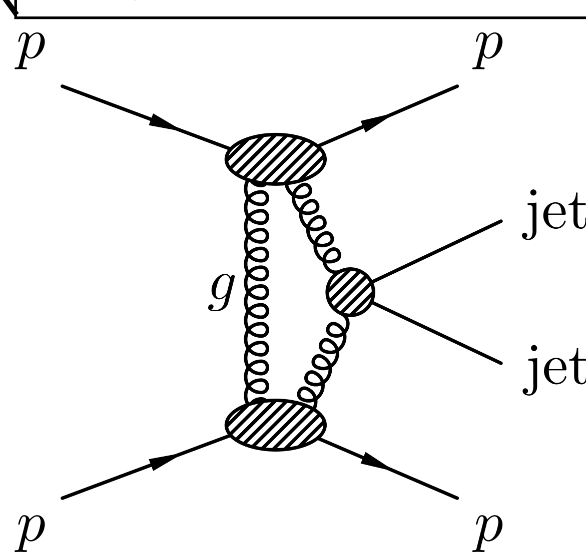

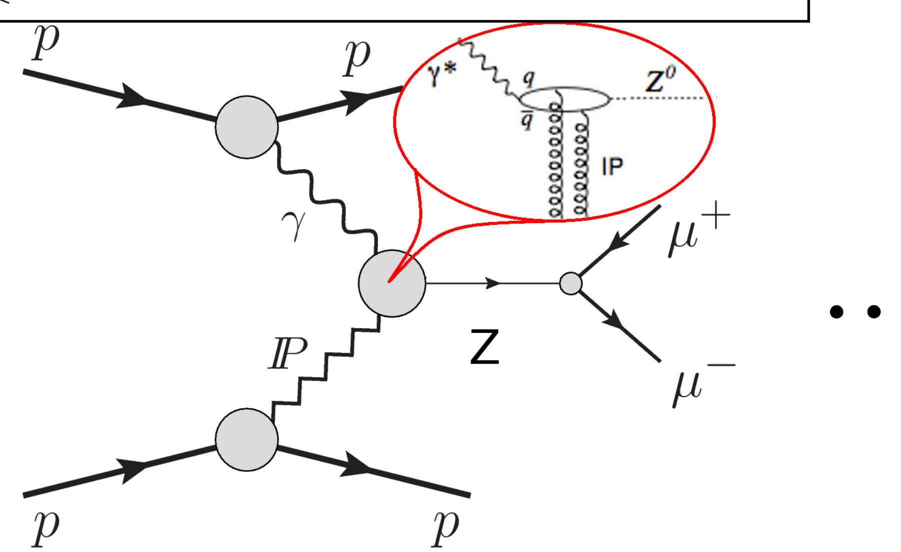

Exclusive WW production

Exclusive WW yields vs detector distance from the beam

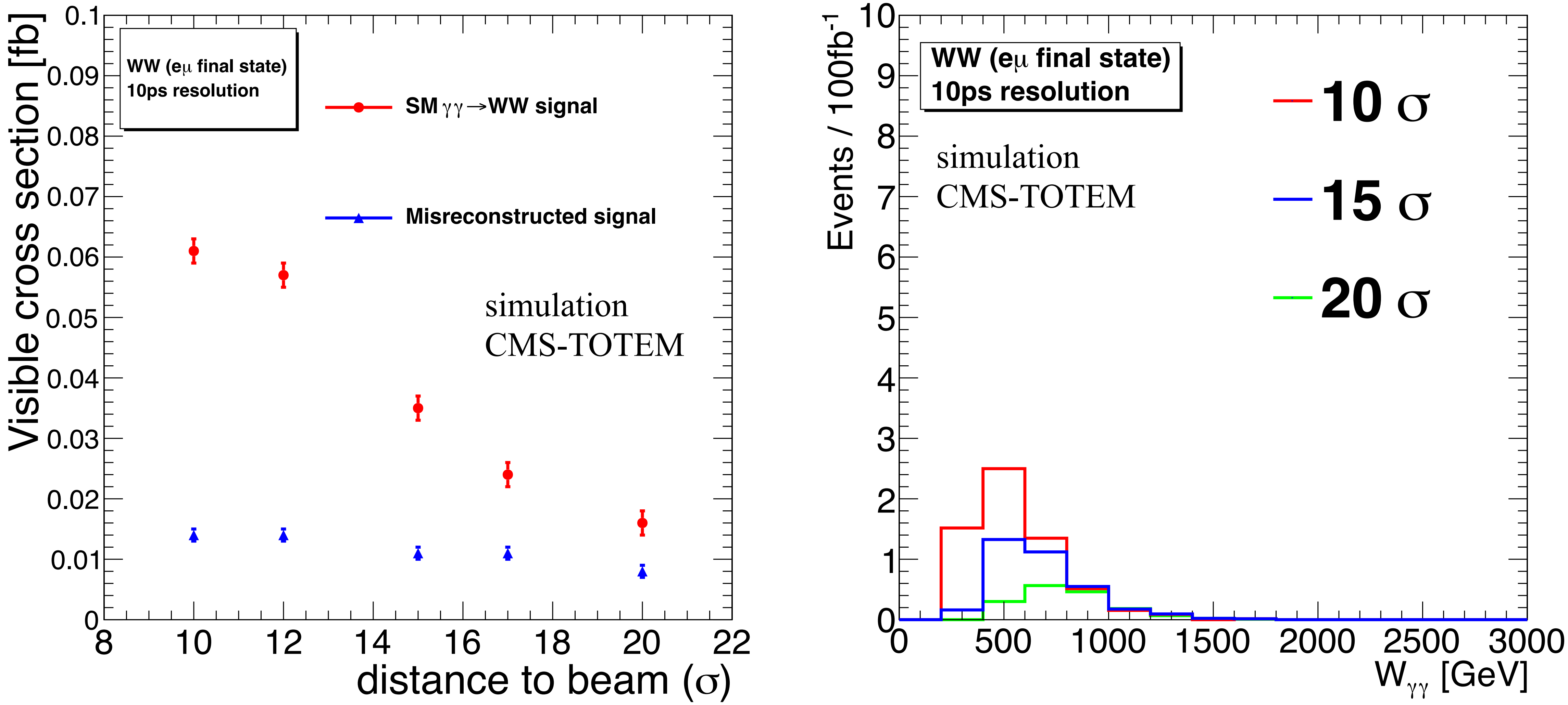

Figure 37: *Left:* The visible cross section for signal exclusive WW events as a function of the distance from the beam (in σ), for SM exclusive WW signal events and for misreconstructed background events. Only the eμ final state is considered; a time resolution of 10 ps is assumed. *Right:* The missing mass is shown for three values of the distance from the beam (10, 15, and 20 σ).

Anomalous quartic couplings

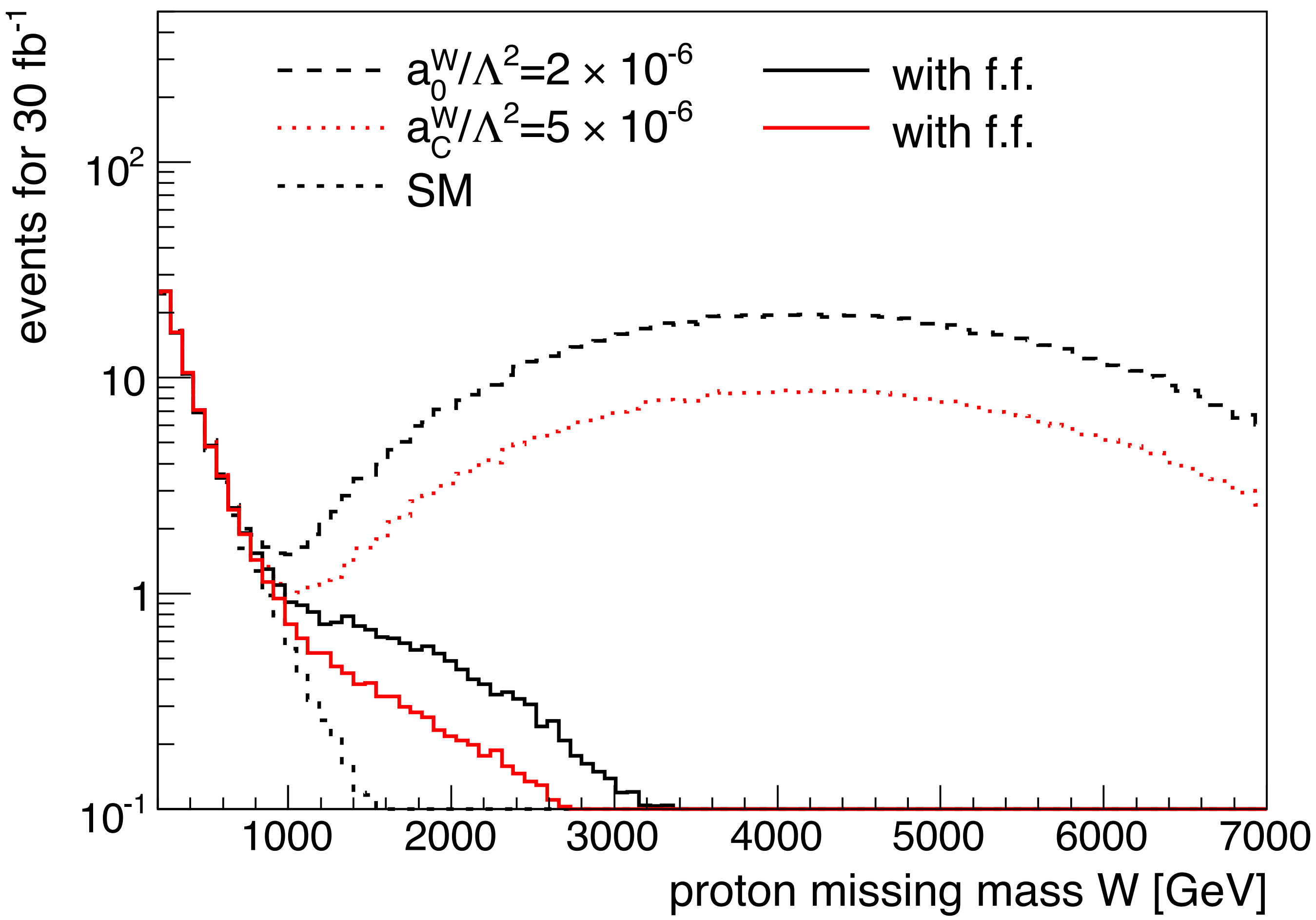

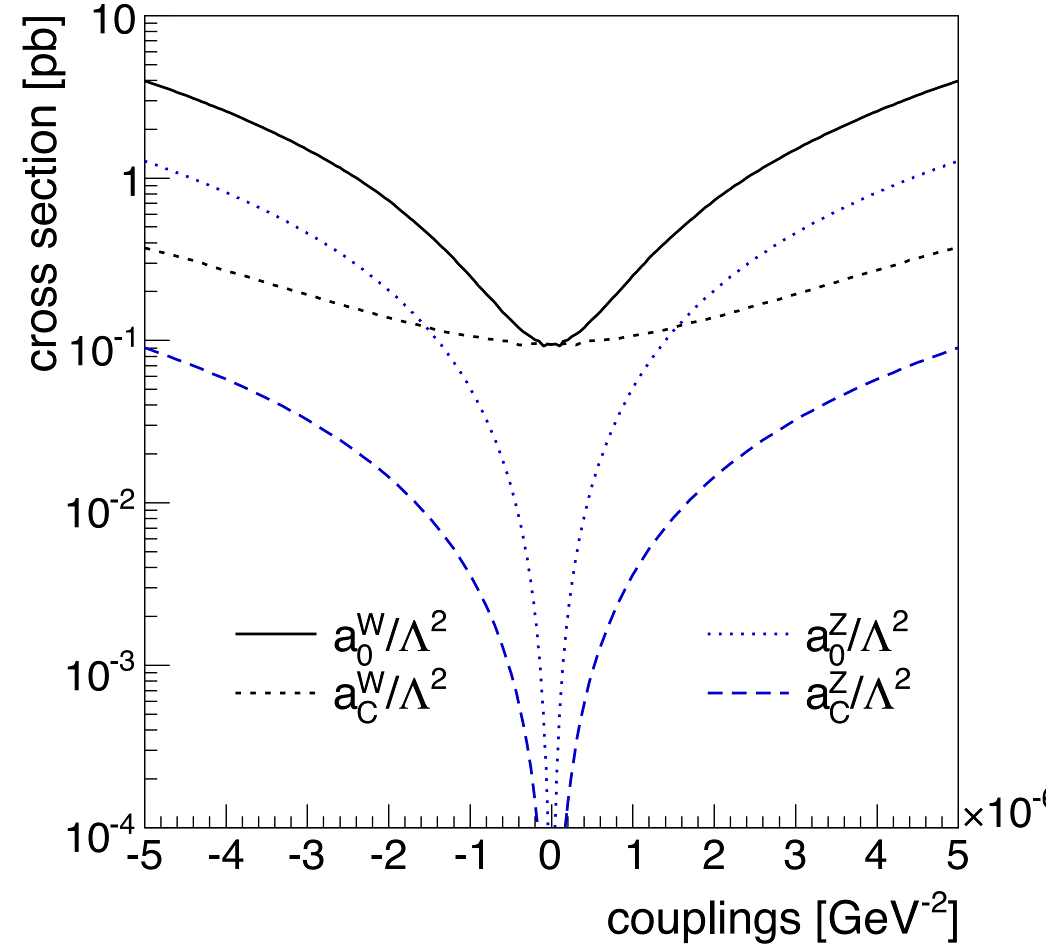

E. Chapon, C. Royon, O. Kepka (2009)

Exclusive diphoton production

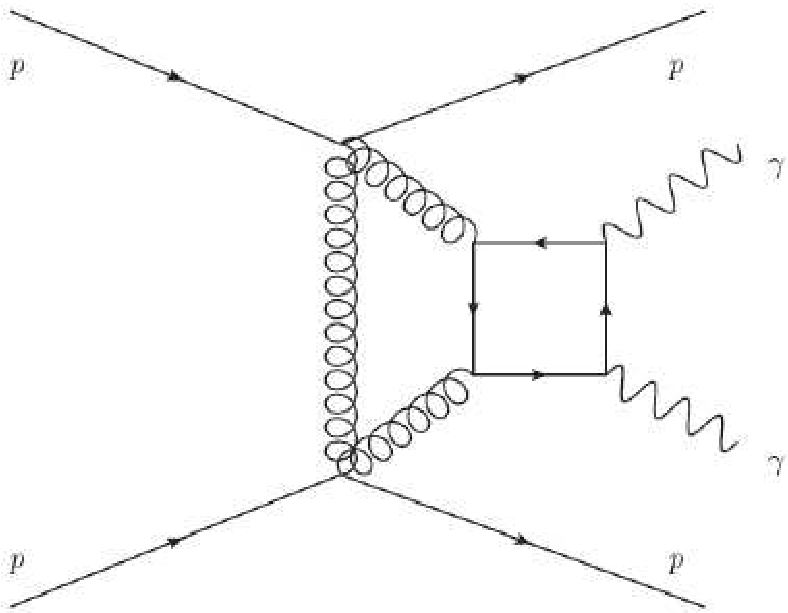

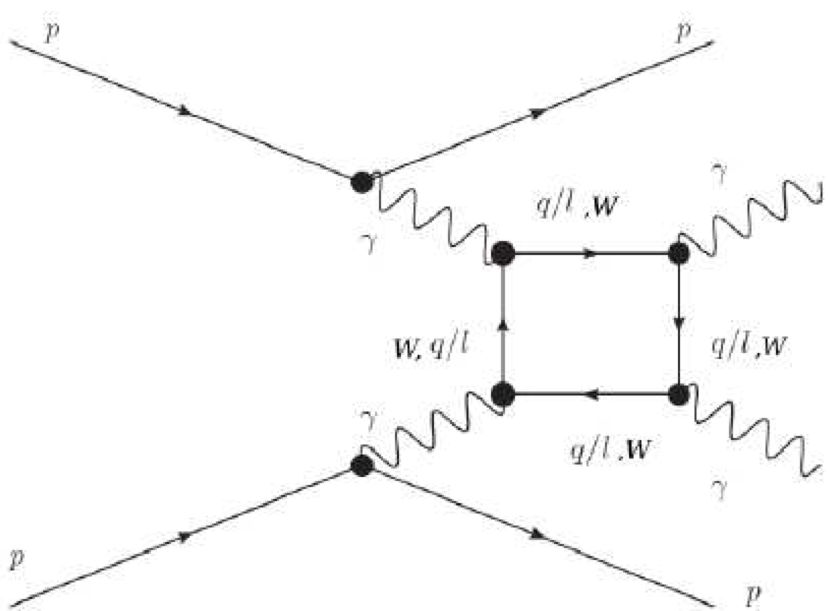

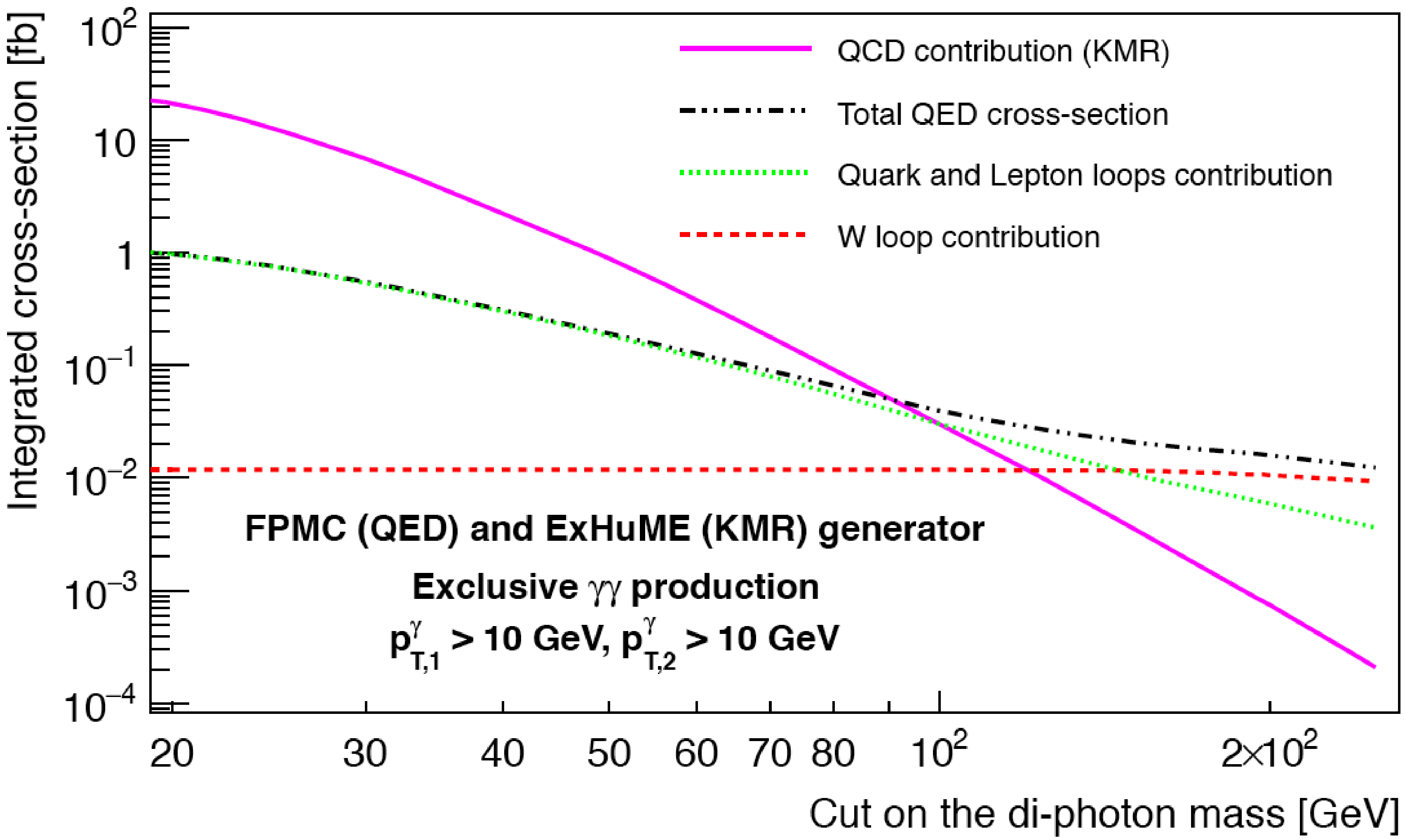

C. Royon et al, 2015

Anomalous quartic photon coupling

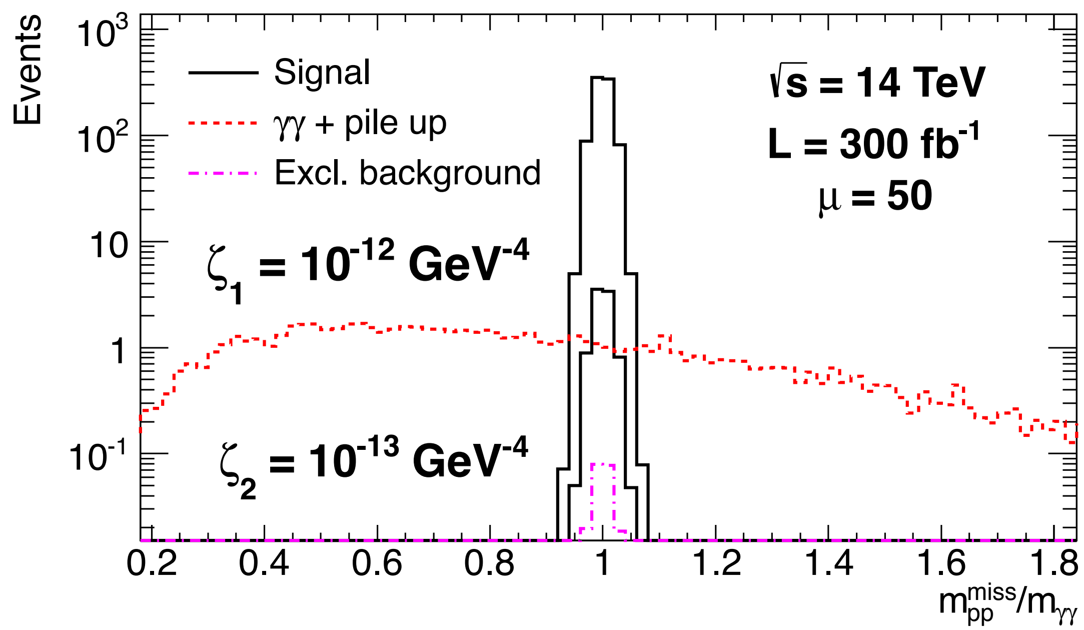

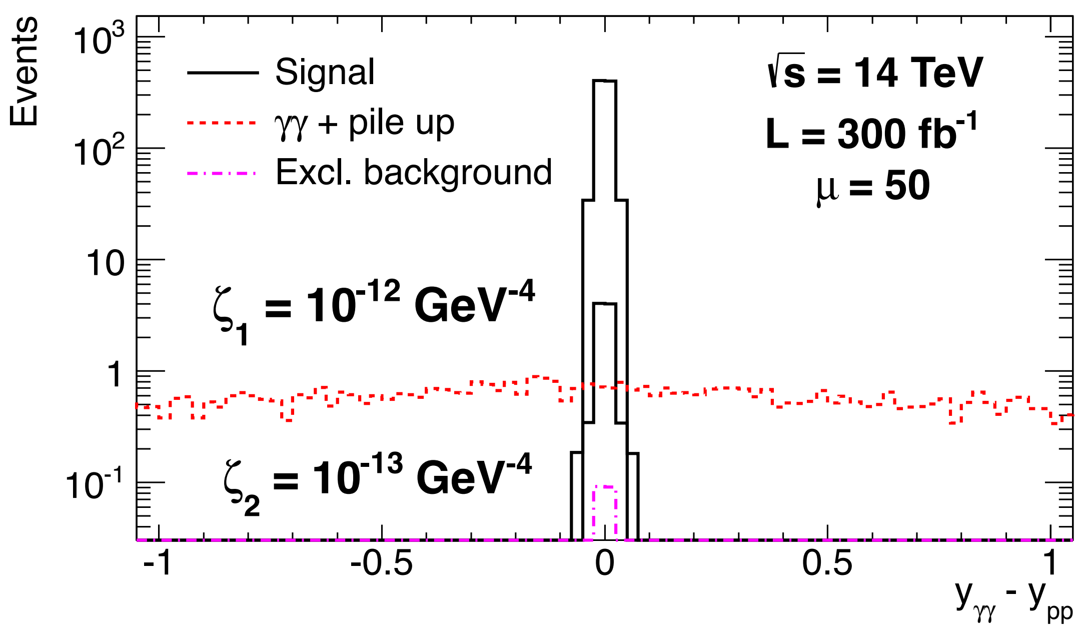

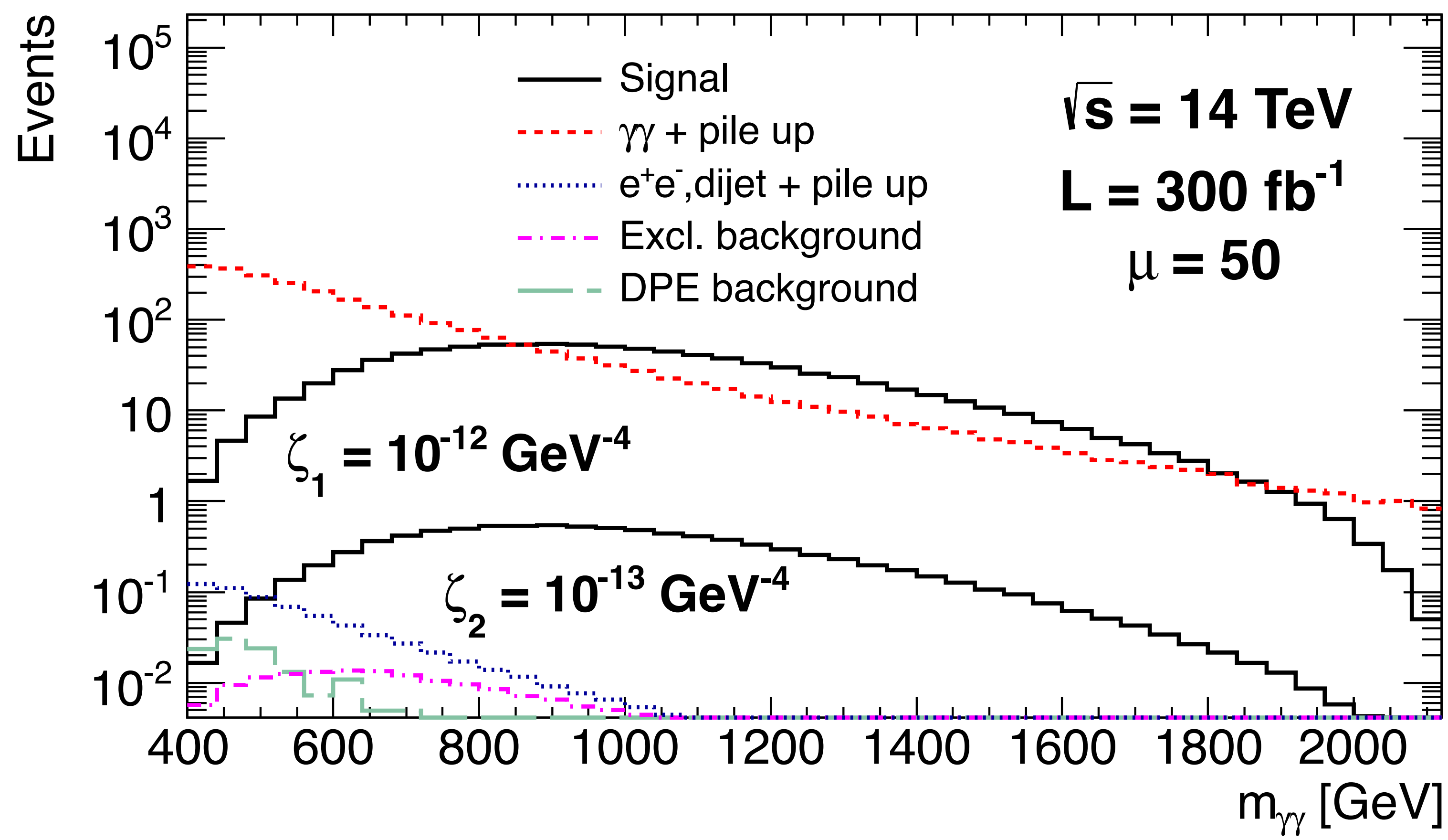

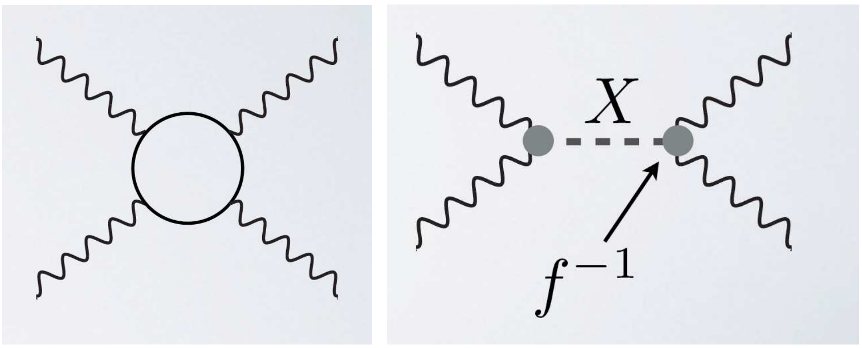

C. Royon et al, 2015

$$\mathcal{L}_{4\gamma} = \zeta_1^\gamma F_{\mu\nu} F^{\mu\nu} F_{\rho\sigma} F^{\rho\sigma} + \zeta_2^\gamma F_{\mu\nu} F^{\nu\rho} F_{\rho\lambda} F^{\lambda\mu}$$

Hit distribution vs (ξ,t)

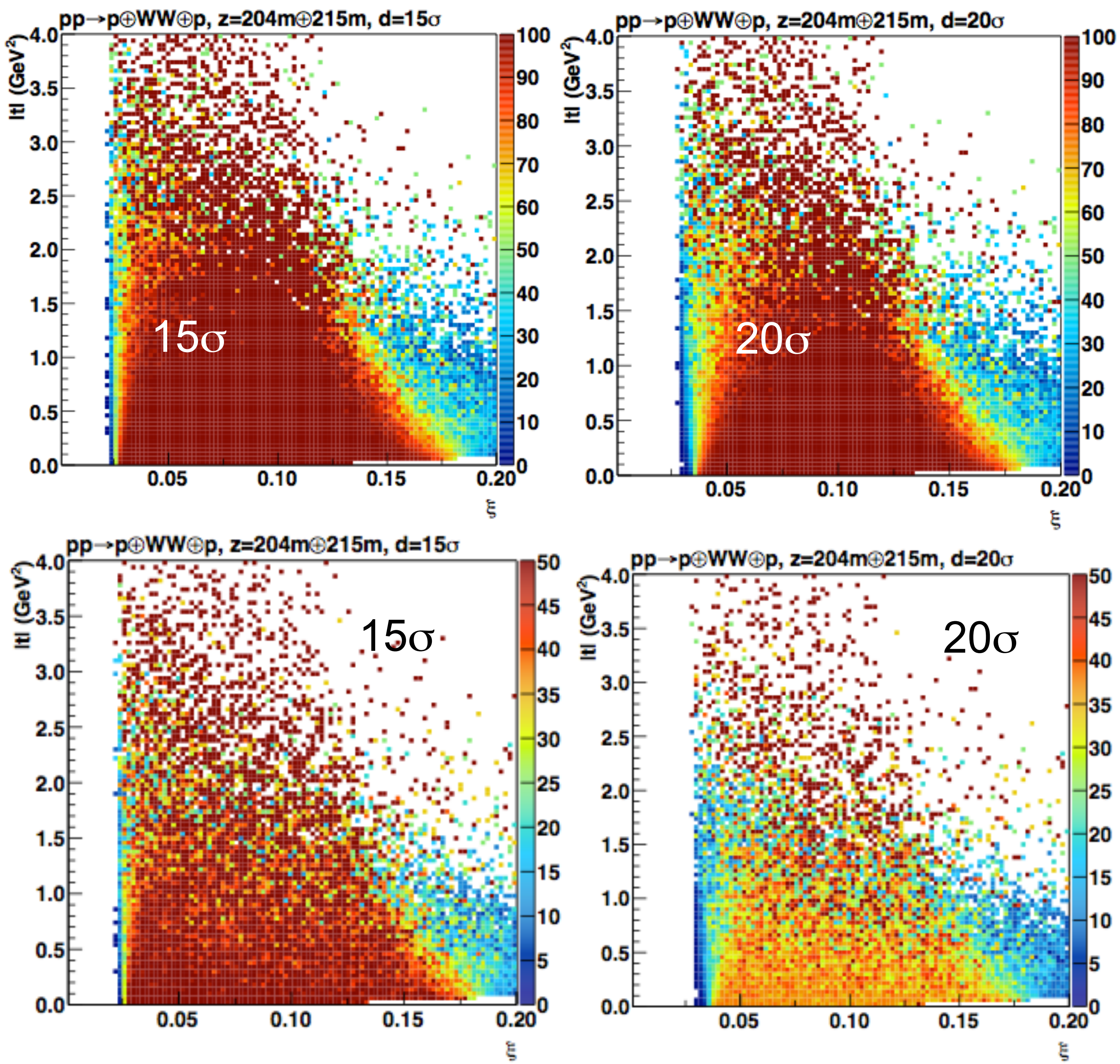

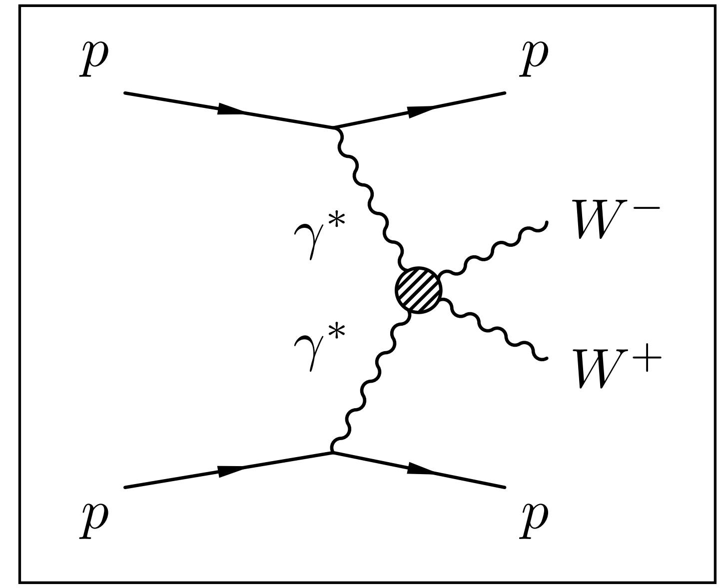

Single arm acceptance:
⇒ ~55% @15σ

Double arm acceptance:
⇒ ~28% @15σ

acceptance in one arm (z>0) when requiring other proton to be within the acceptance of the other arm (z<0)

Detector resolutions in ξ & t